Universidade Federal de Minas Gerais
Instituto de Ciências Biológicas
Departamento de Microbiologia

GUSTAVO JOSÉ COTA DE FREITAS

A BIOLOGIA DE *CRYPTOCOCCUS* SPP.:
Do remodelamento celular e transcricional ao tratamento

Belo Horizonte
2022

Universidade Federal de Minas Gerais
Instituto de Ciências Biológicas
Departamento de Microbiologia

GUSTAVO JOSÉ COTA DE FREITAS

A BIOLOGIA DE *CRYPTOCOCCUS* SPP.:
Do remodelamento celular e transcricional ao tratamento

Tese apresentada ao Programa de Pós-Graduação em Microbiologia do Instituto de Ciências Biológicas da Universidade Federal de Minas Gerais, como requisito para obtenção do título de Doutor em Ciências Biológicas (Microbiologia).

Orientador: Daniel de Assis Santos

Belo Horizonte
2022

043 Freitas, Gustavo José Cota de.
A biologia de Cryptococcus spp.: do remodelamento celular e transcricional ao tratamento [manuscrito] / Gustavo José Cota de Freitas. – 2022.
124 f. : il. ; 29,5 cm.

Orientador: Daniel de Assis Santos.
Tese (doutorado) – Universidade Federal de Minas Gerais, Instituto de Ciências Biológicas. Programa de Pós-Graduação em Microbiologia.

1. Microbiologia. 2. Criptococose. 3. Cryptococcus gattii. 4. Cryptococcus neoformans. 5. Reposicionamento de Medicamentos. 6. Antimaláricos. 7. Hormônios Esteroides Gonadais. 8. Antifúngicos. I. Santos, Daniel de Assis. II. Universidade Federal de Minas Gerais. Instituto de Ciências Biológicas. III. Título.

CDU: 579

Ficha Catalográfica elaborada pela bibliotecária Fabiane C M Reis CRB 6 2680

UNIVERSIDADE FEDERAL DE MINAS GERAIS
INSTITUTO DE CIÊNCIAS BIOLÓGICAS
PÓS-GRADUAÇÃO EM MICROBIOLOGIA

ATA DE DEFESA DE TESE

ATA DA DEFESA DE TESE DE **GUSTAVO JOSÉ COTA DE FREITAS**

Nº REGISTRO: 2019662587

Às 14:00 horas do dia **12 de dezembro de 2022**, reuniu-se, por via remota, a Comissão Examinadora composta pelos Drs. Caio Tavares Fagundes (Departamento de Microbiologia/ICB/UFMG), Márcio Lourenço Rodrigues (FIOCRUZ - CURITIBA), Rafael Wesley Bastos (Universidade Federal do Rio Grande do Norte - UFRN), Livia Kmetzsch Rosa e Silva (Universidade Federal do Rio Grande do Sul - UFRGS) e o Prof. Dr. Daniel de Assis Santos (Orientador), para julgar o trabalho final **"A Biologia de Cryptococcus spp.: do Remodelamento Celular e Transcricional ao Tratamento"** do aluno **Gustavo José Cota de Freitas**, requisito final para a obtenção do Grau de **DOUTOR EM CIÊNCIAS BIOLÓGICAS: MICROBIOLOGIA**. Abrindo a sessão, o Presidente da Comissão, Prof. Dr. Daniel de Assis Santos, após dar a conhecer aos presentes o teor das Normas Regulamentares do Trabalho Final, passou a palavra ao candidato, para a apresentação de seu trabalho. Seguiu-se a arguição pelos Examinadores, com a respectiva defesa do candidato. Logo após, a Comissão se reuniu, sem a presença do candidato e do público, para julgamento e expedição de resultado final. O candidato foi considerado **APROVADO**. O resultado final foi comunicado publicamente ao candidato pelo Presidente da Comissão. Nada mais havendo a tratar, o Presidente encerrou a reunião e lavrou a presente ata, que será assinada por todos os membros participantes da Comissão Examinadora. O candidato tem 60 (sessenta) dias, a partir desta data, para entregar a versão final da tese ao Programa de Pós-graduação em Microbiologia da UFMG e requerer seu diploma.

Belo Horizonte, 12 de dezembro de 2022

Membros da Banca:

Prof. Dr. Caio Tavares Fagundes

Dr. Márcio Lourenço Rodrigues

Prof. Dr. Rafael Wesley Bastos

Profa. Dra. Livia Kmetzsch Rosa e Silva

De acordo:

Prof. Dr. Daniel de Assis Santos

(Orientador)

Profa. Daniele da Glória de Souza

(Coordenadora do Programa de Pós-graduação

em Microbiologia)

Documento assinado eletronicamente por **Rafael Wesley Bastos**, **Usuário Externo**, em 13/12/2022, às 09:40, conforme horário oficial de Brasília, com fundamento no art. 5º do Decreto nº 10.543, de 13 de novembro de 2020.

Documento assinado eletronicamente por **Daniele da Gloria de Souza**, **Coordenador(a) de curso de pós-graduação**, em 13/12/2022, às 09:59, conforme horário oficial de Brasília, com fundamento no art. 5º do Decreto nº 10.543, de 13 de novembro de 2020.

Documento assinado eletronicamente por **Daniel de Assis Santos**, **Professor do Magistério Superior**, em 13/12/2022, às 10:13, conforme horário oficial de Brasília, com fundamento no art. 5º do Decreto nº 10.543, de 13 de novembro de 2020.

Documento assinado eletronicamente por **Caio Tavares Fagundes**, **Professor do Magistério Superior**, em 13/12/2022, às 11:05, conforme horário oficial de Brasília, com fundamento no art. 5º do Decreto nº 10.543, de 13 de novembro de 2020.

Documento assinado eletronicamente por **Marcio Lourenco Rodrigues**, **Usuário Externo**, em 15/12/2022, às 08:38, conforme horário oficial de Brasília, com fundamento no art. 5º do Decreto nº 10.543, de 13 de novembro de 2020.

Documento assinado eletronicamente por **Livia Kmetzsch Rosa e Silva**, **Usuária Externa**, em 09/03/2023, às 10:00, conforme horário oficial de Brasília, com fundamento no art. 5º do Decreto nº 10.543, de 13 de novembro de 2020.

A autenticidade deste documento pode ser conferida no site https://sei.ufmg.br/sei/controlador_externo.php?acao=documento_conferir&id_orgao_acesso_externo=0, informando o código verificador **1904466** e o código CRC **6593267A**.

Referência: Processo nº 23072.230985/2021-91 SEI nº 1904466

AGRADECIMENTOS

Aos meus pais, José Geraldo de Freitas e Maria da Piedade Cota Freitas, que apesar de todas as dificuldades ao longa da vida, sempre estiveram presentes na minha formação pessoal e acadêmica. Sem eles não haveria graduação, mestrado e nem a conclusão desse doutorado. Apesar de não compreenderem a dinâmica da carreira acadêmica, nunca mediram esforços para me apoiar nesta trajetória. Depositaram toda a confiança e possibilitaram a experiência em um mundo que eu jamais imaginei alcançar. Pai e mãe, amo vocês e obrigado por tudo.

Aos meus amigos, Rafael, Diogo, Heliana, Eluzia, Lud Golveia, Lud Baltz, Daniele Leticia, Thais Furtado, Hellem, Noelly, Junya, Carlos BD, Lorena, Maira Juliana, Karen, Gabrielle, Lívia, Camila Nery, Vanessa ES e Cesar; que em meio a toda a loucura da vida acadêmica sempre foram conforto e abraço quando precisei de apoio emocional. Sim! A vida acadêmica possui os seus altos e baixos e isso a gente não coloca no *Lattes*.

Aos atuais colegas de laboratório, Vanessa Caroline, Queila, Victor, Tamires, Geisla, Lívia e a Bruna IC. Obrigado pelo coleguismo, respeito e carinho no convívio da rotina laboratorial.

Ao meu amigo Bala Halls Preta, que ao acaso, abriu as portas para que eu pudesse começar a iniciação científica e dar os primeiros passos para a carreira acadêmica.

Ao meu amigo Rafael Leite, que sempre foi um ótimo amigo e conselheiro na vida profissional. Foi graças a ele que prestei um concurso na UFMG e pude ter uma vida mais tranquila e digna durante o doutorado.

A minha amiga Carla Peres, que apesar de estar longe, sempre foi uma grande luz durante o desenvolvimento do doutorado. Juntos conseguimos sobreviver a uma fase muito difícil no LabMic.

Ao professor Daniel de Assis Santos, que me DESorientou desde a iniciação científica. Sem ele esse agradecimento não seria escrito: "Você não fez isso sozinho, tem que agradecer...não seja ingrato, bota o nome do seu pai e sua mãe ai!". Obrigado pela confiança e possibilidade de fazer pesquisa de uma forma tão agradável; por saber ouvir e sempre estar aberto as discussões no desenvolvimento de projetos e escrita de trabalhos. Obrigado pela humildade, sabedoria e respeito na minha orientação e dos meus colegas.

A professora Cidinha, que me acolheu na primeira iniciação científica e me orientou no desenvolvimento do trabalho de conclusão de curso. Obrigado por guiar os meus passos na introdução ao meio acadêmico.

A professora Nalu, que eu chamo de mocinha e rainha da biologia molecular. Obrigado por todo o carinho e aprendizado durante o doutorado. Sem dúvidas, você se tornou uma grande amiga e inspiração durante esse período.

Ao professor Ary (Zé), que sempre tem uma explicação para tudo. Obrigado pelos conselhos sensatos e pela amizade durante o doutorado.

Aos profissionais da limpeza, em especial a Patrícia e a mocinha do pão de mel. Obrigado por sempre deixar o laboratório limpo e agradável para a realização dos meus experimentos e dos meus colegas.

Ao Thiago e a Débora, por sempre resolverem os meus problemas na secretaria do departamento.

Aos professores do departamento, que de alguma forma contribuíram para a minha formação, em especial: Susana Johann, Elisabeth Neumann, Luís Macedo, Danielle da Glória, Mila, Simone e Silvia Beleza.

A Marisa e a Tatiane do xerox. Obrigado pelo carinho e amizade desde a graduação.

A aqueles que eu não coloquei o nome nesse tópico, mas que de alguma forma contribuíram para a minha formação pessoal e profissional, peço desculpas de antemão, e deixo meus sinceros agradecimentos.

O tamanho dos seus sonhos deve sempre exceder a sua capacidade de alcança-los. Se os seus sonhos não te assustam, eles não são grandes o suficiente.

Ellen Johnson Sirleaf

RESUMO

Cryptococcus gattii e *C. neoformans* são os principais agentes etiológicos da criptococose, uma micose invasiva que acomete os pulmões e pode evoluir para meningoencefalite. O tratamento da doença envolve um arsenal limitado de antifúngicos, associado a elevado toxicidade, custo e indução de resistência, o que impacta diretamente no prognóstico clínico. Durante a interação com o hospedeiro, *Cryptococococcus* spp. pode apresentar diferentes morfologias, que variam desde microcelulas, células de tamanho normal até células titânica. Apesar desse conhecimento, a compreensão sobre a reorganização morfológica em tempos precoces e tardios da infecção permanece pouco explorada. Nesse panorama, esta tese explora o remodelamento celular de *Cryptococcus* spp. durante a infecção e o reposicionamento de fármacos no contexto da criptococose, por meio de quatro estudos. O estudo (i) abordou a dinâmica da reorganização morfológica de *Cryptococcus neoformans* e *C. gattii* em diferentes estágios da infecção. Inicialmente observamos que a indução de células pequenas é importante para o aumento do *fitness* reprodutivo/energético, invasão do epitélio pulmonar e disseminação para o sistema nervoso central. Tardiamente, o aumento da cápsula polissacarídica *in vivo* foi capaz de predizer a virulência de *C. neoformans*, mas não para *C. gattii*. Em (ii) comentamos sobre a importância de compreender o papel do polissacarídeo capsular (PC) de *C. gattii* no reconhecimento de *Cryptococcus* por CD11b e como esse conhecimento pode influenciar nas estratégias para o desenvolvimento de novas vacinas contra a criptococose. Além disso, apresentamos um cenário geral sobre a criptococose, abordando desde a compreensão da biologia fúngica e sua interação no ambiente até as limitações terapêuticas e vacinais atualmente existentes. Na premissa de novas estratégias terapêuticas, o estudo (iii) abordou o reposicionamento de antimaláricos (ATMs) no tratamento da criptococose. Demonstramos que a combinação entre antimaláricos e anfotericina B resultou em uma interação sinérgica e aumento da sobrevida em modelo murino. Em (iv) abordamos o efeito de hormônios sexuais na ação de antifúngicos clínicos frente a *Cryptococcus* spp. Interessantemente, vimos que o estradiol e a testosterona, assim como os ATMs, também apresentam sinergismo com anfotericina B, sendo capazes de reduzir a concentração mínima necessária para a ação fungicida desse antifúngico. Em geral, o conjunto de dados apresentados nesta tese mostram a complexidade biológica de *Cryptococcus* durante a interação com o hospedeiro e a perspectiva de novos tratamentos que poderão ser utilizados no cenário da criptococose.

Palavras chave: Criptococose, *Cryptococcus gattii*, *Cryptococcus neoformans*, remodelamento celular, remodelamento transcricional, reposicionamento de fármacos, antimaláricos, hormônios sexuais, antifúngicos.

ABSTRACT

Cryptococcus gattii and *C. neoformans* are the main etiologic agents of cryptococcosis, an invasive mycosis that affects the lungs and can progress to meningoencephalitis. The treatment of the disease involves a limited arsenal of antifungals, associated with high toxicity, cost and induction of resistance, which directly impacts the clinical prognosis. During the interaction with the host, *Cryptococcus* spp can present different morphologies, ranging from microcells, normal-sized cells to titanic cells. Despite this knowledge, the understanding of morphological reorganization in the initial and late periods of infection remains little explored. In this scenario, this thesis explores the cellular remodeling of *Cryptococcus* spp. during infection and drug repositioning in the context of Cryptococcosis, through four studies. Study (i) addressed the dynamics of morphological reorganization of *Cryptococcus neoformans* and *C. gattii* at different stages of infection. Initially, we observed that the induction of small cells is important for increasing reproductive/energetic fitness, invasion of the pulmonary epithelium and dissemination to the central nervous system. Subsequently, the increase in polysaccharide capsule in vivo was able to predict virulence for *C. neoformans*, but not for *C. gattii*. In (ii) we comment on the importance of understanding the role of capsular polysaccharide (PC) from *C. gattii* in the recognition of *Cryptococcus* by CD11b and how this knowledge can influence strategies for the development of new vaccines against cryptococcosis. In addition, we present an overview of Cryptococcosis, ranging from the understanding of fungal biology and its interaction in the environment to the currently existing therapeutic and vaccine limitations. Based on the premise of new therapeutic strategies, study (iii) addressed the repositioning of antimalarials (ATMs) in the treatment of Cryptococcosis. We demonstrated that the combination of antimalarials and amphotericin B resulted in a synergistic interaction and increased survival in a murine model. In (iv) we address the effect of sex hormones on the action of clinical antifungals against *Cryptococcus* spp. Interestingly, we saw that estradiol and testosterone, as well as ATMs, also present synergism with amphotericin B, which may reduce the minimum concentration required for the fungicidal action of this antifungal. In general, the set of data presented in this thesis shows the biological complexity of *Cryptococcus* during the interaction with the host and the perspective of new treatments that can be used in the scenario of Cryptococcosis.

Keywords: Cryptococcosis, *Cryptococcus gattii*, *Cryptococcus neoformans*, cell remodeling, transcriptional remodeling, drug repurposing, antimalarials, sex hormones, antifungals.

LISTA DE ABREVIATURAS

5-FC: 5-flucitosina

AMB: Anfotericina B

FCZ: Fluconazol

ASD: Ágar Sabouraud Dextrose

SDL: Sabouraud Dextrose líquido

FEC-GM: Fator Estimulador de Colônias de Granulócitos e Macrófagos

MC: Meningite Criptococócica

MM: Meio mínimo

MML: Meio mínimo líquido

MAT: *mating type*

ATCC: *American Type Culture Collection*

BHE: Barreira Hemato-Encefálica

CEUA/UFMG: Comissão de Ética no Uso de Animais da Universidade Federal de Minas Gerais

CIM: Concentração Inibitória Mínima

GXM: Glucoronoxilomanano

GalXM: Galactoxilomanana

ROS: Espécies Reativas de Oxigênio

RNS: Espécies Reativas de Nitrogênio

RPMI-1640 - *Roswell Park Memorial Institute*

SNC: Sistema Nervoso Central

UFC: Unidades Formadoras de Colônia

ROS: Espécies reativas de oxigênio

PRN: Espécies reativas de nitrogênio.

AMSs: Antimaláricos

HSs: Hormônios sexuais

AgCr +: Antigenemia criptococcocica positiva

LISTA DE FIGURAS

SUMÁRIO

1. INTRODUÇÃO

Os patógenos fúngicos apresentam relevante importância na vida vegetal e animal, mais de 300 milhões de pessoas são afetadas anualmente em todo o mundo por infecções fúngicas (BROWN; DENNING; GOW; LEVITZ *et al.*, 2012; FISHER; ALASTRUEY-IZQUIERDO; BERMAN; BICANIC *et al.*, 2022; MOR; RELLA; FARNOUD; SINGH *et al.*, 2015; TUITE; LACEY, 2013). Este contexto está principalmente associado ao aumento da expectativa de vida, procedimentos médicos invasivos e o crescente número de indivíduos imunossuprimidos (MORRIS, 2014). Em destaque, as micoses invasivas normalmente estão associadas a casos mais graves e apresentam taxas de mortalidade superiores a 50% (BROWN; DENNING; GOW; LEVITZ *et al.*, 2012). No entanto, apesar disso, as infecções fúngicas normalmente são negligenciadas, caracterizadas pela ausência de programas de vigilância em saúde e ambiental e pelo baixo financiamento em pesquisa quando comparada a outras doenças infecciosas (BROWN; DENNING; GOW; LEVITZ *et al.*, 2012; RODRIGUES, 2016).

A criptococose, infecção fúngica causada por leveduras encapsuladas do gênero *Cryptococcus,* se tornou ao longo dos anos a principal micose invasiva no mundo, com elevada prevalência e mortalidade (FISHER; ALASTRUEY-IZQUIERDO; BERMAN; BICANIC *et al.*, 2022; MAZIARZ; PERFECT, 2016; PAPPAS, 2013; PARK; WANNEMUEHLER; MARSTON; GOVENDER *et al.*, 2009). Sua etiologia está principalmente relacionada a duas espécies de *Cryptococcus*, *C. neoformans* e *C. gattii,* responsáveis por causar doenças em humanos e animais (COGLIATI, 2013; MORTENSON; BARTLETT; WILSON; LOCKHART, 2013; VOELZ; MAY, 2010). A doença se caracteriza principalmente pelo acometimento primário dos pulmões e subsequentemente do cérebro. As manifestações clínicas variam de assintomática, quando o fungo permanece latente no hospedeiro; até pneumonia, meningoencefalite e manifestações secundárias decorrentes da disseminação do fungo para demais órgãos (MAY; STONE; WIESNER; BICANIC *et al.*, 2016; MAZIARZ; PERFECT, 2016).

Cryptococcus é um gênero de fungos pertencente ao grupo Basidiomycota, ao subfilo Agaricomycotina, à classe Tremellomycetes e à família Tremellaceae da ordem Tremellales (Taxonomy, NCBI). Atualmente, esse gênero possui mais de 80

espécies, sendo que *C. neoformans* e *C. gattii* destacam-se por sua importância médica e veterinária (CHEN; MEYER; SORRELL, 2014; FELL; BOEKHOUT; FONSECA; SCORZETTI *et al.*, 2000) enquanto as demais como *C. albidus*, *C. laurentii* e *C. curvatus* se apresentam como leveduras saprofíticas, apesar de serem frequentemente isoladas em amostras de pacientes imunocomprometidos (LI; MODY, 2010). Esse complexo é composto por células leveduriformes esféricas ou globosas envoltas por uma cápsula polissacarídica. Diferenças estruturais do polissacarídeo capsular glucuronoxilmanana (GXM), que constitui cerca de 90% da cápsula, permite a classificação do complexo *C. neoformans*/ *C. gattii* em cinco sorotipos (A, B, C, D e AD) (HAGEN; KHAYHAN; THEELEN; KOLECKA *et al.*, 2015).

Durante o ciclo de vida, os micro-organismos desse gênero apresentam duas formas de reprodução, assexuada ou sexuada. Na forma assexuada, variedade anamórfica, *C. gattii* e *C. neoformans* se dividem principalmente por brotamento. Enquanto na forma sexuada, variedade teleomórfica, esses dois micro-organismos correspondem a *Filobasidiella neoformans* e *F. bacillispora*, respectivamente (BARNETT, 2010). Nessa forma, no entanto, a reprodução ocorre por meio de um sistema de acasalamento bipolar, denominado *mating type* (MAT): α e a, em que as células leveduriformes sofrem um dimorfismo para o crescimento de hifas e consequente formação de basidiósporos (CHEN; MEYER; SORRELL, 2014) considerados importantes propágulos infecciosos.

2. A plasticidade morfológica de *Cryptococcus* spp.

Cryptococcus ocupa vários nichos ecológicos conhecidos, como árvores, solo, guano de pombos e animais, incluindo diferentes pássaros e espécies de mamíferos (Figura 1) (MAY; STONE; WIESNER; BICANIC *et al.*, 2016). Vários compostos presentes nesses diferentes ambientes estimulam o acasalamento fúngico e consequentemente, alteram a sua morfologia (XU; LIN; ZHAO; KIRKMAN *et al.*, 2017; XUE, 2012; XUE; TADA; DONG; HEITMAN, 2007). Apesar de crescer principalmente na forma leveduriforme, *Cryptococcus* também pode ser encontrado na forma de hifas e pseudo-hifas, sendo essa mudança morfológica dependente do ambiente (SUN; COELHO; DAVID-PALMA; PRIEST *et al.*, 2019).

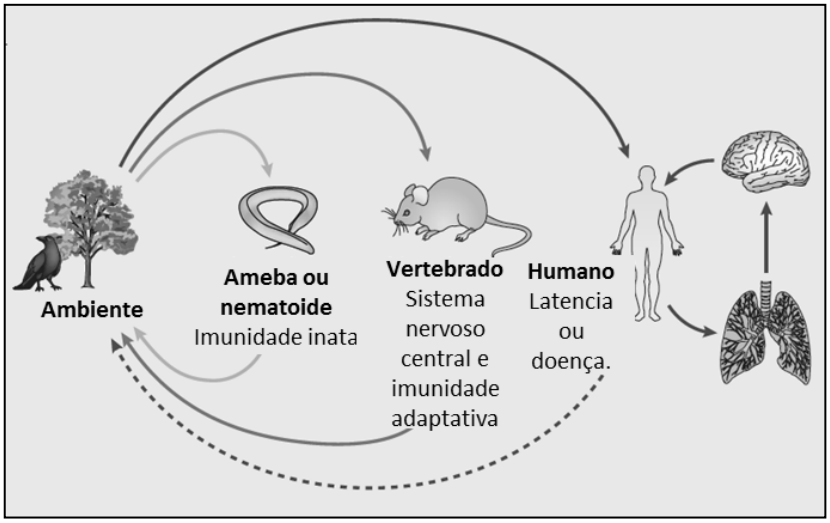

Figura 1. **Diversidade de nichos ecológicos de *Cryptococcus* spp.** (Fonte – Adaptado (MAY; STONE; WIESNER; BICANIC *et al.*, 2016)

A transição de leveduras para hifas envolve uma cascata de sinais de resposta a feromônios relacionada ao acasalamento, aumento da captação de nutrientes e evasão de predadores ambientais (SUN; COELHO; DAVID-PALMA; PRIEST *et al.*, 2019). Após essa resposta, as células de *Cryptococcus* sofrem uma série de alterações morfológicas e celulares para completar o ciclo sexual. Inicialmente, ocorre o acasalamento entre *matings* distintos (bissexual) ou *matings* semelhantes (unissexual), seguido da fusão célula-célula e projeção de um filamento que se diferencia em basídio na sua porção terminal. Posteriormente, ocorre meiose no interior dos basídios e os produtos meióticos passam por sucessivas mitoses levando a formação de cadeias de basidiósporos (Figura 2) (KWON-CHUNG, 1976).

A indução de basidiósporos tem papel crucial na dispersão e sobrevivência de *Cryptococcus* no ambiente(VELAGAPUDI; HSUEH; GEUNES-BOYER; WRIGHT *et al.*, 2009). Essas estruturas conseguem resistir mais facilmente as pressões ambientais (flutuações e extremos de temperatura, UV e estresse oxidativo) do que as células leveduriformes. Além disso, são importantes propágulos infecciosos causadores de doenças em humanos e animais(VELAGAPUDI; HSUEH; GEUNES-BOYER; WRIGHT *et al.*, 2009). As hifas, por sua vez, estão envolvidas no maior sensoriamento ambiental para a captação de nutrientes e evasão da fagocitose de amebas de vida livre. Dessa forma, considera-se que a transição morfológica de leveduras para hifas seja uma estratégia de longo prazo adotada para *Cryptococcus*

sobreviver na natureza (BOTTS; GILES; GATES; KOZEL *et al.*, 2009; SUN; COELHO; DAVID-PALMA; PRIEST *et al.*, 2019).

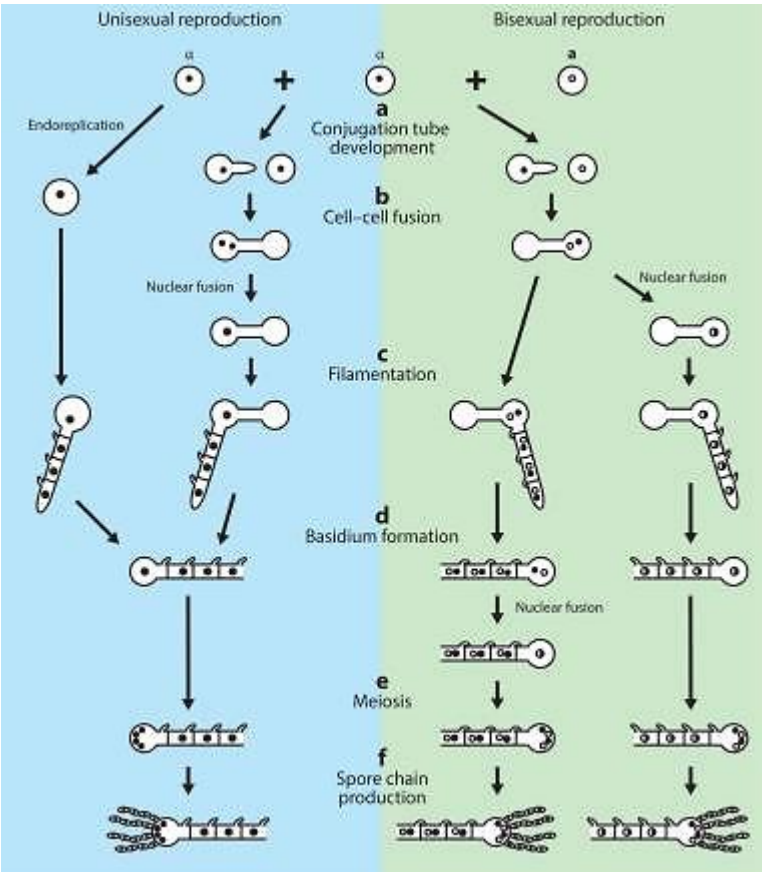

Figura 2: Ciclo de reprodução sexual de *Cryptococcus* (SUN; COELHO; DAVID-PALMA; PRIEST et al., 2019).

Apesar de conferir resistência na natureza, as hifas são estruturas raramente encontradas durante a interação com o hospedeiro (SUN; COELHO; DAVID-PALMA; PRIEST *et al.*, 2019). Após inalação, os basidiosoporos se instalam no parênquima pulmonar e crescem na forma de leveduras, alterando a dinâmica morfológica de *Cryptocoocus* e propiciando o surgimento de outras estratégias de sobrevivência, como a capsula polissacarídica e melanina(SUN; COELHO; DAVID-PALMA; PRIEST *et al.*, 2019). Essa mudança morfológica reflete na variabilidade de tamanhos de leveduras observadas durante a infecção, desde microcélulas (< 2 µm), células típicas de levedura (6 - 8 µm) e células titânicas (> 10 µm) (FERNANDES; BROCKWAY; HAVERKAMP; CUOMO *et al.*, 2018; FERNANDES; DWYER; CAMPBELL; CARTER, 2016; ZARAGOZA, 2011). Ainda, essas células podem apresentar variações no tamanho e estrutura da cápsula polissacarídica, um importante fator de

virulência (Figura 3). Essas alterações morfológicas são importantes para o curso da infecção e proporcionam ao fungo mecanismos para atingir novos ambientes nutricionais, evadir a resposta imune do hospedeiro e disseminar-se pelo organismo(ZARAGOZA, 2011).

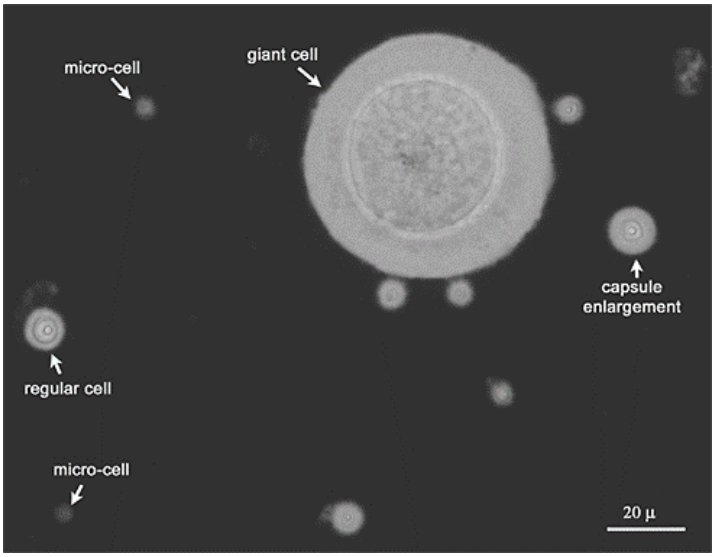

Figura 3: Heterogeneidade da população fúngica extraída do pulmão de camundongos infectados (ZARAGOZA, 2011).

O papel das microcélulas e células pequenas durante a infecção ainda permanece pouco elucidado. Estudo recente descreveu uma população de células pequenas denominadas "*seed cells*", que apresentam tamanho <6µm e alterações em moléculas de superfície de membrana que conferem maior habilidade de escape ao reconhecimento imunológico. Além disso, esse perfil celular possui expressão aumentada de genes envolvidos na aquisição de fosfato e maior habilidade de disseminação em tecidos extrapulmonares (DENHAM; BRAMMER; CHUNG; WAMBAUGH *et al.*, 2022). As microcélulas, por sua vez, apresentam tamanho <2µm e são comuns na infecção por *C. neoformans*. Entretanto, a sua caracterização morfofisiológica ainda permanece incipiente; apesar de um estudo recente relacionar esse perfil morfológico com a virulência em *C. neoformans* (FERNANDES; FRASER; CARTER, 2022).

Por outro lado, as células titânicas são amplamente estudadas e melhor caracterizadas. Além do tamanho aumentado, esse tipo celular é poliplóide, apresenta uma parede celular mais espessa e um único grande vacúolo no

citoplasma (OKAGAKI; STRAIN; NIELSEN; CHARLIER *et al.*, 2010; ZARAGOZA; GARCÍA-RODAS; NOSANCHUK; CUENCA-ESTRELLA *et al.*, 2010). Durante a reprodução, podem gerar células filhas haplóides ou frequentemente aneuplóides (GERSTEIN; FU; MUKAREMERA; LI *et al.*, 2015). As células filhas aneuploides de células titanicas apresentam maior resistência a fatores físico-químicos e a drogas comumente utilizadas na terapia da criptococose (GERSTEIN; FU; MUKAREMERA; LI *et al.*, 2015). No entanto, apesar do tamanho aumentado conferir maior capacidade de evasão da fagocitose por macrófagos, a titanização pode não ser um fator crucial para a patogenicidade, uma vez que alguns isolados clínicos de *C. neoformans* podem não passar por essa transição morfológica (DYLĄG; COLON-REYES; KOZUBOWSKI, 2020; TREVIJANO-CONTADOR; DE OLIVEIRA; GARCÍA-RODAS; ROSSI *et al.*, 2018).

3. Criptococose

3.1 Patogênese e epidemiologia

A criptococose é uma micose invasiva que ocorre pela inalação de leveduras dessecadas do ambiente ou basidiósporos dispersos no ar, que são transportados das vias aéreas superiores, de uma fonte ambiental para os pulmões. Esses propágulos infecciosos são pequenos, de 1,5 a 3,5µm (leveduras) e de 1,0 a 2,0µm (basidiósporos), tamanho ideal para se instalarem rapidamente nos alvéolos pulmonares e serem prontamente reconhecidos por macrófagos alveolares (DATTA; BARTLETT; MARR, 2009; GIBSON; JOHNSTON, 2015). Após a ativação desses macrófagos alveolares, ocorre o recrutamento de outras células imunes pela indução de citocinas e quimiocinas, levando a uma resposta pró-inflamatória e granulomatosa (GIBSON; JOHNSTON, 2015; KWON-CHUNG; FRASER; DOERING; WANG *et al.*, 2014; OLSZEWSKI; ZHANG; HUFFNAGLE, 2010).

Frente ao escape da resposta do hospedeiro, ocorre inicialmente uma colonização dos pulmões por *Cryptococcus* spp, resultando na instalação da infecção. Essa colonização inicial é frequentemente assintomática ou apresenta-se como sintomas gripais, como tosse e febre, podendo evoluir para sintomas mais severos como pneumonia e a síndrome aguda do estresse respiratório (MAZIARZ; PERFECT, 2016). Nesta etapa, o fungo pode se disseminar via hematogênica e atingir outros

orgãos, tais como: baço (KROCKENBERGER; MALIK; NGAMSKULRUNGROJ; TRILLES *et al.*, 2010), fígado (NARA; SANO; OJIMA; ONAYA *et al.*, 2008), supra-renais (MATSUDA; KAWATE; OKISHIGE; ABE *et al.*, 2011) e principalmente o cérebro (CHRÉTIEN; LORTHOLARY; KANSAU; NEUVILLE *et al.*, 2002).

Conhecidamente, *C. neoformans* e *C. gattii*, são capazes de ultrapassar a barreira hematoencefálica se disseminando para o parênquima cerebral, o que ocasiona o quadro da meningoencefalite, principal manifestação clínica característica da infecção e responsável por morte na maioria dos casos. O mecanismo pelo qual o fungo executa esse deslocamento é explicado por três hipóteses bastante discutidas. O primeiro mecanismo é o de paracitose, no qual a célula fúngica ultrapassa a barreira hematoencefálica permeando entre as junções das células endoteliais, usando proteases como Mpr1, que permitem essa migração transendotelial (VU; THAM; UHRIG; THOMPSON *et al.*, 2014). O segundo mecanismo se configura como "cavalo de Tróia", abordagem na qual as células fúngicas ganham acesso ao cérebro por meio do transporte em células fagocíticas, sugerindo que a invasão do cérebro seja célula-associado (CHARLIER; NIELSEN; DAOU; BRIGITTE *et al.*, 2009; CHRÉTIEN; LORTHOLARY; KANSAU; NEUVILLE *et al.*, 2002; IYER; REVIE; FU; ROBBINS *et al.*, 2021). O terceiro mecanismo é o de transcitose, no qual a célula fúngica é capaz de cruzar a barreira endotelial por si mesmo, atravessando o citoplasma da célula endotelial atingindo subsequentemente o parênquima cerebral (CHANG; STINS; MCCAFFERY; MILLER *et al.*, 2004).

Assim, pacientes com meningite criptococócica (MC) apresentam sintomas predominantemente neurológicos, mais tipicamente cefaleia e estado mental alterado, bem como febre, náuseas e vômitos. A duração média desde o início dos sintomas até a manifestação clínica é de duas semanas em pacientes com AIDS e 6-12 semanas em pacientes HIV negativos. Muitos pacientes desenvolvem alterações oftalmológicas, como diplopia e, posteriormente, secundária à alta pressão do líquido céfalo-raquidiano ou envolvimento do nervo e trato óptico, ocorre redução da acuidade visual (MOODLEY; RAE; BHIGJEE; CONNOLLY *et al.*, 2012). Sem tratamento, a doença progride e os sintomas se estendem a confusão mental, convulsões, nível reduzido de consciência e eventualmente coma e morte (WILLIAMSON; JARVIS; PANACKAL; FISHER *et al.*, 2017).

De acordo com estimativas recentes a Criptococose é responsável por 19% da mortalidade global relacionada a AIDS (RAJASINGHAM; GOVENDER; JORDAN; LOYSE *et al.*, 2022). Anualmente, estima-se que ocorram 179.000 casos de antigenemia criptococcocica positiva (AgCr +) globalmente em indivíduos HIV+ (RAJASINGHAM; GOVENDER; JORDAN; LOYSE *et al.*, 2022). Desses, 152.000 evoluem para meningite resultando em 112.000 mortes/ano, sendo a causa mais comum de meningite em adultos que vivem com HIV na África Subsaariana (RAJASINGHAM; GOVENDER; JORDAN; LOYSE *et al.*, 2022). Na América Latina estima-se que ocorram 14.000 casos/ano de AgCr+ em HIV+ e 12.000 casos/ano de meningite criptococócica, resultando em 7.000 mortes (RAJASINGHAM; GOVENDER; JORDAN; LOYSE *et al.*, 2022). De acordo com dados de 2017, Brasil e Colômbia foram os países que apresentaram maior incidência de Criptococose na América Latina, seguidos por Argentina e México (RAJASINGHAM; SMITH; PARK; JARVIS *et al.*, 2017). Atualmente, no Brasil, a prevalência estimada de AgCr+ varia entre 2 – 4% em indivíduos HIV+ (RAJASINGHAM; GOVENDER; JORDAN; LOYSE *et al.*, 2022). Além disso, estudo recente no estado de Minas Gerais encontrou uma mortalidade de 30% devido à criptococose em HIV+ (LIMA *et al*, 2019).

3.2 Tratamento

As estratégias terapêuticas da criptococose estão diretamente relacionadas ao local da infecção no hospedeiro, ao estado imunológico e a severidade dos sintomas (COELHO; CASADEVALL, 2016; PERFECT; DISMUKES; DROMER; GOLDMAN *et al.*, 2010). Os antifúngicos normalmente utilizados, incluem a Anfotericina B, 5-flucitosina ou Fluconazol (COELHO; CASADEVALL, 2016; NOONEY; MATTHEWS; BURNIE, 2005). No entanto, as opções de tratamento são restritas e esse cenário é agravado pelo aumento da resistência microbiana. Além disso, o desenvolvimento de novos antifúngicos é um grande desafio. Tanto os humanos quanto os fungos são eucariotos e, apesar de uma infinidade de alvos potenciais, é necessário haver seletividade e poucas ou nenhuma interação complicadora com as proteínas do hospedeiro e a maquinaria celular.

A anfotericina B pertence à classe dos polienos e vem sendo utilizada no tratamento da Criptococose desde o final da década de 1960 (IYER; REVIE; FU; ROBBINS *et al.*, 2021; KWON-CHUNG; FRASER; DOERING; WANG *et al.*, 2014). Esse

polieno possui um espectro de ação amplo e atua na membrana plasmática se ligando ao ergosterol e formando poros. A formação desses poros leva a um aumento na permeabilidade de cátions do meio extracelular, resultando na morte fúngica (CANNON; LAMPING; HOLMES; NIIMI *et al.*, 2009; IYER; REVIE; FU; ROBBINS *et al.*, 2021; NETT; ANDES, 2016). Além disso, outros mecanismos de ação já foram descritos para a anfotericina B, a droga pode sofrer auto-oxidação e promover o aumento de radicais livres como espécies reativas de oxigênio e de nitrogênio. O acúmulo desses radicais livres ocasiona um estresse oxidativo e nitrosativo culminando a mais danos na célula fúngica (FERREIRA; BALTAZAR; SANTOS; MONTEIRO *et al.*, 2013). Apesar do alto espectro de ação e boa eficácia terapêutica, a anfotericina B está associada a danos hepáticos e renais o que muitas vezes limitam a sua utilização (NETT; ANDES, 2016). No entanto, para pacientes com histórico de doença renal ou hepática, normalmente é indicado a utilização de formulações lipídicas por apresentarem toxicidade reduzida (NETT; ANDES, 2016). A resistência de *Cryptococcus* spp. a anfotericina B ocorre raramente, mas quando ocorre, pode ser devida à redução dos níveis de ergosterol na membrana plasmática (CANNON; LAMPING; HOLMES; NIIMI *et al.*, 2009; SANTOS; GOUVEIA; TAYLOR; RESENDE-STOIANOFF *et al.*, 2012) ou uma mudança desse alvo lipídico, o que determina a diminuição da ligação da anfotericina B na célula fúngica (ELLIS, 2002). Dessa forma, algumas células contendo mutação na via de síntese de ergosterol (mutação no gene *ERG3* e *ERG11*, por exemplo) não produzem ergosterol, mas sim, compostos semelhantes a esse lipídeo que tem menor afinidade pela ligação com AMB (AKINS, 2005) (GEBER *et al.*, 1995; ELLIS, 2002; AKINS, 2005).

O fluconazol (FCZ), outra droga utilizada no tratamento da criptococose, pertence à classe dos triazólicos, atuando como substância fungistática na célula criptocócica. O seu mecanismo de ação envolve a redução da biossíntese de ergostrol por inativação da enzima lanosterol 14-α-demetilase impedindo a conversão do lanosterol em ergosterol (AKINS, 2005; LUPETTI; DANESI; CAMPA; DEL TACCA *et al.*, 2002; ZAVREL; WHITE, 2015). A redução da síntese de ergosterol causa instabilidade na membrana plasmática e altera a permeabilidade da célula fúngica, resultando na interrupção do crescimento (CASALINUOVO; DI FRANCESCO; GARACI, 2004; GHANNOUM; RICE, 1999). No entanto, por se tratar de uma droga

fungistática, a mesma torna a célula fúngica mais susceptível a ação do sistema imunológico. Outros azólicos, como posaconazol, voriconazol e itraconazol podem ser utilizados como terapia alternativa no tratamento da criptococose quando o fluconazol não se encontra disponível ou não é indicado (PERFECT; DISMUKES; DROMER; GOLDMAN *et al.*, 2010), porém o uso do itraconazol não é recomendado para os casos de neurocritpococose, por apresentar baixa permeabilidade no SNC (SUBRAMANIAN; MATHAI, 2005). A resistência aos azólicos tem sido a classe de antifúngicos mais reportada em casos de resistência clínica e laboratorial. Os mecanismos normalmente envolvidos nesse processo são: (i) aumento da expressão e mutação do gene *ERG11*, (ii) diminuição da atividade de ERG3p e outras enzimas da via de síntese do ergosterol e (iii) superexpressão de bombas de efluxo (CANNON; LAMPING; HOLMES; NIIMI *et al.*, 2009; FISHER; ALASTRUEY-IZQUIERDO; BERMAN; BICANIC *et al.*, 2022; ZAVREL; WHITE, 2015)

A heteroressistência é um fenômeno reversível, em que uma subpopulação microbiana consegue crescer na presença de concentrações mais altas de um antimicrobiano(FERREIRA; SANTOS, 2017). Considerando que esse evento é praticamente intrínseco em *C. neoformans* durante a exposição ao fluconazol, o uso de estratégias terapêuticas combinadas com foco na redução da heteroresistência é um caminho promissor no tratamento da Criptococose. Nessa premissa, Stone e colaboradores (2019) avaliaram o papel da heterorresistência ao fluconazol na criptococose humana em um estudo observacional prospectivo. Nesse estudo, pacientes HIV+ receberam monoterapia com fluconazol ou em combinação com 5-flucitosina (5FC). A heteroresistência ao fluconazol foi detectada em todos os isolados de *C. neoformans* durante o diagnóstico de meningite criptococcica e aumentou após duas semanas de monoterapia com o fluconazol (STONE; RHODES; FISHER; MFINANGA *et al.*, 2019). Interessantemente, na terapia combinada (fluconazol + 5-Fluocitosina) nenhuma população heteroresistente foi encontrada no líquor após 14 dias de tratamento (STONE; RHODES; FISHER; MFINANGA *et al.*, 2019). Esse achado reforça a noção de que, embora o arsenal de antifúngicos para a Criptococose seja limitado, é possível reformular os esquemas terapêuticos atualmente existentes de forma a se obter um melhor prognóstico clínico.

A 5-Flucitosina (5-FLU) é um análogo da pirimidina que atua interferindo na

síntese de ácidos nucléicos e consequentemente na síntese proteica (BENNETT; DISMUKES; DUMA; MEDOFF *et al.*, 1979). No entanto, apesar de apresentar bom efeito terapêutico quando associada a Anfotericina B ou Fluconazol, a sua utilização apresenta algumas limitações, por necessitar de uma vigilância farmacológica rigorosa devido a sua alta toxicidade para a medula óssea e fígado (PERFECT; BICANIC, 2015). Além disso, o seu uso como monoterapia não é recomendado devido a seleção de populações resistentes, algo que pode ocorrer em 1 a cada 10^6 – 10^7 células. A resistência a essa droga está principalmente relacionada a mutações na via da pirimidina (AKINS, 2005). Ainda, é importante considerar, que a mesma não se encontra disponível no Brasil.

3.3 Reposicionamento de fármacos

A busca por novas drogas antifúngicas e que apresentem alvos mais seletivos é extremamente importante frente ao arsenal limitado de antifúngicos, a alta toxicidade associada a esses fármacos e a resistência microbiana. Alguns estudos vêm sendo desenvolvidos buscando novos alvos na célula fúngica; como na síntese de glicosilceramida, função mitocondrial e transporte de vesículas (PERFECT, 2017). No entanto, apesar de algumas drogas já estarem em fase clínica de avaliação, os investimentos direcionados para o estudo de infecções fúngicas é reduzido, o que muitas vezes impede o início ou a continuidade de pesquisas voltados para essa vertente (RODRIGUES, 2016). Como alternativa para acelerar esse processo, o reposicionamento de fármacos vem sendo utilizado no campo da micologia.

O reposicionamento de fármacos consiste em uma nova abordagem para o tratamento de diversas infecções (CHEN e DU, 2007; PALOMINO e MARTIN, 2013). Essa estratégia caracteriza-se pela utilização de medicamentos já estabelecidos para o tratamento de novas doenças. Como a farmacologia e toxicologia já são conhecidas, uma droga já estabelecida com uma nova indicação útil pode ser rapidamente implementada para a utilização clínica (CHEN e DU, 2007; PALOMINO e MARTIN, 2013; DELATTIN et al., 2014). São vários os exemplos de medicamentos que já foram descritos para uma função diferente da original (CAVALLA 2013; CASSETA 2014). A finasterida, aprovada inicialmente para tratamentos de hiperplasia prostática, é utilizada no tratamento da queda de cabelo; alopurinol é indicado como antineoplásico, mas foi reposicionado para o tratamento de gota. (ESPOSITO, 2002).

Sildenafil (comercialmente conhecido como Viagra) formulado para o tratamento de hipertensão pulmonar cardíaca foi reposicionado, e agora é prescrito para o tratamento de disfunção eréctil (BOOLELL et al., 1996); e finalmente a anfotericina B, aprovada inicialmente antifúngico e agora é utilizada para o tratamento da Leishmaniose visceral. (SINGHAL et al., 1999).

No contexto da criptococose, o reposicionamento de fármacos pode ser utilizado como agente único ou adjuvante ao tratamento antifúngico padrão (CHEN e DU, 2007; DELATTIN et al., 2014). A combinação de drogas pode exigir doses mais baixas dos agentes antimicrobianos, assim, diminuindo a toxicidade e aumentando a tolerância do hospedeiro ao antimicrobiano (SANTOS et al., 2012). Na literatura já existem alguns relatos de drogas que foram reposicionadas para a criptococose. Blankenship et al, 2003, demonstrou que um inibidor de calcineurina possui atividade antifúngica e sinérgica com fluconazol. Amiodarona, uma droga antiarrítmica, apresentou atividade antifúngica contra *Cryptococcus*, *Aspergillus* e *Candida* (COURCHESNE, 2002). O febendazol, um anti-helmíntico pertencente a classe dos benzimidazóis, também foi capaz de inibir o crescimento de *Cryptococcus in vitro*, fatores de virulência e a capacidade de proliferação no interior de macrófagos. Consequentemente, esses efeitos resultaram em uma maior sobrevida durante o tratamento em modelo murino de Criptococose (DE OLIVEIRA; JOFFE; SIMON; CASTELLI *et al.*, 2020).

Algumas drogas embora não apresentem ação antifúngica, podem alterar a morfofisiologia fúngica, modular a resposta imune do hospedeiro ou reduzir a toxicidade antimicrobiana e atuar de maneira adjuvante a terapia antifúngica padrão. É o caso da atorvastatina e pioglitazona que foram capazes de aumentar a sobrevida em modelo murino de criptococose quando combinadas ao fluconazol e a anfotericinia B, respectivamente (RIBEIRO; COSTA; MAGALHÃES; CARNEIRO *et al.*, 2017). A combinação Atorvastatina + Fluconazol levou a redução do conteúdo de ergosterol fúngico, alteração da cápsula polissacarídica, maior produção de espécies reativas de oxigênio por macrófagos e redução da proliferação intracelular. Enquanto para a pioglitazona, o seu efeito adjuvante foi associado a redução da toxidade causada pela Anfotericina B. Atualmente, um ensaio clínico com a pioglitazona combinada a AMB está sendo desenvolvido em um Hospital de Belo

Horizonte - MG, referência no diagnóstico e tratamento da Criptococose na região(GOUVEIA-EUFRASIO; RIBEIRO; SANTOS; DA COSTA *et al.*, 2021). Não obstante, outros estudos também já demonstraram o efeito adjuvante da sertralina e do tamoxifeno no tratamento da criptococose (DOLAN; MONTGOMERY; BUCHHEIT; DIDONE *et al.*, 2009; PERFECT, 2017; ZHAI; WU; WANG; SACHS *et al.*, 2012).

Apesar dos esforços para o desenvolvimento de novos antifúngicos e para o reposicionamento de fármacos, a avaliação de melhores estratégias para o uso dos antifúngicos já existentes também é importante. Nesse sentido, Santos e colaboradores (2107) avaliaram em modelo murino de criptococose o efeito da combinação entre fluconazol e anfotericina B. Os autores observaram que uma dose maior de fluconazol combinada a anfotericina B é mais eficiente no tratamento da criptococose murina do que quando usado em monoterapia (SANTOS; RIBEIRO; BASTOS; HOLANDA *et al.*, 2017). Além disso, formulações lipídicas da anfotericina B também tem sido desenvolvidas na tentativa de reduzir a sua toxicidade. Estudo de fase II, por exemplo, demonstrou que uma dose única de Anfotericina B lipossômica apresenta eficácia equivalente ao tratamento de 7 dias com a anfotericina B convencional (JARVIS; LEEME; MOLEFI; CHOFLE *et al.*, 2019). Uma formulação oral de Anfotercina B lipossomal também tem sido estudada, o que poderia reduzir os custos envolvidas na administração intravenosa (LU; HOLLINGSWORTH; QIU; WANG *et al.*, 2019). Entretanto, apesar dos avanços, o uso de formulações lipossomais tem sido limitado devido ao elevado custo.

4. OBJETIVOS

4.1 Objetivo geral

Avaliar a dinâmica do remodelamento celular de *Cryptococcus* spp*. in vivo* e o reposicionamento de antimaláricos e hormônios sexuais para o tratamento da criptococose.

4.2 Objetivos específicos

4.2.1 Capítulo 1

✓ **Estratégias *in vivo***

- Avaliar a dinâmica das alterações morfológica de *C. neoformans* e *C. gattii* em diferentes tempos de infecção no espaço broncoalveolar e epitélio pulmonar.
- Realizar o transcriptoma do lavado broncoalveolar de camundongos infectados com *C. neoformans*.

Estratégias *in sílico*

- Analisar os dados de transcriptoma do lavado broncoalveolar de camundongos infectados com *C. neoformans* - H99.

4.2.2 Capítulo 2

Realizar um comentário sobre o trabalho intitulado "*Cryptococcus gattii* evades CD11b-mediated fungal recognition by coating itself with capsular polysaccharides".

4.2.3 Capítulo 3

✓ **Estratégias *in vitro***

- Determinar a atividade antifúngica de antimaláricos para diferentes linhagens de *C. neoformans* e *C. gattii*.

- Determinar a concentração inibitória fracional (CIF) dos antimaláricos estabelecidos em combinação com o fluconazol e anfotericina B.
- Avaliar diferentes parâmetros em *C. neoformans* e *C. gattii* após exposição aos antimaláricos:
    - Resposta frente a estresse osmótico, estresse de membrana, parede celular e reticulo endoplasmático;
    - Espécies reativas de oxigênio e nitrogênio.
    - Ergosterol;
    - Atividade de lacase;
    - Fenótipo de melanização
    - Síntese de cápsula polissacarídica
- Realizar análise químico-genética dos antimaláricos frente a coleções de mutantes *C. neoformans* deletados para diferentes genes não essenciais.

✓ **Estratégias *Ex vivo***

- Avaliar a toxicidade da combinação entre os antimaláricos e antifúngicos frente a macrófagos murinos derivados de medula.

✓ **Estratégias *in vivo***

- Avaliar a influência do tratamento com antimaláricos isolados e combinados a anfotericina na sobrevida, em modelo murino de criptococose.
- Avaliar a carga fúngica no pulmão, lavado broncoalveolar, e cérebro após infecção e tratamento com os antimaláricos isolados e combinados a anfotericina.

✓ **Estratégias *in sílico***

- Analisar os dados da triagem químico-genética dos antimaláricos frente a coleções de mutantes *C. neoformans* deletados para diferentes genes não essenciais.

4.2.4 Capítulo 4

✓ **Estratégias *in vitro***

- Determinar a atividade antifúngica de estradiol e testosterona para diferentes linhagens de *C. neoformans* e *C. gattii*.
- Determinar a concentração inibitória fracional (CIF) de estradiol e testosterona em combinação com o fluconazol e anfotericina B.
- Avaliar a capacidade de estradiol e testosterona induzir estresse oxidativo e nitrosativo em *Crypococcus* spp.

5. RESULTADOS

Os resultados desta tese serão apresentados em 4 capítulos, conforme listados a seguir.

Capítulo 1: The dynamics of *Cryptococcus neoformans* cell and transcriptional remodeling during infection.

Nesse capitulo apresentamos a dinâmica das alterações morfológicas e transcricionais de *C. neoformans* em tempos precoces e tardios da infecção. Vimos que a indução de células pequenas e o aumento da regulação ribossomal foi importante para adaptação inicial ao espaço broncoalveolar, invasão do epitélio pulmonar e escape dos pulmões para o sistema nervoso central. Tardiamente, o aumento da capsula polissacarídica e da regulação do metabolismo de inositol foram determinantes para a virulência. Em continuidade ao capítulo e de maneira complementar ao estudo de *C. neoformans,* também apresentamos a dinâmica do remodelamento celular para *C. gattii* nos diferentes estágios da infecção. Nesse contexto, vimos que as alterações morfológicas no início da infecção se assemelham aos achados de *C. neoformans*. Porém, o aumento da cápsula polissacarídica ao longo da infecção não foi suficiente para predizer a virulência de *C. gattii*, como visto para *C. neoformans*.

Capítulo 2: Polysaccharide capsule: An insight on fungal-host interactions and vaccine studies.

Baseados na compreensão preliminar sobre o remodelamento celular de *Cryptococcus* spp. durante a infecção, publicamos um comentário sobre o trabalho intitulado "*Cryptococcus gattii* evades CD11b-mediated fungal recognition by coating itself with capsular polysaccharides". Aqui, destacamos a importância de compreender o papel do polissacarídeo capsular (PC) de *C. gattii* no reconhecimento de *Cryptococcus* spp. por CD11b e como esse conhecimento pode influenciar nas estratégias para o desenvolvimento de novas vacinas contra a criptococose. Posteriormente, apresentamos um cenário geral sobre a criptococose, abordando desde a compreensão da biologia fúngica e sua interação no ambiente até as limitações terapêuticas e vacinais atualmente existentes.

Capítulo 3: Antimalarials and amphotericin B interact synergistically and are new options to treat cryptococcosis.

Na premissa de busca por novas estratégias terapêuticas, nesse capítulo abordamos o reposicionamento de antimaláricos no contexto da criptococose. Demonstramos que a combinação entre antimaláricos e anfotericina B resultou em uma interação sinérgica e aumento da sobrevida em modelo murino. Considerando a elevada toxidade e custo da AMB, acreditamos que, futuramente, esses achados podem oferecer um avanço importante no tratamento da Criptococose.

Capítulo 4: Testosterona e Estradiol apresentam sinergismo com anfotericina B contra *Cryptococcus* spp.

Aqui, abordamos o papel de hormônios sexuais na ação de antifúngicos normalmente utilizados na criptococose. Interessantemente, vimos que o estradiol e a testosterona apresentam sinergismo com anfotericina B, sendo capazes de reduzir a concentração mínima necessária para a ação fungicida desse antifúngico. Para o fluconazol a interação foi indiferente. Esses achados reforçam a possibilidade de otimizar os tratamentos atualmente existentes e tornar mais rápida a disponibilização de novas estratégias terapêuticas contra a criptococose.

CAPÍTULO 1
The dynamics of *Cryptococcus neoformans* cell and transcriptional remodeling during infection

Gustavo J. C. Freitas; Ludmila Gouveia-Eufrasio; Eluzia C.P. Emidio; Hellem C. S. Carneiro, Ludmila de M. Baltazar, Marliete C. Costa; Susana Frases, Glauber R. de Sousa Araújo, Tatiane A. Paixão, Brunno G. Sossai, Melissa Caza, James W. Kronstad, Nalu T. A. Peres, Daniel A. Santos.

ABSTRACT

The phenotypic plasticity of *Cryptococcus neoformans* is widely studied and demonstrated *in vitro*, but its influence on pathogenicity remains unclear. In this study we investigated the dynamics of cryptococcal cell and transcriptional remodeling during pulmonary infection in a murine model. We showed that in *Cryptococcus neoformans*, cell size reduction (cell body ≤ 3μm) is important for initial adaptation during infection. This change was associated with reproductive fitness and tissue invasion. Subsequently, the fungus develops mechanisms aimed at resistance to the host's immune response, which is determinant for virulence. We investigated the transcriptional changes involved in this cellular remodeling and found an up-regulation of transcripts related to ribosome biogenesis at the beginning (6 hours) of infection and a later (10 days) up-regulation of transcripts involved in the inositol pathway, energy production and the proteasome. Consistent with a role for the proteasome, we found that its inhibition delayed cell remodeling during infection with the H99 strain. Altogether, these results further our understanding of the infection biology of *C. neoformans* and provide perspectives to support therapeutic and diagnostic targets for cryptococcosis

Keywords: Cell size, ribosome biogenesis, inositol pathway, proteasome, cell remodeling; cryptococcosis.

cells

MDPI

Article

The Dynamics of *Cryptococcus neoformans* Cell and Transcriptional Remodeling during Infection

Gustavo J. C. Freitas [1], Ludmila Gouveia-Eufrasio [1], Eluzia C. P. Emidio [1], Hellem C. S. Carneiro [1], Ludmila de Matos Baltazar [2], Marliete C. Costa [1], Susana Frases [3], Glauber R. de Sousa Araújo [3], Tatiane A. Paixão [4], Brunno G. Sossai [4], Melissa Caza [5], James W. Kronstad [5], Nalu T. A. Peres [1] and Daniel A. Santos [1,*]

1 Laboratório de Micologia, Departamento de Microbiologia, Universidade Federal de Minas Gerais, Belo Horizonte 31270-901, Brazil
2 Instituto de Patologia Tropical e Saúde Pública, Universidade Federal de Goiás, Goiânia 74605-020, Brazil
3 Laboratório de Ultraestrutura Celular Hertha Meyer, Instituto de Biofísica Carlos Chagas Filho, Universidade Federal do Rio de Janeiro, Rio de Janeiro 21941-902, Brazil
4 Laboratório de Patologia Celular e Molecular, Departamento de Patologia, Universidade Federal de Minas Gerais, Belo Horizonte 31270-901, Brazil
5 Michael Smith Labs, University of British Columbia, Vancouver, V6T 1Z4, Canada
* Correspondence: dasufmg@gmail.com

Abstract: The phenotypic plasticity of *Cryptococcus neoformans* is widely studied and demonstrated in vitro, but its influence on pathogenicity remains unclear. In this study, we investigated the dynamics of cryptococcal cell and transcriptional remodeling during pulmonary infection in a murine model. We showed that in *Cryptococcus neoformans*, cell size reduction (cell body ≤ 3 µm) is important for initial adaptation during infection. This change was associated with reproductive fitness and tissue invasion. Subsequently, the fungus develops mechanisms aimed at resistance to the host's immune response, which is determinant for virulence. We investigated the transcriptional changes involved in this cellular remodeling and found an upregulation of transcripts related to ribosome biogenesis at the beginning (6 h) of infection and a later (10 days) upregulation of transcripts involved in the inositol pathway, energy production, and the proteasome. Consistent with a role for the proteasome, we found that its inhibition delayed cell remodeling during infection with the H99 strain. Altogether, these results further our understanding of the infection biology of *C. neoformans* and provide perspectives to support therapeutic and diagnostic targets for cryptococcosis.

Keywords: cell size; ribosome biogenesis; inositol pathway; proteasome; cell remodeling; cryptococcosis

check for updates

Citation: Freitas, G.J.C.; Gouveia-Eufrasio, L.; Emidio, E.C.P.; Carneiro, H.C.S.; de Matos Baltazar, L.; Costa, M.C.; Frases, S.; de Sousa Araújo, G.R.; Paixão, T.A.; Sossai, B.G.; et al. The Dynamics of *Cryptococcus neoformans* Cell and Transcriptional Remodeling during Infection. *Cells* **2022**, *11*, 3896. https://doi.org/10.3390/cells11233896

Academic Editor: Suleyman I. Allakhverdiev

Received: 21 October 2022
Accepted: 29 November 2022
Published: 2 December 2022

1. Introduction

Cryptococcus neoformans is the leading agent of cryptococcosis, an invasive fungal infection that occurs by inhaling desiccated yeasts or basidiospores dispersed in the environment [1,2]. The yeast initially settles in the lung, causing pneumonia, and then spreads to other organs, such as the central nervous system (CNS), leading to cryptococcal meningitis, the most severe form of the disease [2]. Cryptococcosis is responsible for 152,000 new cases of meningitis annually, resulting in 112,000 deaths [3].

The cells of *Cryptococcus* spp. switch morphology in response to environmental conditions, a plasticity that may enhance survival. Several morphotypes have been described, such as hyphae, pseudohyphae, seed cells, microcells (<2 µm), typical yeast cells (6–8 µm), and titan cells (>10 µm) [4–7]. Desiccated yeast cells or spores are thought to be the morphological types that are inhaled to initiate infection [8]. Cells of *Cryptococcus* spp. are generally found in the yeast phase inside the host, presenting as small cells, typical cells, and titan cells. In this context, titan cells are often associated with higher virulence [9–11]. However, titan cells are a minority of cryptococcal cells and are rarely observed outside

of the lungs. Considering that most studies are focused on morphological assessment at late stages of infection, little is known about the kinetics of in vivo morphological transitions at the beginning of infection and how this may be determinant for fungal survival and disease progression. The size and morphology can affect the virulence of pathogenic microorganisms. For example, the reduction in bacterial size allows evasion of the immune response by *Streptococcus pneumoniae* [12]. In *Candida albicans*, hyphae are essential for tissue invasion, and yeast cells are crucial for hematogenous and lymphatic dissemination [13,14]. More recently, the seed cells of *C. neoformans* have been shown to be better at spreading into extrapulmonary tissues and in surviving intracellularly [6,15]. However, further studies on the morphophysiological adaptation of *C. neoformans* in the bronchoalveolar space and in the pulmonary epithelium are still needed.

The polysaccharide capsule is considered the main virulence factor of the *Cryptococcus* genus [16]. In the environment, it confers resistance to desiccation and phagocytosis by free-living amoebae, while in the host, it has antioxidant and antiphagocytic roles in addition to the modulating of the host's immune response [17]. Melanin, another determining factor of virulence, is associated with resistance to UV radiation and oxidative stress and has antiphagocytic properties [18]. The synthesis of the polysaccharide capsule and melanin may vary according to the culture condition, the time of infection, and the anatomical site where the yeast is found [19–23]. Usually, studies evaluate these virulence factors using different in vitro/ex vivo culture conditions or infection models [6,24,25] that do not reproduce the natural route of infection (lung–blood–brain). Thus, it is necessary to establish whether the in vitro/ex vivo phenotypes are observed in vivo, and how they impact fungal virulence and the course of the infection. For instance, the VGI genotype has been associated with a thicker polysaccharide capsule in vitro. However, this is not the only parameter that impacts virulence, since strains of the same genotype may have different virulence profiles [22,26].

In this study, we observed the morphological, physiological, and transcriptional reorganization of *C. neoformans* in the bronchoalveolar space and pulmonary epithelium throughout the infection, which we call cellular and transcriptional remodeling. We demonstrate that this is a dynamic process during infection and promotes different levels of virulence. An analysis of fungal and host transcriptomes during infection revealed that fungal transcriptional response is initially focused on strategies to adapt and reproduce during host colonization. Subsequently, transcriptional patterns reflected cellular mechanisms focusing on resistance to the immune response and fungal virulence. The murine transcriptional response was consistent with phagocytosis and an inflammatory response. We also identified transcriptional profiles in the early and late stages of infection in fungi and mice.

2. Materials and Methods

2.1. Fungal Strains and Media

Five strains of *C. neoformans* were used, including the reference strain H99 from the Duke University Medical Center, North Carolina (United States), and four strains representing other genotypes/serotypes (WM 626, WM 628, WM 629, and WM 148) (Table 1). All strains were maintained at −80 °C and were cultured on Yeast Extract Peptone Dextrose (YPD—2% glucose, 2% peptone, and 1% yeast extract) or M = minimal medium (MM—15 mM glucose, 10 mM $MgSO_4 \cdot 7H_2O$, 29.4 mM KH_2PO_4, 13 mM glycine, and 3 mM thiamine-HCl, pH 5.5) for 48 h/72 h (exponential phase) at 37 °C for each experiment.

Table 1. *C. neoformans* strains used in this study (American Type Culture Collection).

Strain	Genotype/Serotype	Isolation Source	Origin
WM 148 (ATCC® MYA-4564™)	VNI A	CSF	Clinical–Australia
WM 626 (ATCC® MYA-4565™)	VNII A	CSF	Clinical–Australia
WM 628 (ATCC® MYA-4566™)	VNIII AD	CSF	Clinical–Australia
WM 629 (ATCC® MYA-4567™)	VNIV D	Blood	Clinical–Australia
H99 (ATCC® 208821™)	VNI–A	CSF	Clinical–North Carolina-USA

CSF: cerebrospinal fluid.

2.2. Phenotypic Characterization In Vitro

Growth curves, pigmentation, morphology, laccase, and urease activity were analyzed for each strain. Initially, to validate the growth analysis in the spectrophotometer, we compared the OD600 data with the plating in culture medium for the H99 strain. We observed that the OD600 results reproduced the profile observed when CFU was determined (data not shown). Thus, for experimental optimization, we used the OD600 analysis for the growth curve of the other strains. For this, 5×10^5 cells/mL of each strain were dispensed into a 96-well plate with liquid YPD or MM and incubated for 72 h in a spectrophotometer (OD 600 nm) at 37 °C. For each strain, eight replicates were performed. The area under the curve (AUC) was used to compare the groups. Melanin production was visually determined by growing the strains in solid MM supplemented with 1 mM L-3,4-dihydroxphenylalanine L-DOPA (Sigma-Aldrich, Burlington, MA, USA) and incubation for five days at 37 °C. Laccase and urease activity were quantified as previously described [27–30].

For the morphometric analysis, the strains were cultivated in YPD and MM broth for 72 h at 37 °C. After incubation, yeasts were suspended on a slide with India ink, followed by visualization under an optical microscope and image capture. Cell body and capsule sizes of at least 100 specimens from each condition were measured using the Image J program (http://rsb.info.nih.gov/ij/ (accessed on 4 September 2020); National Institutes of Health, NIH, Bethesda, MD, USA) (Araujo et al., 2012). Cell body diameter was defined as the diameter without the capsule. Capsule size was calculated by the ratio of capsule thickness to cell body radius. The total cell size was defined as the diameter of the cell body, including the capsule. In addition, the surface/volume ratio was determined using the formula 3/r, where r = radius [21]. All phenotypic assays were performed in triplicate.

2.3. Mice Experimentation

2.3.1. Ethics Statement

This work was approved (protocol 235/2017) by the Ethics Committee in the Use of Animals (CEUA) from Universidade Federal de Minas Gerais. We followed the Brazilian Society of Zootechnics/Brazilian College of Animal Experimentation guidelines (available online http://www.cobea.org.br/ (accessed on 10 January 2019)) and Federal Law 11,794. Water and food were provided ad libitum and light/dark cycles were maintained. All efforts to minimize the suffering of the animals were carried out.

2.3.2. Mice Survival and Behavior

The inoculum of 1×10^5 CFU/30 μL of each strain was used to infect C57/BL6 male mice. Inoculum preparation was based on the Neubauer chamber count of viable cells stained with Trypan Blue. Animals were infected intratracheally under anesthesia with ketamine (100 mg/kg) and xylazine (16 mg/kg) [31,32]. Animals were monitored daily for survival analysis and behavior assessment using the SmithKline/Harwell/ImperialCollege/Royal Hospital/PhenotypeAssessment (SHIRPA) protocol. This protocol provides reliable information about murine brain dysfunction and its general status. The individual parameters evaluated were grouped into five functional categories: neuropsychiatric status, motor be-

havior, autonomic function, muscle tone and strength, and reflex and sensory function. The score for each category was calculated as previously described [32]. Table S3 describes the parameters analyzed.

According to the mean lethality time (MLt), the strains were classified as hypervirulent (MLt = 21–25 days), virulent (MLt = 26–31 days), hypovirulent (MLt = 32–40 days), and non-lethal (MLt > 100 days).

2.3.3. Fungal Burden

After analysis of survival and behavior, another group of mice was anesthetized and infected intratracheally to assess fungal burden in the bronchoalveolar space (BS), the pulmonary epithelium (PE), and the brain after 10 days of infection. Animals were euthanized under anesthesia, and the organs and bronchoalveolar lavage fluid (BALF) were aseptically removed to quantify the fungal burden in the BS. BALF was isolated by inserting a catheter in the trachea of terminally anesthetized mice, through which 1 mL PBS solution was instilled into the bronchioles. The fluid was gently retracted to maximize BAL fluid retrieval. Lungs and brains were weighed and ground in Petri dishes with 1 mL sterile PBS. Then, the suspensions were cultivated on YPD agar for 48 h at 37 °C. Colonies were counted and the results were expressed in CFU/g or CFU/mL.

2.3.4. Macrophage Assays

Bone-marrow-derived macrophages (BMDM) were used to evaluate the susceptibility of *C. neoformans* strains to the fungicidal activity of macrophages. Briefly, bone marrow cells were harvested from the tibias and femurs of C57BL/6 male mice. Then, cells were cultured in BMDM differentiation medium (RPMI (Gibco, Thermo Fisher Scientific, Waltham, MA, USA) supplemented with 30% L929 growth-conditioning media, 20% fetal bovine serum (Gibco), 2 mM glutamine (Sigma-Aldrich, Burlington, MA, USA), 100 units/mL of penicillin-streptomycin (Gibco, Thermo Fisher Scientific, Waltham, MA, USA), 50 μM of 2-mercaptoethanol (Gibco, Thermo Fisher Scientific, Waltham, MA, USA)) for 1 week at 37 °C/5% CO_2 (25). Aderant cells differentiated into macrophages were resuspended and transferred to a sterile polypropylene tube. BMDMs were centrifuged at 200× *g*/5 min at 4 °C and resuspended in 5 mL of RPMI 1640 medium containing 10% BFS, 2 mM glutamine, 25 mM HEPES (Gibco, Thermo Fisher Scientific, Waltham, MA, USA) pH 7.2, 100 units/mL G penicillin, and 5% L929 cell culture supernatant. Cell viability was determined with Trypan Blue (Sigma-Aldrich, Burlington, MA, USA), followed by plating in 24-well plates for phagocytosis percentage (PP) and fungicidal activity (FA) determination, or in 96-well plates for reactive oxygen species (ROS) and peroxynitrite quantification (PRN) [32].

PP and killing assays were determined after 2 and 24 h of BMDM infection. Briefly, for PP analyses, glass slides were placed at the bottom of 24-well plates, and cells were plated and infected in a proportion of 5:1 (yeast:macrophages). After 2 and 24 h of infection, the glass coverslips were removed and stained with Panotico Rapido dye (Laborclin, Pinhais, Parana, Brazil). PP was determined by counting the percentage of BMDM with internalized yeasts under an optical microscope. For the killing assay, supernatants were removed, and non-internalized and non-adherent yeast cells were removed by two washes with PBS. BMDMs were lysed with 200 μL of sterile distilled water for 30 min at 37 °C [32]. Both phagocytosis and killing assays were performed in six replicate techniques, and the data presented represent three independent experiments.

To quantify ROS and PRN, 2,7-dichlorofluorescein diacetate (DCFH-DA; Invitrogen, Thermo Fisher Scientific, Waltham, MA, USA) and dihydrorhodamine 123 (DHR 123; Invitrogen, Thermo Fisher Scientific, Waltham, MA, USA) were used, respectively. After incubation of the dyes with infected BMDMs for 3 and 24 h at 37 °C, the fluorescence was read at excitation wavelengths of 485 nm and emission of 530 nm. Data were expressed as arbitrary fluorescence units (AU) ± SE [32–34] representing the levels of intracellular ROS and PRN of the fungus and macrophage.

2.3.5. Kinetics of *C. neoformans* Morphology In Vivo

After analysis of survival, one strain representing each virulence profile (H99—hypervirulent, WM628—virulent, WM148—hypovirulent, and WM626—non-lethal) was selected for the morphological evaluation of fungal cells at different times of infection (0, 6 h, 24 h, and 240 h). Time 0 represents the yeasts used for infection, previously cultured in YPD. Animals were infected intratracheally and euthanized at the established times. BALF, lungs, and brain were removed, ground, and fixed on a slide with India ink, followed by visualization under an optical microscope and image capture. Cell and capsule sizes of at least 100 yeasts from each condition were measured using the Image J program (http://rsb.info.nih.gov/ij/ (accessed on 4 January 2021); National Institutes of Health, NIH, Bethesda, MD, USA) [17]. In addition, BALF was also used for scanning electron microscopy and RNA analyses.

2.3.6. Scanning Electron Microscopy of BALF

BALF was fixed in 2.5% glutaraldehyde type I, in 0.1 M sodium cacodylate buffer (pH 7.2), for 1 hour at room temperature. After fixation, cells were washed in 0.1 M sodium cacodylate buffer (pH 7.2) containing 0.2 M sucrose and 2 mM $MgCl_2$. Cell surface was observed by scanning electron microscopy (SEM) [35]. Obtained images were colored using Photoshop software.

2.3.7. Kinetics of Fungal Burden in the Brain after Intratracheal Infection

Analysis of fungal burden in the brain after 6 h, 24 h, and 240 h was performed. Animals were infected intratracheally and euthanized at the established times. The tissue was weighed and ground in Petri dishes with 1 mL of sterile PBS. Then, the solution was cultured in YPD agar and incubated for 48 h at 37 °C. Colonies were counted, and results expressed as CFU/g.

2.3.8. Histopathology of Brain

To evaluate the melanin phenotype in the brain, mice were infected by intracranial inoculation. An inoculum of 1×10^2 CFU/5 µL was prepared and counted in a Neubauer chamber with Trypan Blue. Only the strains that did not produce melanin in vitro (WM628 and WM626) were analyzed in this assay, and H99 was used as control. After preparing the inoculum, the animals were anesthetized and immobilized, and intracranial infection was performed with a 30-gauge needle, fixed to an insulin syringe with a cuff to prevent penetration > 1 mm. A midline puncture through the cranial vault was made 6 mm posterior to the orbit, and the inoculum was injected [36]. After 10 days of infection, the animals were euthanized, and their brains removed. The tissue was fixed in formalin, embedded in paraffin, and then subjected to Fontana–Masson (FMS) staining [37]. After microscopic analysis, the presence of melanin was considered as the brown to black color in the yeast.

2.3.9. Dual RNA Sequencing

Sample Preparation

C57BL/6 mice were infected intratracheally with the H99 strain previously grown in YPD to analyze the transcriptome. BALF obtained from 6 mice of each condition was pooled together, generating two replicates at 6 h and 240 h (10 d). BALF was centrifuged at 1200× *g* and resuspended in 1 mL TRIzol Reagent (Invitrogen, Thermo Fisher Scientific, Waltham, MA, USA) for RNA isolation, according to the manufacturer's protocol. RNA from H99 yeasts grown in YPD was used as control.

Library Preparation and Sequencing

RNA quality, library preparation, sequencing reactions, and initial bioinformatics analyses were conducted at GENEWIZ Inc. (South Plainfield, NJ, USA). RNA samples were quantified by fluorometry (Qubit 2.0, Thermo Fisher Scientific, Waltham, MA, USA), and RNA integrity was checked with a 2100 Bioanalyzer (Agilent Technologies, Santa Clara, CA,

USA). Transcriptome sequencing was performed via rRNA depletion using the Illumina HiSeq platform (Illumina, San Diego, CA, USA) in the 2 × 150 bp Paired-End configuration.

Data Analysis

Quality reads were filtered using the FastQC software, and adapters were removed by the Trimmomatic v.0.36 [38]. Trimmed reads were mapped to the *C. neoformans* H99 or the Mus musculus GRCm38 reference genomes, both available on ENSEMBL, using the STAR aligner v.2.5.2b [39]. STAR aligner detects splice junctions, incorporating them to align the entire read sequences and generating the BAM files. Table 3 show the statistics of genome mapping. Unique gene hit counts were calculated using feature Counts from the Subread package v.1.5.2 [40], and unique reads that fell within exon regions were counted. Differentially expressed genes (DEGs) were obtained using a 5% false discovery rate (FDR), using the DESeq2 Bioconducter package [41].

GO Analysis and Regulatory Network Constructions

Fungal DEGs were functionally categorized using Gene Ontology (GO) and KEGG (Kyoto Encyclopedia of Genes and Genomes), using FungiDB ((http://fungidb.org/fungidb/ (accessed on 5 March 2020)) and FungiFun2 (https://elbe.hki-jena.de/fungifun/ (accessed on 5 March 2020)). Mouse DEGs were categorized using the ShinyGO v0.75 database [42]. Highly represented categories under each condition were determined by enrichment analysis. All data were submitted in the GEO (Gene Expression Omnibus) database GSE206758.

2.3.10. *C. neoformans* (H99) Morphology in Mice under Treatment with a Proteasome Inhibitor

After analyzing the transcriptome results, a new infection was performed to assess the effect of treatment with a proteasome inhibitor (Bortezomib-Sigma-Aldrich, Burlington, MA, USA) on the morphology of *C. neoformans*. Bortezomib (BTZ—1.4 mg/kg, humanized dose) [43] was administered intraperitoneally 1 hour before infection. After 6 h and 10 days of infection, the animals were euthanized to obtain BALF and evaluate fungal morphology. The infected and untreated (NT) groups were used as controls.

2.4. Statistical Analysis

All statistical analyses were performed using GraphPad Prism, version 5.00, for Windows (GraphPad Software, San Diego, CA, USA), and the results were considered significant at $p < 0.05$. The survival curve was plotted by Kaplan–Meier analysis and the results were analyzed by the log rank test; for behavior parameters, the area under the curve was analyzed. Laccase, urease, morphology, phagocytosis, IPR assay, ROS and PRN measurements, and CFU per gram were analyzed by analysis of variance (ANOVA) followed by Tukey's multiple comparison test. All correlation measurements used throughout this manuscript are Pearson correlations.

3. Results

3.1. Strain Growth and Morphological Characteristics in Culture

To study morphological and transcriptional responses to pulmonary infection, we focused on the serotype A strain H99 (VNI genotype) commonly used for evaluating virulence traits, and we selected four additional strains for comparison (Table 1). The additional strains included two of serotype A (WM148, genotype VNI and WM626, VNII), a serotype D strain (WM629, VNIV) and a serotype AD strain (WM628, VNIII). Initially, we evaluated the growth of the five strains in rich medium (Yeast Extract Peptone Dextrose (YPD)) and in minimal medium (MM) at 37 °C. All the strains demonstrated reduced growth in YPD compared to MM (Figure 1A–E). Results were confirmed by the plating method (data not shown). We also tested growth and melanin production after five days of culture in medium with the substrate L-DOPA. The WM628 and WM626 strains demonstrated a reduced melanization compared to H99, and WM626 additionally showed

reduced growth (Figure 1F). An assay for laccase activity confirmed the visual analysis of melanin production (Figure 1G). Urease activity was also analyzed, but no significant difference was observed among the strains (data not shown). In the context of the growth studies, we next determined whether morphological differences were apparent. The strains were incubated in YPD or MM, and cell morphology was analyzed by microscopy (Figure 1H–K). Notably, we observed that all of the strains produced smaller cells upon growth in MM (Figure 1H,K). We also noted that the WM629 strain had a smaller cell body and a higher surface/volume ratio (S/V ratio) than H99 in YPD (Figure 1H,I). Under the growth conditions in YPD, a capsule was observed for WM629 and H99, and the size was larger for strain WM629 (Figure 1J). All of the strains produced a capsule in MM with the exception of WM148 (Figure 1J,K). Taken together, these results indicated conserved cell size responses to rich and minimal medium for the strains but revealed differences between the strains in the virulence traits of melanin and capsule production.

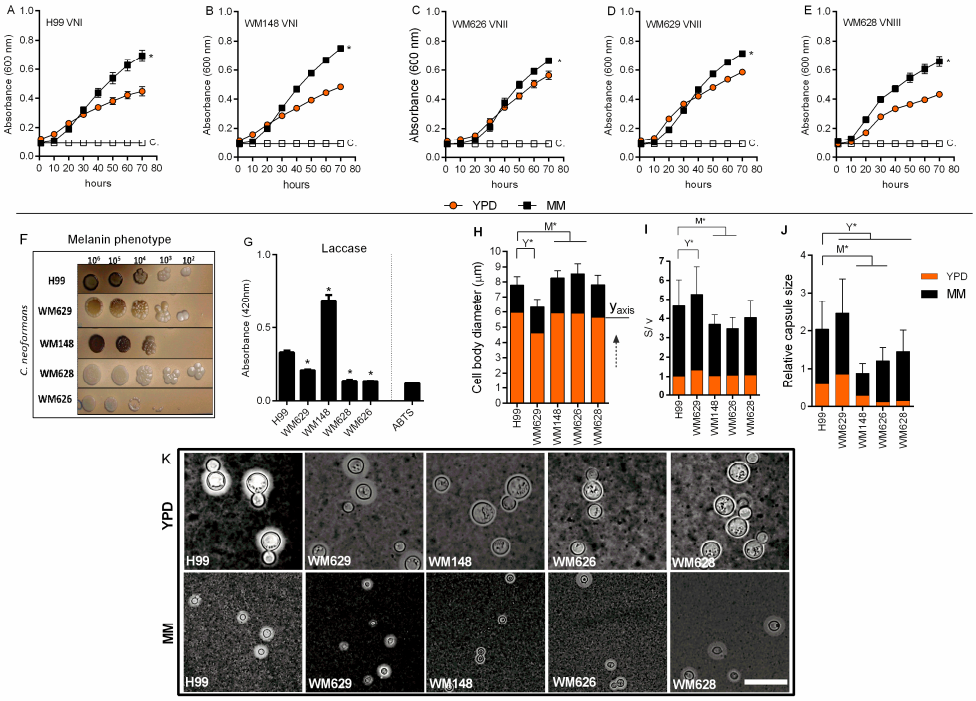

Figure 1. Phenotypic analysis of *C. neoformans* strains in vitro. (**A**–**E**) Growth curves of each strain in Yeast Extract Peptone Dextrose (YPD) or in minimal medium (MM) at 37 °C (blank squares represent only the culture media). (**F**) Visual analysis of melanin production after fungal growth in solid minimal medium with L-DOPA at 37 °C for 5 days. (**G**) Laccase activity measured in MM (ABTS: 2,2′-azinobis(3-ethylbenzthiazoline-6-sulfonate). (**H**) Cell body diameter in YPD or in MM at 37 °C after 72 h. Dashed arrow: indicates that the MM y-axis starts at the end of each YPD bar. (**I**) Surface/volume ratio in YPD or in MM at 37 °C after 72 h. (**J**) Relative capsule sizes in YPD or in MM at 37 °C. Mean values were compared with H99 (* $p < 0.05$; M* = strain analysis on MM; Y* = strain analysis on YPD). (**K**) India ink counter-staining of *C. neoformans* after growth in YPD or MM. Scale bar: 10 µm.

3.2. C. neoformans Strains Display Different Disease Profiles in Murine Cryptococcosis

After investigating growth and the in vitro virulence-related attributes, we evaluated whether these factors could be associated with the ability of each strain to cause disease in a murine model of cryptococcosis. Mice were infected intratracheally with cells grown in YPD, and survival, behavior, and fungal burden were evaluated. Differences in lethality were found for all strains (Figure 2A). Strains H99 (mean lethality time—MLt = 22 days) and WM629 (MLt = 23 days) caused an early lethality profile, while longer survival was observed for the WM628 (MLt = 28 days) and WM148 (MLt = 32 days) strains

(Figure 2A). WM626 did not cause death and was classified as a non-lethal (NL) strain, although it induced behavioral changes at the beginning of the infection (Figure 2D–H). Thus, according to the survival data, the strains were classified as hypervirulent (H99, WM629 MLt = 21–25 days), virulent (WM628 MLt = 26–31 days), hypovirulent (WM148 MLt = 32–40 days), and non-lethal (WM626).

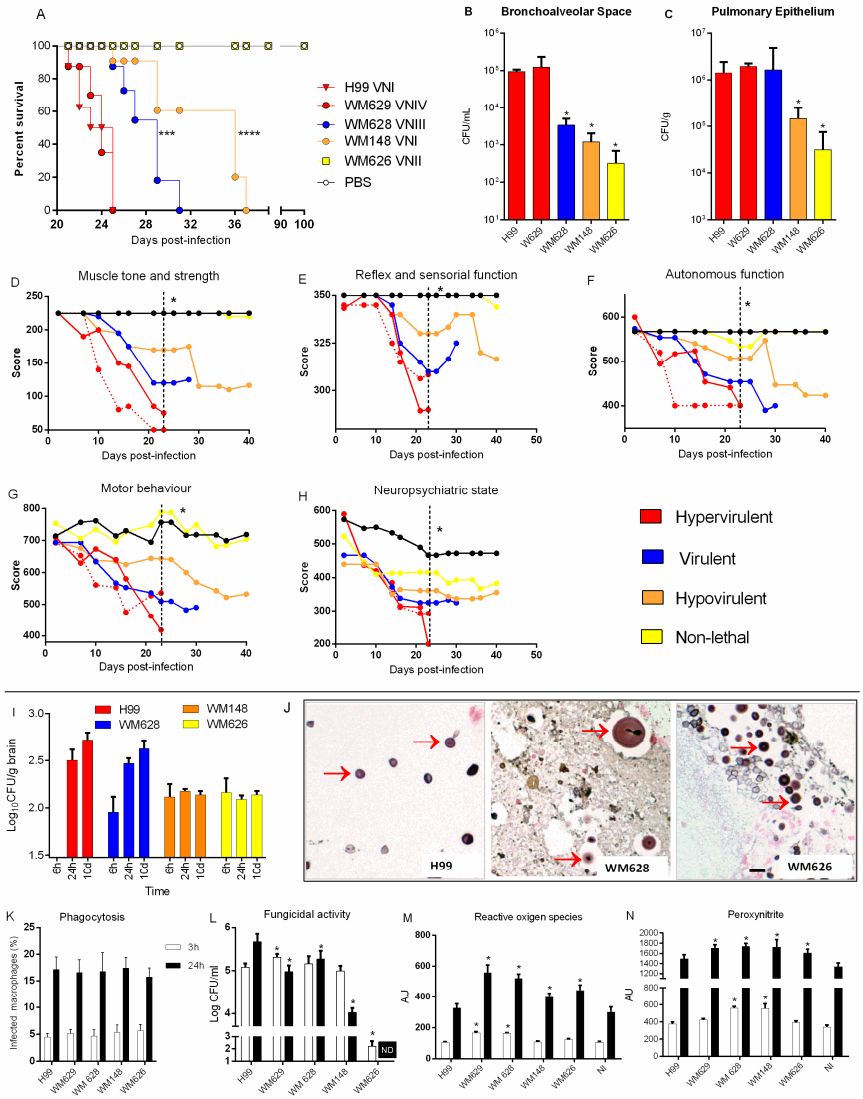

Figure 2. Virulence analysis of *C. neoformans* strains in vivo and ex vivo. (**A**) Mortality curve of mice after intratracheal infection with 1×10^5 cells (*** $p < 0.001$ and **** $p < 0.001$). (**B**,**C**) Fungal burden determination from the bronchoalveolar space (BS) and pulmonary epithelium (PE) 10 days post infection. (**D**–**H**) Behavior analysis after infection with *C. neoformans* strains. Dashed lines indicate the statistical difference in virulent, hypovirulent, and non-lethal strains compared with H99 (* $p < 0.05$). Virulence was classified according to the mean lethality time (MLt), with hypervirulent (red) range of MLt = 21–25 days, virulent (blue) range of MLt = 26–31 days, hypovirulent (orange) range of MLt = 32–40 days, and non-lethal (yellow) range of MLt => 100 days. (**I**) Fungal burden in the brain after 6 h, 24 h, and 10 days of intratracheal infection. (**J**) Brain stained with Fontana–Masson after 10 days of intracranial infection. Red arrow indicates the stained fungus due to the presence of melanin in the cell wall. Scale bar: 10 µm. (**K**) Phagocytic index after 3 h and 24 h infection. (**L**) Colony forming unit (CFU) determination represents viable yeast cells internalized by macrophages in each time point. (**M**) ROS and (**N**) PRN production after 3 and 24 h of infection by *C. neoformans*. Mean values were compared with H99 (* $p < 0.05$). AU: arbitrary units of fluorescence. NI: non-infected macrophages.

We next analyzed fungal burden in the two compartments of the lungs, considering the sequence of tissue colonization: the bronchoalveolar space (BS, obtained from bronchoalveolar lavage fluid) and the pulmonary epithelium (PE). Fungal burden recovered from the PE and bronchoalveolar lavage fluid was similar for the H99 and WM629 strains (Figure 2B,C). Compared to H99, a lower fungal burden was recovered from the bronchoalveolar space (BS) of mice infected with WM628 but not from the PE (Figure 2B,C). The hypovirulent WM148 and non-lethal WM626 strains presented lower fungal burdens in the PE and BS than H99 (Figure 2B,C).

The behavior of infected animals was analyzed using the SHIRPA protocol, which mimics human signs and symptoms caused by neurological diseases [44]. All the strains were able to influence the following parameters evaluated at ten days post infection: muscle tone and strength, neuropsychiatric status, autonomic function, motor behavior, and function and sensory reflex (Figure 2D–H). The hypervirulent and virulent strains showed more intense behavioral changes when compared to the hypovirulent strain after 22 days of infection (Figure 2D–H).

3.3. Hypervirulent and Virulent Strains Increased Fungal Burden in the Brain

As *C. neoformans* is associated with meningoencephalitis, we evaluated the fungal burden in the brain throughout infection for the strains with different virulence phenotypes. Unfortunately, we could not analyze fungal cell morphology directly from the brain tissue, although several protocols were tested. However, we verified that all strains were able to disseminate to the CNS after 6 or 24 h of intratracheal infection. In addition, the hypervirulent and virulent strains increased fungal burden over time, while the less virulent or non-lethal strains had a similar fungal burden in the CNS throughout the infection, with a lower fungal burden compared to H99 (Figure 2I).

Melanization is considered one of the main factors related to the tropism of *Cryptococcus* spp. to the CNS [16,18]. However, strains that were not able to produce melanin in vitro were able to translocate to the CNS and maintain a stable fungal burden. Therefore, we evaluated whether in vivo melanization was compatible with the in vitro observations for these strains. An intracranial mice infection was performed, and histological analysis of the brain was performed after ten days using Fontana–Masson stain. In the histological analysis, we observed cryptococcal cells with brown staining, characteristic of melanized cells. Interestingly, the strains that did not produce melanin in vitro (WM628 and WM626) were able to produce it in the brain (Figure 2J).

3.4. C. neoformans Hypervirulent Strains Are Less Susceptible to the Fungicidal Activity of Macrophages

In general, the evaluation of the ability of the strains to cause cryptococcosis did not strictly correlate with the elaboration of virulence traits. We therefore evaluated the interaction between the fungus and murine macrophages considering the importance of *C. neoformans* ability to survive inside the host's immune cells. Phagocytosis did not vary according to the virulence of *C. neoformans* strains (Figure 2K). However, the virulent strains H99, WM629, and WM628 showed higher intracellular survival (Figure 2L) and were associated with an increase in intracellular levels of reactive oxygen species (ROS) and peroxynitrite (PRN) when compared to the H99 strain after 3 h of infection. However, the survival mechanism was overall independent of oxidative and nitrosative stress for the other strains (Figure 2M,N).

3.5. The Kinetics of In Vivo Morphology Revealed Small Cells at Early Stages of Infection with Later Capsule Enlargement

Considering the in vitro morphological response of *C. neoformans* to culture conditions, we next evaluated whether this variation in cell size occurred during murine lung infection and the possible relationship to virulence. Mice were infected with one representative strain of each virulence phenotype and euthanized after 6, 24, or 240 h of infection. Cell morphology was determined directly from the BS (BALF) and PE. *C. neoformans* cells were

not detected in the brain by microscopy at these early stages of infection. We found that murine infection led to morphological changes that were related to the virulence of the strains. Specifically, all strains presented a smaller cell body (≤3 μm) in the BS and PE than the initial inoculum after 6 h of infection (Table 2), leading to a predominance of small cells with a higher S/V ratio (Figure 3A–F). Furthermore, the hypervirulent strain (H99) had a cell body 20% smaller in the PE (mean = 2.0 μm) when compared to the cells in the BS (Mean = 2.5 μm).

Table 2. Cell body diameter variation in *C. neoformans* in vivo.

Cell Body Diameter (μm)	Cells (%)							
	Bronchoalveolar Space 6 h				Pulmonary Epithelium 6 h			
	H99	WM628	WM148	WM626	H99	WM148	WM628	WM626
≤3	100	100	100	100	100	100	100	100
4–5	0	0	0	0	0	0	0	0
6–9	0	0	0	0	0	0	0	0
>10	0	0	0	0	0	0	0	0
	24 h				**24 h**			
≤3	46.3	43.4	96.7	100	84.5	82.6	95.8	96.3
4–5	25.9	56.6	3.3	0	15.5	11.5	4.2	3.7
6–9	18.5	0	0	0	0	5.9	0	0
>10	9.2	0	0	0	0	0	0	0
	240 h (10 days)				**240 h (10 days)**			
≤3	20.3	7.8	33.3	76.1	46.2	3.9	37.1	84.7
4–5	33.5	61.5	24.0	22.6	38.7	63.3	22.2	13.4
6–9	34.6	30.7	42.7	1.3	15.1	32.6	40.7	1.9
>10	11.8	0	0	0	0	0	0	0

After 24 h, the hypervirulent (H99) and virulent (WM628) strains showed an increase in cell body size, accompanied by a lower S/V ratio in the BS (Table 2) (Figure 3A–F). However, the same increase did not occur in the PE, where we observed the predominance of smaller cells, thus providing evidence for tissue compartmentalization (Figure 3H). Furthermore, the relative capsule size increased for all strains in the BS and PE throughout the infection, but this increase was significantly higher for the virulent strains (H99, WM628, and WM148). Further, there is a positive correlation between capsule size and virulence in mice, but not for the in vitro data (Figure 3G). Notably, the NL strain did not increase in cell size after ten days of infection (Figure 3A–F). Interestingly, after ten days of infection, the cells returned to their original total diameter (capsule + cell body); however, they had a larger polysaccharide capsule and a smaller cell body (Figure 3I). Thus, these results highlight that before capsule enlargement, *C. neoformans* reproduce and generate daughter cells with a small size initially after infection. After that, cell body enlargement and capsule synthesis occur throughout the infection. However, some cells may present an intense enlargement of the cell body leading to the formation of titan cells (>10 μm), as seen for the hypervirulent strain in BL, after 24 h and 10 days of infection (Table 2). Cell morphology and the dynamics of the morphological variation were observed under an optical microscope after staining with India ink (Figure 3J). The scanning electron microscopy of the BALF was performed to examine the hypervirulent (H99) and NL (WM626) yeasts (blue) after 6 and 240 h (10 days) of infection (Figure 3K). Bronchoalveolar space cells and red blood cells are pictured in green and red, respectively (Figure 3K). A delay in re-growing the cell body was seen in low virulent strains, pointing to a reduced microbial fitness. We therefore focused our subsequent transcriptome analyses on the H99 strain during lung infection.

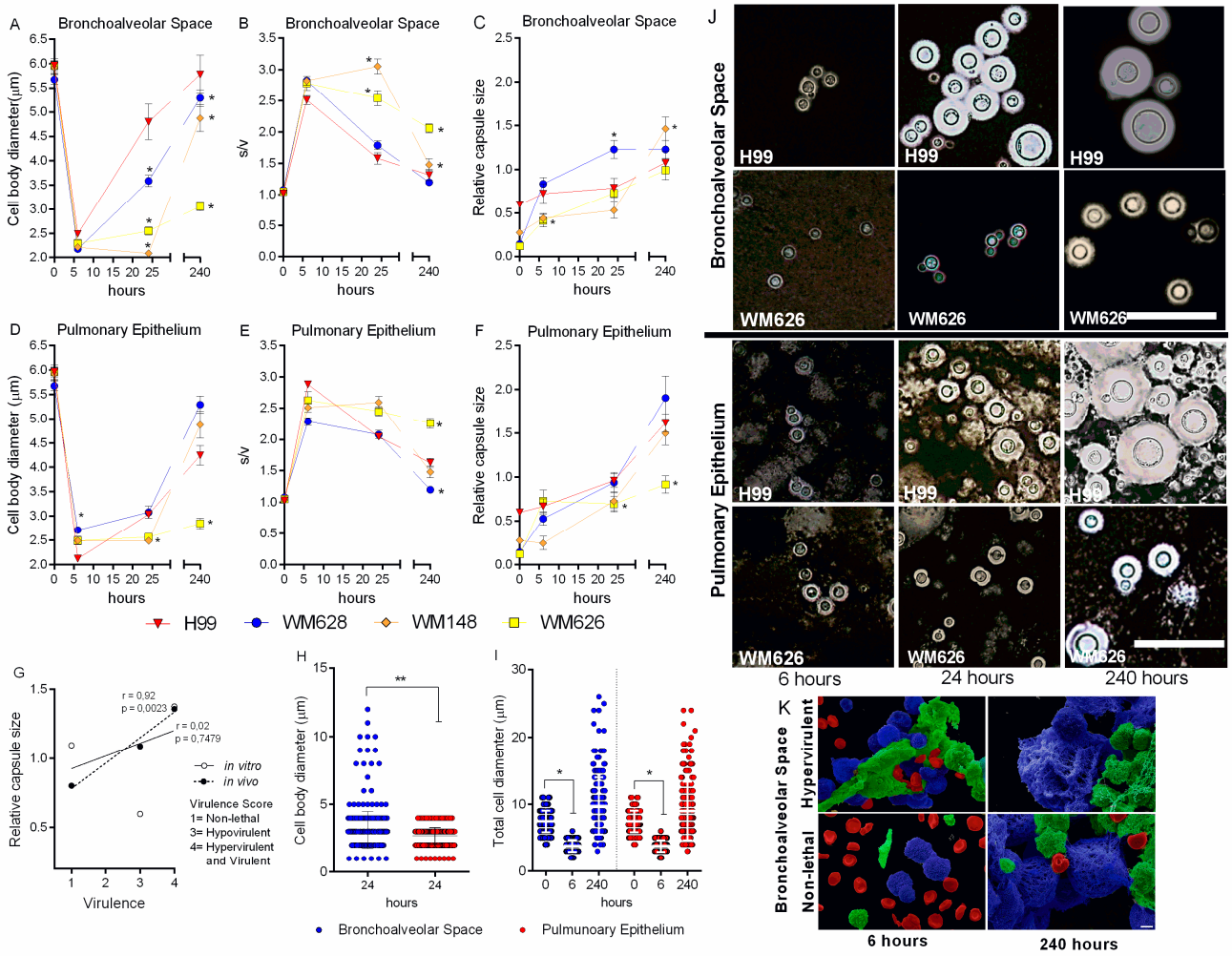

Figure 3. Dynamics of morphological variation of *C. neoformans* in vivo. (**A**–**F**) Morphological variation in bronchoalveolar space (BS) and pulmonary epithelium (PE) of four strains of *C. neoformans* after 6, 24, and 240 h of intratracheal infection. Mean values were compared with H99 (* $p < 0.05$). (**G**) Correlation between virulence and relative capsule size after 240 h infection. R values are included next to lines of best fit and are based on Pearson correlation. (**H**) Cell body diameter in BS and PE after 24 h of infection. Mean values were compared with bronchoalveolar space (** $p < 0.01$). (**I**) Total cell diameter in BS and PE after 0 and 240 h infection. Mean values were compared with 0 h of infection (* $p < 0.05$). (**J**) India ink counter-staining of the yeasts recovered from infected mice. Scale bar: 10 µm. (**K**) Scanning electron microscopy (SEM) of hypervirulent and non-lethal strains after infection: yeasts are colored in blue, bronchoalveolar space cells in green, and blood cells in red. Scale bar: 2 µm.

3.6. Dual RNA-Seq Analysis of C. neoformans and Mice Revealed Transcriptional Profiles of Early and Late Events of Infection

To evaluate the transcription changes underlying morphological and other responses during lung infection, we characterized the fungal and host transcriptomes for early and late stages of infection, considering the BS as the first compartment of colonization. For these studies, mice were infected with the H99 strain, and the BALF was obtained after 6 h or 10 days of infection to perform dual RNA-seq. Yeast cells grown in YPD (before infection) were used as a control. We analyzed the upregulated and downregulated genes after 6 h and 10 days of infection, compared to the inoculated yeast (YPD vs. 6 h and YPD vs. 10 d) and the differentially expressed genes (DEGs) between 6 h and 10 days of infection (designated BAL6h vs. BAL10d). Table 3 describes the RNA-seq statistics. The low mapping to the *C. neoformans* H99 reference genome in the infection libraries is

consistent with dual RNA-seq analysis, as previously shown by other studies, ensuring the quality of our results [45,46]. These analyses revealed transcriptional profiles of early and late stages of infection, and the profiles shared between these two time points as well (Figure 4A). In the later stages of infection, 860 genes were modulated, with 488 being upregulated and 372 downregulated (YPD vs. 10 d). Moreover, 602 genes at 6 h and 540 genes at 10 d were uniquely expressed. The regulation of these genes represents the potential adaptation mechanisms used by *C. neoformans* in vivo, compared to the yeast cells found in the environment. During mice infection, there were 83 DEGs, with 81 upregulated and 2 downregulated genes in 10 d compared to 6 h (6 h vs. 10 d) (Figure 4A). *C. neoformans* DEGs are shown in Table S1.

Table 3. Dual RNA-seq statistics of mapping the reads to the reference genome.

			C. neoformans		Mouse	
Sample	**Raw Reads**	**High-Quality Reads**	**Mapped Reads**	**Total Mapped Reads (%)**	**Mapped Reads**	**Total Mapped Reads (%)**
BAL10d I	35,858,545	34,810,495	415,287	1.19	20,978,194	60.26
BAL10d II	36,346,653	35,320,291	579,106	1.64	20,921,124	59.23
BAL6h I	34,773,919	33,841,813	283,360	0.84	20,098,380	59.39
BAL6h II	45,536,641	44,382,642	650,886	1.47	24,160,652	54.44
YPD IC	26,632,962	26,025,358	25,820,614	99.21	-	-
YPD2C	25,955,261	25,380,479	25,185,198	99.23	-	-

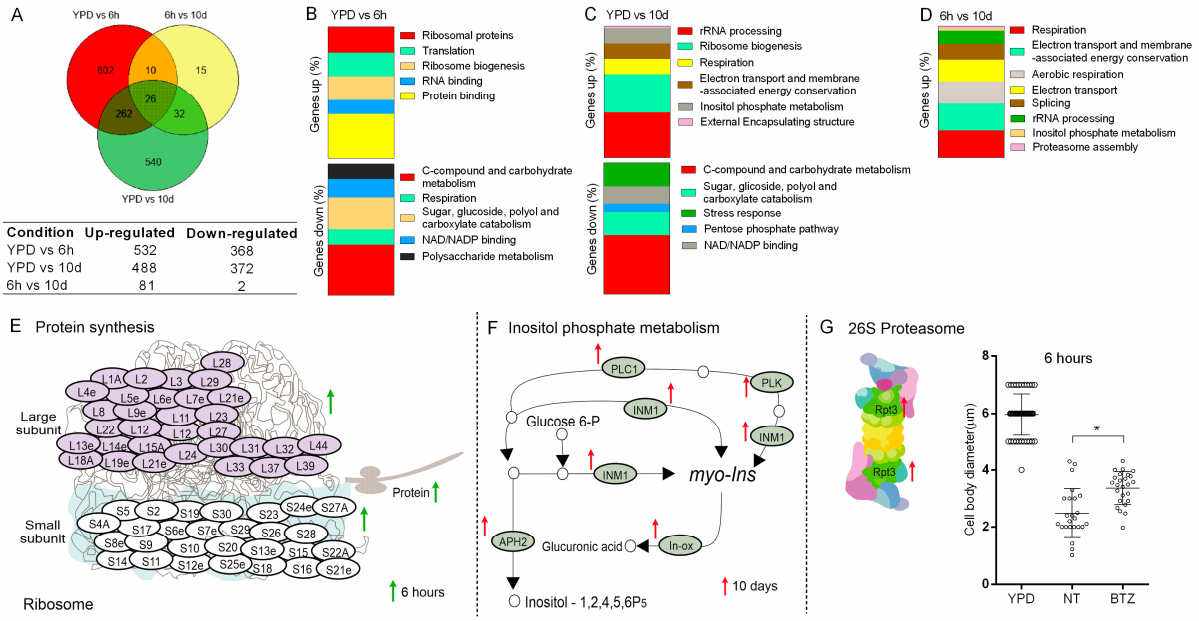

Figure 4. Differentially expressed genes (DEGs) in *C. neoformans* strain H99 during mice infection. (**A**) Venn diagram showing the number of H99 transcripts modulated comparing 6 h and 10 d of infection and YPD cultured yeasts. (**B**–**D**) GO biological processes enriched in H99 after 6 h and 10 days of intratracheal infection, for each comparison. (**E**) Upregulated transcripts related to ribosome subunits after 6 h of infection compared to YPD. (**F**) Genes involved in inositol metabolism differentially expressed after 10 days of infection (CNAG_00038, CNAG_00730, CNAG_00869, CNAG_01823, CNAG_01947, CNAG_02867, CNAG_04209, CNAG_04335, CNAG_04869, CNAG_05316, CNAG_05884, CNAG_06348, CNAG_06623, CNAG_06785, CNAG_06967, and CNAG_07799). (**G**) Differentially expressed genes related to fungal proteasome 10 d post infection, and the influence of bortezomib (BTZ) (proteasome inhibitor) on cell body diameter. Mean values were compared with NT (* $p < 0.05$). Upward arrows indicate induction of gene expression. Upregulated genes after 6 h are indicated by green arrows and upregulated genes after 10 days are indicated by red arrows.

Functional classification of the differentially expressed transcripts was performed using FunCat (Functional Catalogue), GO (Gene Ontology), and KEGG (Kyoto Encyclopedia of Genes and Genomes). Nineteen biological processes were significantly enriched (YPD vs. 6 h, YPD vs. 10 d, and BAL6h vs. BAL10d) (Figure 4B–D). Biological processes such as protein binding, ribosomal proteins, ribosome biogenesis, and translation were upregulated after 6 h of infection compared to the yeast grown in YPD (Figure 4B) (Table S1). Melanin and the polysaccharide capsule are virulence factors classically described for *C. neoformans* [15,17]. Interestingly, after 6 h of infection, we identified genes upregulated for these virulence factors (LAC2, CAP64, CAP2, and CAS3) (Table S1). This is consistent with the increase in the polysaccharide capsule observed in the AS and PE after 10 days of infection and the presence of melanin in the cell wall in intracranial infection after 10 days. A gene for chromatin remodeling (SNF59) was also upregulated (Table S1). Ten days post infection (YPD vs. 10 d, BAL6 h vs. BAL10 d), several transcripts related to respiration, electron transport and membrane-associated energy conservation, aerobic respiration, and splicing were upregulated (Figure 4C,D) (Table S1).

3.7. Ribosomal Modulation Is Important for C. neoformans Adaptation in the Early Time of Infection

Transcripts for five hundred and thirty-two genes were upregulated in *C. neoformans* in the BS after 6 h of infection (Figure 4A). Seventy-five of them were involved in ribosomal regulation, specifically thirty-two related to the small subunit, forty-two to the large subunit, one (RPF2 CNAG_01187) to 60S pre-ribosomal formation, and one (UTP10 CNAG_04370) for 18S ribosomal RNA biogenesis (Figure 4E) (Table S1). This finding is consistent with proliferation and the morphological analysis of *C. neoformans* throughout infection. Initially, we observed smaller and more metabolically active yeasts, compatible with the higher S/V ratio. Thus, the transcriptional response likely reflects the protein synthesis necessary for the reproduction and initial adaptation of the fungus.

3.8. Inositol Metabolism and Proteasome Modulation Are Involved in the Late Adaptation of C. neoformans during Infection

Previous studies have demonstrated that inositol catabolism is involved in the virulence of *C. neoformans* [47–49]. Consistent with these studies, our results showed the upregulation of genes related to inositol metabolism after 10 days of infection compared to YPD (YPD vs. BAL10d) and 6 h (BAL6h × BAL10d) (Table S1). Transcripts for sixteen genes related to inositol metabolism were upregulated, including two related to myo-inositol oxygenase (MIO) that converts myo-inositol to D-glucuronic acid, a substrate of the pentose phosphate cycle and a component of the polysaccharide capsule (Figure 4F) (Table S1). These findings are consistent with the increase in the relative capsule size observed for the most virulent strains after 10 days of infection.

The proteasome is important for the degradation of cellular proteins and is involved in synthesizing the polysaccharide capsule in *C. neoformans* [50–52]. Interestingly, the proteasome-related gene RPT3 (26S proteasome regulatory subunit—CNAG_03904) was upregulated after 10 days post infection, compared to 6 h (BAL6h vs. BAL10d) (Figure 4G). Considering these findings, we evaluated whether the proteasome inhibitor bortezomib affects the morphology of *C. neoformans* recovered from the BS. Yeast cells recovered after 6 h of infection from treated mice exhibited increased cell body diameter compared to the yeasts recovered from non-treated mice (Figure 4G), pointing to the importance of the proteasome for *C. neoformans* cell remodeling during infection. The treatment did not alter the morphology after 10 days of infection (data not shown).

3.9. Transcripts Related to Energy Production Are Differentially Modulated during Infection

Throughout infection, transcripts for 22 genes were differentially modulated in all comparisons (YPD vs. BAL6h, YPD vs. BAL10d, and BAL6h vs. BAL10d), involving different biological processes such as respiration, electron transport, membrane-associated energy conservation, metabolism of energy reserves, the pentose phosphate pathway,

and electron transport (Figure 5A,B). Most transcripts (15) were downregulated at the beginning of infection and upregulated after 10 days (Figure 5A) (Table S1). Oxidative phosphorylation, a pathway related to energy production, was the main enriched pathway (Figure 5C) (Table S1).

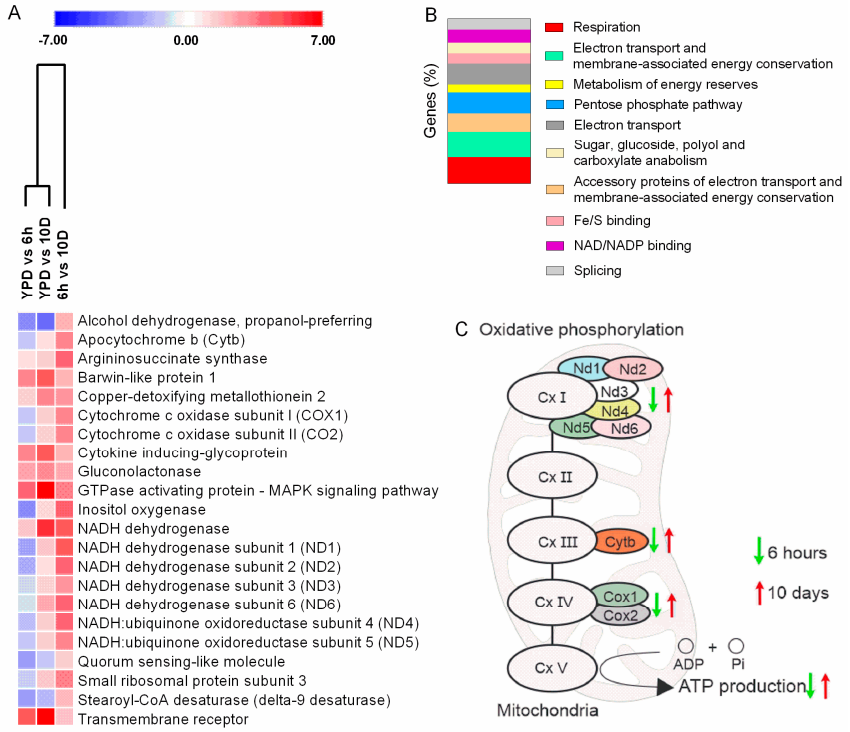

Figure 5. Transcriptional profile of *C. neoformans* in the bronchoalveolar space of mice. (**A**) Heatmap of the significantly enriched GO categories of regulated fungal genes at 6 h and 10 days post infection. (**B**) Enriched GO biological processes of fungal genes expressed in the bronchoalveolar space. (**C**) Modulated genes from the oxidative phosphorylation pathway expressed 6 h and 10 days post infection. Upward arrows indicate induction of gene expression and downward arrows indicate repression of gene expression at 10 days, compared to 6 h. Differently regulated genes after 6 h are indicated by green arrows, and differentially regulated genes after 10 days are indicated by red arrows.

3.10. The Mouse Transcriptional Response to the Early and Late Stages of Infection

The comparison of the in situ mice transcriptional profiles between 6 h and 10 d post *C. neoformans* infection allowed the identification of transcripts for 4575 genes involved in the early and late host responses. In particular, we found that 1375 genes were upregulated at 6 h and 1823 were upregulated at 10 d (Table S2). To categorize the differentially expressed transcripts and characterize their functions, the ShinyGO v0.75, GO (Gene Ontology), and KEGG (Kyoto Encyclopedia of Genes and Genomes) classifications were used. Functional enrichment showed that at the early stage of infection (6 h), there is an over-representation of genes coding for proteins involved in phagocytosis, such as integrins and cell receptors (*CD18, MR, TLR2,* and *TLR4*), proteins related to lysosomes (*LAMP*, *LIMP*, *DMXL*, *WDR7*, and *NCOA7*), and components of the NF-kB signaling pathway (*LYN*, *VAV*, *BCAP*, *NFKB*, *NFAT*, *API*, and *CARMA1*) (Figure 6A,B) (Table S2). The phagosome, lysosome, and B-cell signaling pathways were also enriched in response to *C. neoformans* in the early stage of the infection (Figure 6C) (Table S2). These results are consistent with phagocytosis and cell-migration-related genes being important for the early mice response to infection (Table S2). The connection with phagocytosis is further emphasized by our observation of the upregulation of transcripts for SOD1 (superoxide dismutase [Cu-Zn]—CNAG 01019) in *C. neoformans*, an important enzyme for oxidative stress resistance within phagocytes [53].

On the other hand, functional enrichment of the upregulated genes at 10 days (compared to 6 h) was over-represented with genes involved in cell morphogenesis/migration, components of the Phosphoinositide 3-kinase (PI3K)/Akt (PI3K-AKT) signaling pathways, focal adhesion, and inflammation and cytokine/chemokine pathways (Table S2). The identification of these genes begins to build a view of the host molecular profile at the later (10 d) stage of cryptococcosis (Figure 6D,E). Notably, the host transcriptome response to *C. neoformans* resembled that of other infectious or inflammatory diseases, including rheumatoid arthritis, legionellosis, salmonella infection, tuberculosis, Chagas disease, and leishmaniasis (Figure 6F) (Table S2).

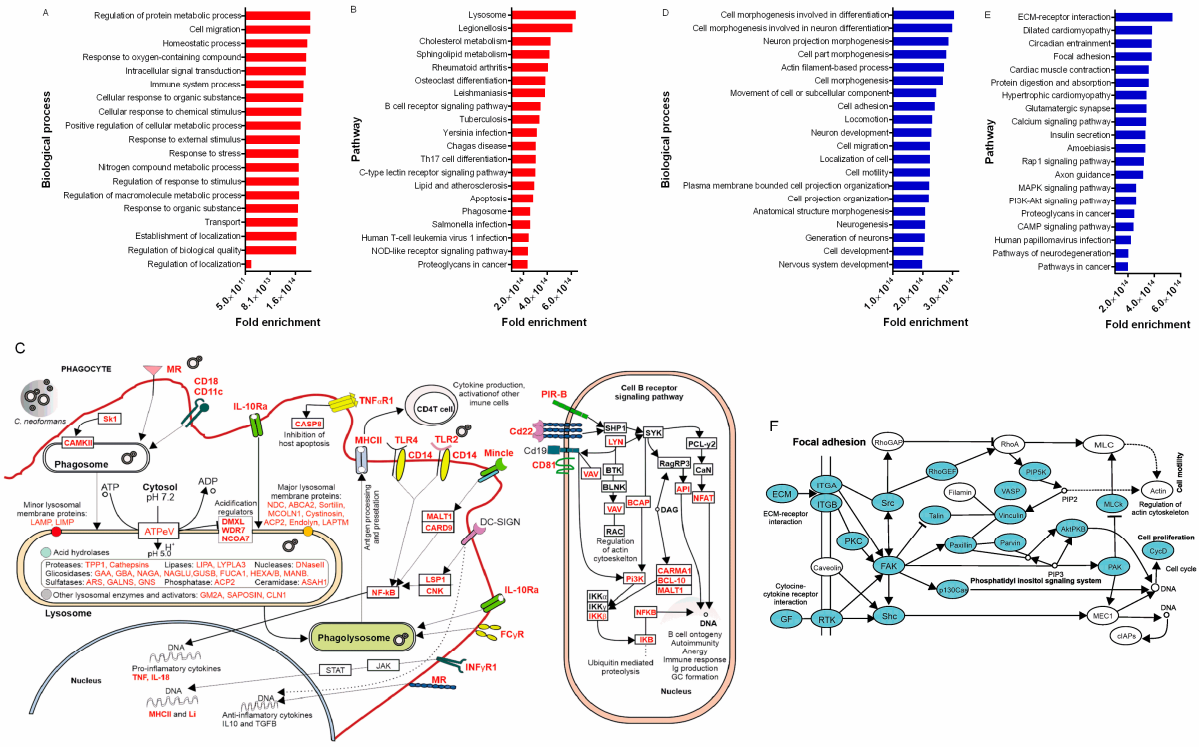

Figure 6. In situ transcriptional profile in the early and late mouse response to *C. neoformans* infection. Genes are upregulated at 6 h compared to 10 d. (**A**) Biological processes and (**B**) pathways enriched in the BS of mice 6 h post infection. (**C**) Gene regulation of phagocytosis and B-cell receptor signaling in the BS. After deposition in the lungs, *C. neoformans* can be recognized by pattern recognition receptors (MR, CD18, CD11C, DC-SIGN, TLR4, and TLR2) on phagocytes and internalized, leading to the formation of the phagosome and consequently the phagolysosome. The acidification of this compartment combined with respiratory burst and degradative enzymes are important factors for antimicrobial activity. After the degradation of *C. neoformans* in the phagolysosome, microbial antigens can be targeted to the MHC-II pathway for presentation to CD4 T cells. Furthermore, cell wall components of *C. neoformans* (GXM, GalGXM, and mannoproteins) can also be recognized by B-cell receptors, leading to signaling for antibody production. Upregulated genes in red. Based on KEGG and Gene Ontology (GO) analyses. Genes are upregulated at 10 days compared to 6 h. (**D**) Biological processes and (**E**) pathways enriched in the BS of mice 10 days post infection. (**F**) Focal adhesion pathway showing the upregulated genes (blue) in the BS 10 days post infection. Based on KEGG and Gene Ontology (GO) analyses.

As summarized in Figure 7, our results demonstrate the dynamics of cellular remodeling of *C. neoformans* during infection.

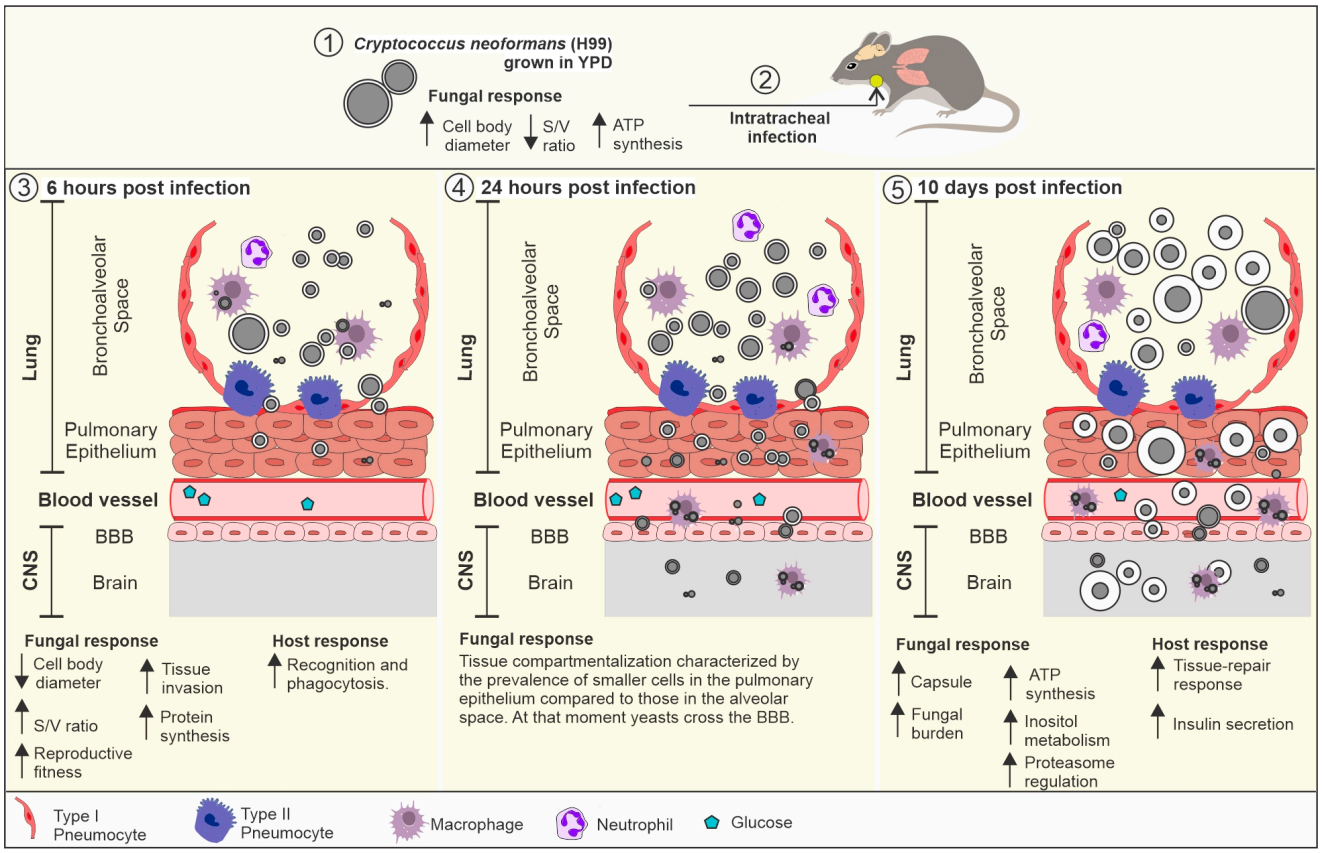

Figure 7. The dynamics of *Cryptococcus neoformans* cell remodeling during infection. (**1**) The growth of the H99 strain on YPD resulted in cells with a larger cell body diameter (mean: 5.6 µm), reduced capsule (mean: 0.5), reduced surface-to-volume ratio (mean: 1.16), and upregulation of pathways related to energy production. This profile mimics yeasts found in the environment. (**2**) After mice intratracheal infection with these cells, we observed a time- and location-dependent cell remodeling. (**3**) At 6 h post infection, we observed a predominance of small cells in the BS compared to the initial size. These cells have a smaller cell body and a higher surface-to-volume ratio. This contributes to increased fitness and pulmonary epithelium invasion. This cellular profile was associated with upregulation of pathways related to protein synthesis and upregulations of recognition and phagocytosis pathways in the host. (**4**) At 24 h post infection, we observed tissue compartmentalization characterized by the prevalence of smaller cells in the pulmonary epithelium (variation: 1.0–4.0 µm) compared to cells in the BS (variation: 1.0–12.0 µm). This evidence confirmed our hypothesis that small cells are important for PE invasion during interaction with the host. At this stage, the cells were able to reach the bloodstream, free or internalized by phagocytes, and cross the blood–brain barrier (BBB) and infect the central nervous system (CNS). (**5**) At 10 days post infection, we observed an increase in the polysaccharide capsule and upregulation of pathways related to energy production, inositol, and proteasome metabolism. In the host, this cellular profile led to the upregulation of tissue repair pathways and insulin secretion.

4. Discussion

C. neoformans is an important human pathogen related to cryptococcosis, a public health issue with a high mortality rate [54]. This fungus can be found as a free-living cell and as an intracellular pathogen, therefore it is exposed to several environmental pressures, such as temperature and pH changes, soil nutrient availability, phagocytosis by free-living amoebae, interaction with other microorganisms and plants, and exposure to UV radiation [55]. The exposure to these hostile environments may have contributed to the evolution of virulence factors that also support the survival and interaction with mammalian cells [55]. Despite knowledge about the virulence attributes of *C. neoformans*, the influence of cellular

morphogenesis on virulence and disease outcome and the mechanisms involved in cell plasticity during infection remain poorly understood.

In this study, we combined in vitro and in vivo assays to examine differences in the virulence of a set of five *C. neoformans* strains. Using a murine model of cryptococcosis, we found that the lethality of each strain ranged from hypervirulent (H99 and WM629), to virulent (WM628), to hypovirulent (WM148), to non-lethal (WM626). These differences provided a useful set of strains for better understanding virulence attributes, such as the ability to survive inside macrophages, morphological changes in vivo, dissemination, and the ability to proliferate in the CNS. Initially, we determined that the strains generally had a smaller cell body and larger polysaccharide capsule when grown in MM, compared to growth in the YPD. Interestingly, after 6 h of mice lung infection, we observed a predominance of small cells in the BS compared to the initial size of the inoculated cells. Presumably, these smaller cells result from initial proliferation at the early time of infection. We refer to this event as cell remodeling, and it was observed in all strains independent of the virulence level. It is well established that fungal cells adopt different strategies during tissue invasion, such as the filamentation in *Candida albicans* [13,56]. In *C. neoformans*, the generation of small cells at the early stages of infection may be a determining factor for the invasion of the PE, since they may have an increased ability to cross barriers compared to the regular cells. This possibility is consistent with the tissue compartmentalization at 24 h post infection, in which smaller cells were detected in the PE. Moreover, smaller cells may be more active metabolically since they have a higher S/V ratio, facilitating the exchange of nutrients with the environment and increasing their fitness [21]. Considering that the lung environment is stressful, the initial cellular remodeling may be critical for optimizing *C. neoformans* energy expenditure and PE invasion.

The ability to cross the blood–brain barrier is essential for CNS infection [57]. The mechanisms involved in this process (e.g., a Trojan horse process) are well described, and it is likely that fungal cell size influences fungal dissemination, since small cells may be more readily phagocytosed, exhibit higher intracellular proliferation and survival [15], and may spread quickly from the lungs throughout the bloodstream to reach the CNS. In this study, the predominance of small cells in the PE at the beginning of the infection is likely contribute to pulmonary escape and early detection in the CNS. Furthermore, we speculate that these small cells (<3 μm) may be the precursors of the seed cells (<6 μm), as recently described [6]. Interestingly, the seed cells present changes on the cell surface that impair immunological response and favor the dissemination to extrapulmonary tissues [6]. Thus, our findings, in light of the previous studies, demonstrate how *C. neoformans* remodels itself in the lungs at the beginning of the infection and promotes the development of a systemic disease.

Despite our evidence, the role of small cells during *Cryptococcus* spp. infection remains poorly understood. A recent study demonstrated a relationship between small cells and virulence after culture under laboratory conditions [7]. However, in our morphological analyses in vivo, the predominance of small cells at the beginning of the infection was independent of the virulence profile. However, the ability to re-growth the cell body after 24 h and 10 days of infection can be associated with increased microbial fitness. Therefore, we believe that this cell type is essential for initial adaptation to the lung tissue and escape to other tissues, but it is not a virulence determinant. We assume that subsequent cellular events (capsule enlargement and cell body re-growth) determine the pathogenic potential of *C. neoformans.*

After the invasion of the CNS, *C. neoformans* has access to catecholamines that can be used to synthesize melanin, an important virulence factor. Therefore, the melanin phenotype and laccase activity observed in vitro may explain the higher fungal burden in the CNS found for the hypervirulent strains. However, this correlation is not absolute, because strain WM628 was not able to produce melanin in vitro but showed an increase in melanin and the capsule in vivo. Perhaps this is a compensatory mechanism to ensure the survival of the fungus in the CNS.

Deployment of the capsule, for example, is the most studied *C. neoformans* virulence factor. Several aspects regarding capsule structure, antigenic properties, and role in virulence have already been reported [17,18,58]. In our study, in vivo capsule enlargement was positively correlated with mice mortality and was associated with a higher fungal burden in the BS and PE 10 days post infection for the virulent strains. The absence of or reduction in the capsule facilitates the host's defense response and disease outcome [16,17]. However, it is worth mentioning that in vitro capsule enlargement in MM alone did not predict virulence in vivo. These findings highlight in vivo morphology studies' importance in establishing an association with virulence.

C. neoformans cellular remodeling is dynamic, and in our study varied according to the time and compartment of infection. Considering the chronological events of cellular morphogenesis during infection, remodeling strategies related to survival, tissue invasion, and fungal dissemination may be expected early, while mechanisms related to evasion of the immune response and colonization of the host, favoring fungal maintenance within the host may appear later. Based on these ideas, we performed dual RNA-seq analyses of fungal and host cells from the BS using the hypervirulent strain H99. Previous studies have also performed transcriptional analysis of *Cryptococcus* from the cerebrospinal fluid [6,48,59] and cell culture. However, in general, we did not observe a similar transcriptional response comparing these studies. This difference may be related to differences in the fungal response to host niches. Here, we analyzed yeasts directly from the bronchoalveolar space, a totally different environment compared to cerebrospinal fluid and cell culture in laboratory conditions.

We initially observed that transcripts for many genes encoding ribosomal subunits were upregulated early after infection, a finding consistent with the adaptation to the host and the initiation of proliferation. That is, cells with higher ribosomal expression would show a higher growth rate [60]. This information aligns with our hypothesis that small cells from the BS show increased cell replication early in the infection, contributing to tissue invasion. Previous reports demonstrated alterations in ribosomal modulation in *C. neoformans*; however, little is known about the in vivo regulation of protein biosynthesis in *C. neoformans* [61–63]. Our results demonstrate this modulation in a murine model, considering early and late stages of infection, pointing to the importance in cell remodeling. This reinforces the importance of ribosomal regulation during infection, opening perspectives for further evaluation of its role in virulence and the search for new targets for antifungals.

We also found that transcripts encoding functions for energy metabolism were modulated throughout the infection. For example, a downregulation of transcripts involved in ATP synthesis was observed in the early stage of infection, possibly because cells were still adapting to the host from the pre-culture in a rich medium (YPD). We did note increased HXS1 (CNAG_03772) transcripts at the early stage, and this high-affinity glucose transporter is regulated by glucose and involved in fungal virulence [64]. In this context, the level of glucose in the BS seems to possibly be an early signal for the adaptation of *C. neoformans*. This idea is consistent with the expression of monosaccharide transporters previously observed during murine lung colonization [23]. Consequently, this regulation may contribute to cellular remodeling of *C. neoformans*, favoring the optimization of energy expenditure and increase in reproductive fitness. However, increased levels of transcripts involved in ATP synthesis in mitochondria were detected later in the infection, reinforcing previously published data that pointed to the importance of this organelle in fungal virulence [65–68]. This shift in the transcriptional profile occurred concomitantly with the increase in polysaccharide capsule, a high-energy-requiring process. Furthermore, we observed an increase in the regulation of insulin secretion in mice, corroborating previous data [46]. Therefore, this would possibly lead to lower glucose levels and stimulate the regulation of pathways for obtaining energy in *C. neoformans*. Thus, our findings reinforce the idea that *C. neoformans* needs to cope with a variety of stresses during infection (temperature, phagocytosis, oxidative and nitrosative stress, hypoxia, and low glucose levels)

that activate energy-dependent resistance mechanisms (polysaccharide capsule synthesis, inositol, and proteasome regulation), which are critical for fungal survival.

Our RNA-seq analysis revealed additional features of fungal adaptation, including the upregulation of transcripts coding for proteins from the inositol pathway 10 days post infection, consistent with a previous study [48]. This pathway contains three genes that encode myo-inositol oxygenases, which convert myo-inositol into d-glucuronic acid, a substrate of the pentose phosphate cycle and a component of the polysaccharide capsule [48]. Furthermore, the upregulation of this pathway is consistent with increased polysaccharide capsule and higher fungal replication in the CNS, since inositol plays a role in *C. neoformans* brain invasion [49]. We also found that the transcript of the RPT3 gene (CNAG_03904) encoding a putative subunit of the proteasome 2 was upregulated 10 days post infection. The proteasome is essential in cell cycle regulation, transcription, signal transduction, apoptosis, and polysaccharide capsule synthesis [50,52]. The importance of the proteasome is supported by our observation that treatment of infected mice with a proteasome inhibitor (bortezomib) impaired *C. neoformans* cell remodeling after 6 h of infection. In addition, a previous study demonstrated that bortezomib inhibited the polysaccharide capsule synthesis in vitro [52]. However, this does not exclude the possibility that BTZ also affected the mouse proteasome, or another pathway, contributing to the observed effect on fungal cell size. These findings reinforce the role of the proteasome in *C. neoformans* cell remodeling and generate perspectives for the repositioning of bortezomib and other proteasome inhibitors for the treatment of cryptococcosis. Although we did not observe morphological differences after 10 days of treatment (data not shown), this does not exclude the possibility that the treatment induces physiological changes in the fungal cell, such as changes in cell viability and replicative rate. We believe that proteasome assembly is important throughout the infection, and it may help the fungus to cope with the strong immune response against it. However, further studies are still needed to better understand the effect of bortezomib and the proteasome on late times of *C. neoformans* infection.

Considering the mouse response to infection by *C. neoformans*, the most highly upregulated transcripts after 6 h of infection were involved in recognition, uptake, and phagocytosis, including IL-18 and TNF. IL-18 is critical in TH1 responses via IFN-y production, while TNF is associated with activating innate and adaptive responses against *C. neoformans* [69,70]. After phagocytosis, the fungal cell finds an environment with reduced oxygen levels, explaining the downregulation of COX1 and COX2 genes in *C. neoformans*. These genes are involved in Complex IV of the electron transport chain, and their activity requires oxygen as the final electron acceptor [71]. Consistent with our results, previous findings also demonstrated that the in vitro macrophage-induced hypoxia environment leads to the downregulation of COX1 regulation in *C. neoformans* [71]. However, the mouse response is ineffective in controlling *C. neoformans* growth, as evidenced by the higher fungal burden in the organs after 10 days post infection. We hypothesize that small cells may be more readily engulfed by macrophages. However, a higher fungal reproductive fitness of small cells may increase the capability for intracellular proliferation, favoring the selection of these cells to facilitate persistence and disease. Although the timing of the host response plays a role in determining the extent of tissue damage [72], it is ineffective in fungal control. It is unclear how the dynamic response differs for the hypovirulent and non-virulent strains, and this is an important area for future study. Still, we hypothesize that the balance of the pro-inflammatory and anti-inflammatory responses added to immunomodulatory mechanisms (polysaccharide capsule) [73] may be decisive. Since non-lethal and hypovirulent strains have a reduced capsule at late times of infection, this may contribute to the maintenance of a more effective inflammatory response.

5. Conclusions

In conclusion, our findings support a scenario in which the fungus initially deploys mechanisms aimed at survival, proliferation, and tissue invasion. Later, the fungus may focus on mechanisms aimed at resistance to the immune response and colonization, which

are crucial for disease development. A limitation of this study is that it used only four strains of *C. neoformans* to evaluate fungal cell remodeling in vivo. As most of the experiments were conducted in a murine model, this makes the use of many strains unfeasible. In fact, how the differences shown here work for other lineages of the *C. neoformans* complex still need to be elucidated. Despite this, the study brings important contributions on the dynamics of cellular remodeling of *C. neoformans* during infection and generates perspectives for the survey of new therapeutic and diagnostic targets for cryptococcosis.

Supplementary Materials: The following supporting information can be downloaded at: https://www.mdpi.com/article/10.3390/cells11233896/s1, Table S1: H99 transcriptome analysis after infection in murine model. Table S2: Mice transcriptome analysis after infection with *C. neoformans* (H99). Table S3: SHIRPA.

Author Contributions: G.J.C.F., L.G.-E., E.C.P.E., H.C.S.C., L.d.M.B., M.C.C. and D.A.S. prepared the experimental design and conducted the phenotyping, CFU analysis, and animal experimentation. G.J.C.F., S.F. and G.R.d.S.A. performed the MEV assay. J.W.K., M.C. and D.A.S. performed RNA isolation for sequencing and transcriptome analysis. G.J.C.F., N.T.A.P. and D.A.S. performed GO analysis, regulation network constructions, discussed the results, and wrote and approved the final manuscript. T.A.P. and B.G.S. performed histopathology of the brain. All authors have read and agreed to the published version of the manuscript.

Funding: This study was supported by Fundação de Amparo a Pesquisa do Estado de Minas Gerais-FAPEMIG (PPM-00061-18), Coordenação de Aperfeiçoamento de Pessoal de Nível Superior (CAPES), Conselho Nacional de Desenvolvimento Científico e Tecnológico-CNPq (402200/2021-7) Brazilian Ministry of Health (440010/2018-7), and the Canadian Institutes for Health Research (to J.W.K.). D.A.S. (303762/2020-9) is a research fellow of the CNPq.

Institutional Review Board Statement: The animal study protocol was approved by the Institutional Review Board (or Ethics Committee) of Universidade Federal de Minas Gerais (protocol code 235/2017–02/10/2017).

Informed Consent Statement: Not applicable.

Data Availability Statement: Datasets were submitted to the Gene Expression Omnibus database (http://www.ncbi.nlm.nih.gov/geo/, accessed on 1 November 2022), accession number GSE206758.

Acknowledgments: Paul Anderson Souza Guimarães for technical support in transcriptome analysis.

Conflicts of Interest: The authors declare no conflict of interest.

References

1. Chen, S.C.; Meyer, W.; Sorrell, T.C. *Cryptococcus gattii* infections. *Clin. Microbiol. Rev.* **2014**, *27*, 980–1024. [CrossRef] [PubMed]
2. Ballou, E.R.; Johnston, S.A. The cause and effect of *Cryptococcus* interactions with the host. *Curr. Opin. Microbiol.* **2017**, *40*, 88–94. [CrossRef] [PubMed]
3. Rajasingham, R.; Govender, N.P.; Jordan, A.; Loyse, A.; Shroufi, A.; Denning, D.W.; Meya, D.B.; Chiller, T.M.; Boulware, D.R. The global burden of HIV-associated cryptococcal infection in adults in 2020: A modelling analysis. *Lancet Infect. Dis.* **2022**, *22*, 1748–1755. [CrossRef]
4. Lin, X. *Cryptococcus neoformans*: Morphogenesis, infection, and evolution. *Infect. Genet. Evol.* **2009**, *9*, 401–416. [CrossRef] [PubMed]
5. Wang, L.; Lin, X. The morphotype heterogeneity in *Cryptococcus neoformans*. *Curr. Opin. Microbiol.* **2015**, *26*, 60–64. [CrossRef] [PubMed]
6. Denham, S.T.; Brammer, B.; Chung, K.Y.; Wambaugh, M.A.; Bednarek, J.M.; Guo, L.; Moreau, C.T.; Brown, J.C.S. A dissemination-prone morphotype enhances extrapulmonary organ entry by *Cryptococcus neoformans*. *Cell Host Microbe* **2022**, *30*, 1382–1400.e8. [CrossRef]
7. Fernandes, K.E.; Fraser, J.A.; Carter, D.A. Lineages Derived from *Cryptococcus neoformans* Type Strain H99 Support a Link between the Capacity to Be Pleomorphic and Virulence. *mBio* **2022**, *13*, e0028322. [CrossRef]
8. Velagapudi, R.; Hsueh, Y.P.; Geunes-Boyer, S.; Wright, J.R.; Heitman, J. Spores as infectious propagules of *Cryptococcus neoformans*. *Infect. Immun.* **2009**, *77*, 4345–4355. [CrossRef]
9. Crabtree, J.N.; Okagaki, L.H.; Wiesner, D.L.; Strain, A.K.; Nielsen, J.N.; Nielsen, K. Titan cell production enhances the virulence of *Cryptococcus neoformans*. *Infect. Immun.* **2012**, *80*, 3776–3785. [CrossRef]

10. Dambuza, I.M.; Drake, T.; Chapuis, A.; Zhou, X.; Correia, J.; Taylor-Smith, L.; LeGrave, N.; Rasmussen, T.; Fisher, M.C.; Bicanic, T.; et al. The *Cryptococcus neoformans* Titan cell is an inducible and regulated morphotype underlying pathogenesis. *PLoS Pathog.* **2018**, *14*, e1006978. [CrossRef]
11. Okagaki, L.H.; Nielsen, K. Titan cells confer protection from phagocytosis in *Cryptococcus neoformans* infections. *Eukaryot. Cell* **2012**, *11*, 820–826. [CrossRef] [PubMed]
12. Dalia, A.B.; Weiser, J.N. Minimization of bacterial size allows for complement evasion and is overcome by the agglutinating effect of antibody. *Cell Host Microbe* **2011**, *10*, 486–496. [CrossRef] [PubMed]
13. Jayatilake, J.A.; Samaranayake, Y.H.; Samaranayake, L.P. An ultrastructural and a cytochemical study of candidal invasion of reconstituted human oral epithelium. *J. Oral Pathol. Med.* **2005**, *34*, 240–246. [CrossRef] [PubMed]
14. Mavor, A.L.; Thewes, S.; Hube, B. Systemic fungal infections caused by Candida species: Epidemiology, infection process and virulence attributes. *Curr. Drug Targets* **2005**, *6*, 863–874. [CrossRef]
15. Hommel, B.; Sturny-Leclère, A.; Volant, S.; Veluppillai, N.; Duchateau, M.; Yu, C.H.; Hourdel, V.; Varet, H.; Matondo, M.; Perfect, J.R.; et al. *Cryptococcus neoformans* resists to drastic conditions by switching to viable but non-culturable cell phenotype. *PLoS Pathog.* **2019**, *15*, e1007945. [CrossRef]
16. Alspaugh, J.A. Virulence mechanisms and *Cryptococcus neoformans* pathogenesis. *Fungal Genet. Biol.* **2015**, *78*, 55–58. [CrossRef]
17. Araujo, G.e.S.; Fonseca, F.L.; Pontes, B.; Torres, A.; Cordero, R.J.; Zancopé-Oliveira, R.M.; Casadevall, A.; Viana, N.B.; Nimrichter, L.; Rodrigues, M.L.; et al. Capsules from pathogenic and non-pathogenic *Cryptococcus* spp. manifest significant differences in structure and ability to protect against phagocytic cells. *PLoS ONE* **2012**, *7*, e29561. [CrossRef]
18. Casadevall, A.; Rosas, A.L.; Nosanchuk, J.D. Melanin and virulence in *Cryptococcus neoformans*. *Curr. Opin. Microbiol.* **2000**, *3*, 354–358. [CrossRef]
19. Feldmesser, M.; Kress, Y.; Casadevall, A. Dynamic changes in the morphology of *Cryptococcus neoformans* during murine pulmonary infection. *Microbiology* **2001**, *147*, 2355–2365. [CrossRef]
20. Rivera, J.; Feldmesser, M.; Cammer, M.; Casadevall, A. Organ-dependent variation of capsule thickness in *Cryptococcus neoformans* during experimental murine infection. *Infect. Immun.* **1998**, *66*, 5027–5030. [CrossRef]
21. Ferreira, G.F.; Santos, J.R.; Costa, M.C.; Holanda, R.A.; Denadai, Â.; Freitas, G.J.; Santos, Á.; Tavares, P.B.; Paixão, T.A.; Santos, D.A. Heteroresistance to Itraconazole Alters the Morphology and Increases the Virulence of *Cryptococcus gattii*. *Antimicrob. Agents Chemother.* **2015**, *59*, 4600–4609. [CrossRef] [PubMed]
22. Fernandes, K.E.; Dwyer, C.; Campbell, L.T.; Carter, D.A. Species in the *Cryptococcus gattii* Complex Differ in Capsule and Cell Size following Growth under Capsule-Inducing Conditions. *mSphere* **2016**, *1*, e00350-16. [CrossRef] [PubMed]
23. Hu, G.; Cheng, P.Y.; Sham, A.; Perfect, J.R.; Kronstad, J.W. Metabolic adaptation in *Cryptococcus neoformans* during early murine pulmonary infection. *Mol. Microbiol.* **2008**, *69*, 1456–1475. [CrossRef] [PubMed]
24. Charlier, C.; Chrétien, F.; Lortholary, O.; Dromer, F. [Early capsule structure changes associated with *Cryptococcus neoformans* crossing of the blood-brain barrier]. *Med. Sci.* **2005**, *21*, 685–687. [CrossRef]
25. Fries, B.C.; Goldman, D.L.; Casadevall, A. Phenotypic switching in *Cryptococcus neoformans*. *Microbes Infect.* **2002**, *4*, 1345–1352. [CrossRef]
26. Barcellos, V.A.; Martins, L.M.S.; Fontes, A.C.L.; Reuwsaat, J.C.V.; Squizani, E.D.; de Sousa Araújo, G.R.; Frases, S.; Staats, C.C.; Schrank, A.; Kmetzsch, L.; et al. Genotypic and Phenotypic Diversity of *Cryptococcus gattii* VGII Clinical Isolates and Its Impact on Virulence. *Front. Microbiol.* **2018**, *9*, 132. [CrossRef]
27. Li, C.; Lev, S.; Saiardi, A.; Desmarini, D.; Sorrell, T.C.; Djordjevic, J.T. Identification of a major IP5 kinase in *Cryptococcus neoformans* confirms that PP-IP5/IP7, not IP6, is essential for virulence. *Sci. Rep.* **2016**, *6*, 23927. [CrossRef]
28. Missall, T.A.; Moran, J.M.; Corbett, J.A.; Lodge, J.K. Distinct stress responses of two functional laccases in *Cryptococcus neoformans* are revealed in the absence of the thiol-specific antioxidant Tsa1. *Eukaryot. Cell* **2005**, *4*, 202–208. [CrossRef]
29. Singh, A.; Panting, R.J.; Varma, A.; Saijo, T.; Waldron, K.J.; Jong, A.; Ngamskulrungroj, P.; Chang, Y.C.; Rutherford, J.C.; Kwon-Chung, K.J. Factors required for activation of urease as a virulence determinant in *Cryptococcus neoformans*. *mBio* **2013**, *4*, e00220-13. [CrossRef]
30. Fu, M.S.; Coelho, C.; De Leon-Rodriguez, C.M.; Rossi, D.C.P.; Camacho, E.; Jung, E.H.; Kulkarni, M.; Casadevall, A. *Cryptococcus neoformans* urease affects the outcome of intracellular pathogenesis by modulating phagolysosomal pH. *PLoS Pathog.* **2018**, *14*, e1007144. [CrossRef]
31. Santos, J.R.A.; Ribeiro, N.Q.; Bastos, R.W.; Holanda, R.A.; Silva, L.C.; Queiroz, E.R.; Santos, D.A. High-dose fluconazole in combination with amphotericin B is more efficient than monotherapy in murine model of cryptococcosis. *Sci. Rep.* **2017**, *7*, 4661. [CrossRef] [PubMed]
32. Oliveira, L.V.N.; Costa, M.C.; Magalhães, T.F.F.; Bastos, R.W.; Santos, P.C.; Carneiro, H.C.S.; Ribeiro, N.Q.; Ferreira, G.F.; Ribeiro, L.S.; Gonçalves, A.P.F.; et al. Influenza A Virus as a Predisposing Factor for Cryptococcosis. *Front. Cell. Infect. Microbiol.* **2017**, *7*, 419. [CrossRef] [PubMed]
33. Santos, J.R.; Holanda, R.A.; Frases, S.; Bravim, M.; Araujo, G.e.S.; Santos, P.C.; Costa, M.C.; Ribeiro, M.J.; Ferreira, G.F.; Baltazar, L.M.; et al. Fluconazole alters the polysaccharide capsule of *Cryptococcus gattii* and leads to distinct behaviors in murine Cryptococcosis. *PLoS ONE* **2014**, *9*, e112669. [CrossRef] [PubMed]

34. Ferreira, G.F.; Baltazar, L.e.M.; Santos, J.R.; Monteiro, A.S.; Fraga, L.A.; Resende-Stoianoff, M.A.; Santos, D.A. The role of oxidative and nitrosative bursts caused by azoles and amphotericin B against the fungal pathogen *Cryptococcus gattii*. *J. Antimicrob. Chemother.* **2013**, *68*, 1801–1811. [CrossRef]
35. Araújo, G.R.S.; Freitas, G.J.C.; Fonseca, F.L.; Leite, P.E.C.; Rocha, G.M.; de Souza, W.; Santos, D.A.; Frases, S. The environmental yeast *Cryptococcus liquefaciens* produces capsular and secreted polysaccharides with similar pathogenic properties to those of *C. neoformans*. *Sci. Rep.* **2017**, *7*, 46768. [CrossRef]
36. Thompson, G.R.; Wiederhold, N.P.; Najvar, L.K.; Bocanegra, R.; Kirkpatrick, W.R.; Graybill, J.R.; Patterson, T.F. A murine model of *Cryptococcus gattii* meningoencephalitis. *J. Antimicrob. Chemother.* **2012**, *67*, 1432–1438. [CrossRef]
37. Bishop, J.A.; Nelson, A.M.; Merz, W.G.; Askin, F.B.; Riedel, S. Evaluation of the detection of melanin by the Fontana-Masson silver stain in tissue with a wide range of organisms including Cryptococcus. *Hum. Pathol.* **2012**, *43*, 898–903. [CrossRef]
38. Bolger, A.M.; Lohse, M.; Usadel, B. Trimmomatic: A flexible trimmer for Illumina sequence data. *Bioinformatics* **2014**, *30*, 2114–2120. [CrossRef]
39. Dobin, A.; Davis, C.A.; Schlesinger, F.; Drenkow, J.; Zaleski, C.; Jha, S.; Batut, P.; Chaisson, M.; Gingeras, T.R. STAR: Ultrafast universal RNA-seq aligner. *Bioinformatics* **2013**, *29*, 15–21. [CrossRef]
40. Liao, Y.; Smyth, G.K.; Shi, W. featureCounts: An efficient general purpose program for assigning sequence reads to genomic features. *Bioinformatics* **2014**, *30*, 923–930. [CrossRef]
41. Love, M.I.; Huber, W.; Anders, S. Moderated estimation of fold change and dispersion for RNA-seq data with DESeq2. *Genome Biol.* **2014**, *15*, 550. [CrossRef] [PubMed]
42. Ge, S.X.; Jung, D.; Yao, R. ShinyGO: A graphical gene-set enrichment tool for animals and plants. *Bioinformatics* **2020**, *36*, 2628–2629. [CrossRef] [PubMed]
43. Reagan-Shaw, S.; Nihal, M.; Ahmad, N. Dose translation from animal to human studies revisited. *FASEB J.* **2008**, *22*, 659–661. [CrossRef] [PubMed]
44. Rogers, D.C.; Fisher, E.M.; Brown, S.D.; Peters, J.; Hunter, A.J.; Martin, J.E. Behavioral and functional analysis of mouse phenotype: SHIRPA, a proposed protocol for comprehensive phenotype assessment. *Mamm. Genome* **1997**, *8*, 711–713. [CrossRef]
45. Seelbinder, B.; Wallstabe, J.; Marischen, L.; Weiss, E.; Wurster, S.; Page, L.; Löffler, C.; Bussemer, L.; Schmitt, A.L.; Wolf, T.; et al. Triple RNA-Seq Reveals Synergy in a Human Virus-Fungus Co-infection Model. *Cell Rep.* **2020**, *33*, 108389. [CrossRef]
46. Li, H.; Li, Y.; Sun, T.; Du, W.; Li, C.; Suo, C.; Meng, Y.; Liang, Q.; Lan, T.; Zhong, M.; et al. Unveil the transcriptional landscape at the Cryptococcus-host axis in mice and nonhuman primates. *PLoS Negl. Trop. Dis.* **2019**, *13*, e0007566. [CrossRef]
47. Henry, J.; Guillotte, A.; Luberto, C.; Del Poeta, M. Characterization of inositol phospho-sphingolipid-phospholipase C 1 (Isc1) in *Cryptococcus neoformans* reveals unique biochemical features. *FEBS Lett.* **2011**, *585*, 635–640. [CrossRef]
48. Wang, Y.; Wear, M.; Kohli, G.; Vij, R.; Giamberardino, C.; Shah, A.; Toffaletti, D.L.; Yu, C.A.; Perfect, J.R.; Casadevall, A.; et al. Inositol Metabolism Regulates Capsule Structure and Virulence in the Human Pathogen *Cryptococcus neoformans*. *mBio* **2021**, *12*, e0279021. [CrossRef]
49. Liu, T.B.; Kim, J.C.; Wang, Y.; Toffaletti, D.L.; Eugenin, E.; Perfect, J.R.; Kim, K.J.; Xue, C. Brain inositol is a novel stimulator for promoting *Cryptococcus* penetration of the blood-brain barrier. *PLoS Pathog.* **2013**, *9*, e1003247. [CrossRef]
50. Bijlmakers, M.J. Ubiquitination and the Proteasome as Drug Targets in Trypanosomatid Diseases. *Front. Chem.* **2020**, *8*, 630888. [CrossRef]
51. Hossain, S.; Veri, A.O.; Cowen, L.E. The Proteasome Governs Fungal Morphogenesis via Functional Connections with Hsp90 and cAMP-Protein Kinase A Signaling. *mBio* **2020**, *11*, e00290-20. [CrossRef] [PubMed]
52. Geddes, J.M.; Caza, M.; Croll, D.; Stoynov, N.; Foster, L.J.; Kronstad, J.W. Analysis of the Protein Kinase A-Regulated Proteome of *Cryptococcus neoformans* Identifies a Role for the Ubiquitin-Proteasome Pathway in Capsule Formation. *mBio* **2016**, *7*, e01862-15. [CrossRef] [PubMed]
53. Cox, G.M.; Harrison, T.S.; McDade, H.C.; Taborda, C.P.; Heinrich, G.; Casadevall, A.; Perfect, J.R. Superoxide dismutase influences the virulence of *Cryptococcus neoformans* by affecting growth within macrophages. *Infect. Immun.* **2003**, *71*, 173–180. [CrossRef]
54. Kwon-Chung, K.J.; Fraser, J.A.; Doering, T.L.; Wang, Z.; Janbon, G.; Idnurm, A.; Bahn, Y.S. *Cryptococcus neoformans* and *Cryptococcus gattii*, the etiologic agents of cryptococcosis. *Cold Spring Harb. Perspect. Med.* **2014**, *4*, a019760. [CrossRef]
55. May, R.C.; Stone, N.R.; Wiesner, D.L.; Bicanic, T.; Nielsen, K. Cryptococcus: From environmental saprophyte to global pathogen. *Nat. Rev. Microbiol.* **2016**, *14*, 106–117. [CrossRef] [PubMed]
56. Akins, R.A. An update on antifungal targets and mechanisms of resistance in *Candida albicans*. *Med. Mycol.* **2005**, *43*, 285–318. [CrossRef] [PubMed]
57. Ma, H.; May, R.C. Virulence in *Cryptococcus* species. *Adv. Appl. Microbiol.* **2009**, *67*, 131–190. [CrossRef]
58. García-Rodas, R.; Cordero, R.J.; Trevijano-Contador, N.; Janbon, G.; Moyrand, F.; Casadevall, A.; Zaragoza, O. Capsule growth in *Cryptococcus neoformans* is coordinated with cell cycle progression. *mBio* **2014**, *5*, e00945-14. [CrossRef]
59. Chen, Y.; Toffaletti, D.L.; Tenor, J.L.; Litvintseva, A.P.; Fang, C.; Mitchell, T.G.; McDonald, T.R.; Nielsen, K.; Boulware, D.R.; Bicanic, T.; et al. The *Cryptococcus neoformans* transcriptome at the site of human meningitis. *mBio* **2014**, *5*, e01087-13. [CrossRef]
60. Zhao, Y.; Sohn, J.H.; Warner, J.R. Autoregulation in the biosynthesis of ribosomes. *Mol. Cell. Biol.* **2003**, *23*, 699–707. [CrossRef]
61. Cheng, Z.; Mugler, C.F.; Keskin, A.; Hodapp, S.; Chan, L.Y.; Weis, K.; Mertins, P.; Regev, A.; Jovanovic, M.; Brar, G.A. Small and Large Ribosomal Subunit Deficiencies Lead to Distinct Gene Expression Signatures that Reflect Cellular Growth Rate. *Mol. Cell* **2019**, *73*, 36–47.e10. [CrossRef] [PubMed]

62. Leipheimer, J.; Bloom, A.L.M.; Campomizzi, C.S.; Salei, Y.; Panepinto, J.C. Translational Regulation Promotes Oxidative Stress Resistance in the Human Fungal Pathogen *Cryptococcus neoformans*. *mBio* **2019**, *10*, e02143-19. [CrossRef] [PubMed]
63. Li, C.; Hou, S.; Ma, X.; Li, J.; Huo, L.; Zhang, P.; Hao, X.; Zhu, X. Epigenetic regulation of virulence and the transcription of ribosomal protein genes involves a YEATS family protein in *Cryptococcus deneoformans*. *FEMS Yeast Res.* **2021**, *21*, foab001. [CrossRef]
64. Liu, T.B.; Wang, Y.; Baker, G.M.; Fahmy, H.; Jiang, L.; Xue, C. The glucose sensor-like protein Hxs1 is a high-affinity glucose transporter and required for virulence in *Cryptococcus neoformans*. *PLoS ONE* **2013**, *8*, e64239. [CrossRef] [PubMed]
65. Steen, B.R.; Zuyderduyn, S.; Toffaletti, D.L.; Marra, M.; Jones, S.J.; Perfect, J.R.; Kronstad, J. *Cryptococcus neoformans* gene expression during experimental cryptococcal meningitis. *Eukaryot. Cell* **2003**, *2*, 1336–1349. [CrossRef]
66. Missall, T.A.; Pusateri, M.E.; Donlin, M.J.; Chambers, K.T.; Corbett, J.A.; Lodge, J.K. Posttranslational, translational, and transcriptional responses to nitric oxide stress in *Cryptococcus neoformans*: Implications for virulence. *Eukaryot. Cell* **2006**, *5*, 518–529. [CrossRef]
67. Upadhya, R.; Campbell, L.T.; Donlin, M.J.; Aurora, R.; Lodge, J.K. Global transcriptome profile of *Cryptococcus neoformans* during exposure to hydrogen peroxide induced oxidative stress. *PLoS ONE* **2013**, *8*, e55110. [CrossRef]
68. Lev, S.; Li, C.; Desmarini, D.; Liuwantara, D.; Sorrell, T.C.; Hawthorne, W.J.; Djordjevic, J.T. Monitoring Glycolysis and Respiration Highlights Metabolic Inflexibility of *Cryptococcus neoformans*. *Pathogens* **2020**, *9*, 684. [CrossRef]
69. Kawakami, K.; Qureshi, M.H.; Zhang, T.; Okamura, H.; Kurimoto, M.; Saito, A. IL-18 protects mice against pulmonary and disseminated infection with *Cryptococcus neoformans* by inducing IFN-gamma production. *J. Immunol.* **1997**, *159*, 5528–5534.
70. Fa, Z.; Xu, J.; Yi, J.; Sang, J.; Pan, W.; Xie, Q.; Yang, R.; Fang, W.; Liao, W.; Olszewski, M.A. TNF-α-Producing *Cryptococcus neoformans* Exerts Protective Effects on Host Defenses in Murine Pulmonary Cryptococcosis. *Front. Immunol.* **2019**, *10*, 1725. [CrossRef]
71. Derengowski, L.d.S.; Paes, H.C.; Albuquerque, P.; Tavares, A.H.; Fernandes, L.; Silva-Pereira, I.; Casadevall, A. The transcriptional response of *Cryptococcus neoformans* to ingestion by Acanthamoeba castellanii and macrophages provides insights into the evolutionary adaptation to the mammalian host. *Eukaryot. Cell* **2013**, *12*, 761–774. [CrossRef] [PubMed]
72. Shourian, M.; Qureshi, S.T. Resistance and Tolerance to Cryptococcal Infection: An Intricate Balance That Controls the Development of Disease. *Front. Immunol.* **2019**, *10*, 66. [CrossRef] [PubMed]
73. Decote-Ricardo, D.; LaRocque-de-Freitas, I.F.; Rocha, J.D.B.; Nascimento, D.O.; Nunes, M.P.; Morrot, A.; Freire-de-Lima, L.; Previato, J.O.; Mendonça-Previato, L.; Freire-de-Lima, C.G. Immunomodulatory Role of Capsular Polysaccharides Constituents of *Cryptococcus neoformans*. *Front. Med.* **2019**, *6*, 129. [CrossRef] [PubMed]

O remodelamento celular em *Cryptococcus gattii*: descobertas e perspectivas

1. INTRODUÇÃO

Cryptococcus gattii é a segunda espécie principalmente relacionada a Criptococose e que geralmente infecta pacientes imunocompetentes (BYRNES; HEITMAN, 2009). Essa espécie emergiu em 1999, quando foi responsável por um surto na Ilha de Vancouver e se espalhou para o noroeste do Pacífico (PNW) dos Estados Unidos (FYFE; MACDOUGALL; ROMNEY; STARR *et al.*, 2008; STEPHEN; LESTER; BLACK; FYFE *et al.*, 2002). Tradicionalmente apresentou restrição geográfica às regiões tropicais e subtropicais, porém em 2006 causou um surto na região temperada da Ilha de Vancouver, indicando que esta espécie também pode ter um ambiente ecológico mais amplo, assim como *C. neoformans* (UPTON; FRASER; KIDD; BRETZ *et al.*, 2007).

Semelhante a *C. neoformans*, *C. gattii* também pode invadir o trato respiratório, causar doença pulmonar, se espalhar para outros órgãos e causar meningoencefalite (CHEN; MEYER; SORRELL, 2014). Ainda, ambas as espécies compartilham de fatores de virulência classicamente descritos para o gênero *Cryptococcus*, como síntese de cápsula polissacarídica, melanina, urease e fosfolipase (BARCELLOS; MARTINS; FONTES; REUWSAAT *et al.*, 2018; GARCÍA-RODAS; CORDERO; TREVIJANO-CONTADOR; JANBON *et al.*, 2014). Portanto, considerando a semelhança de rota infecciosa e fatores de virulência entre ambas as espécies, nós decidimos avaliar a dinâmica das alterações morfológicas para 10 linhagens de *C. gattii* durante a infecção.

Em geral, nós observamos que no estágio inicial da infecção, *C. gattii* apresenta uma reorganização morfológica semelhante a observada para *C. neoformans*. Nesse momento observamos um predomínio de células pequenas (<3um) no trato respiratório, associada a invasão do epitélio pulmonar e disseminação para o sistema nervoso central. Tardiamente, observamos um aumento da cápsula polissacarídica para todas as linhagens. Entretanto, esse aumento não foi suficiente para predizer a virulência como visto em *C. neoformans*. Especulamos que diferenças estruturais na cápsula polissacarídica de *C. gattii* podem ser mais determinantes para a virulência do que o tamanho em si.

2. MATERIAIS E MÉTODOS

Para o desenvolvimento deste estudo, utilizamos a mesma metodologia descrita no artigo anterior "The dynamics of *Cryptococcus neoformans* cell and transcriptional remodeling during infection".

3. RESULTADOS E DISCUSSÃO

A análise da sobrevida para as linhagens de *C. gattii* revelou diferentes perfis de letalidade (Figura 1). Para o isolado WM779 (Lt50=24 dias) encontramos um perfil de letalidade precoce em relação a R265 (Lt50=29 dias). Para WM178

(Lt50=40 dias) e WM179 (Lt50=41 dias) observou-se uma maior sobrevida quando comparadas a R265 (Lt50=29 dias). A cepa WM161 não foi capaz de levar a letalidade (Não letal – NL) dos camundongos. Assim, conforme a sobrevida, nós classificamos as linhagens como hipervirulentas (Lt=21 – 27 dias), virulentas (Lt=28 – 32 dias), pouco virulentas (Lt=27 – 45 dias) e não-letais.

Posteriormente, ao avaliar a morfologia diretamente dos tecidos, nós vimos que todas as linhagens apresentaram redução do corpo celular após 6 horas de infecção, em relação ao inóculo inicial (Figura 1). Esses achados corroboraram com os resultados do estudo de *C. neoformans* e reforçaram a nossa tese de que as células pequenas são importantes para a adaptação inicial ao contexto do hospedeiro, invasão do tecido pulmonar e disseminação para o sistema nervoso central.

Após 24 horas de infecção observamos um "recrescimento" do corpo celular acompanhado de um aumento da capsula polissacarídica para todas as linhagens. Esse perfil ascendente se manteve após 10 dias de infecção e surpreendetemente, o aumento da cápsula polissacarídica não foi suficiente para predizer a virulência em *C. gattii*, sendo uma diferença importante em relação aos achados para *C. neoformans* (Figura 1). Urai *et al* (2015) ao comparar cepas de *C. gattii* e *C. neoformans* com dimensões capsulares semelhantes, demonstraram que a desacetilação de GXM, observada apenas para *C. gattii*, é importante para a virulência desta espécie (URAI; KANEKO; UENO; OKUBO *et al.*, 2015). Além disso, a capsula polissacarídica de *C. gattii* também é capaz de inibir a maturação de células dendriticas e a proliferação de Celulas T (SYME; SPURRELL; AMANKWAH; GREEN *et al.*, 2002; YAUCH; LAM; LEVITZ, 2006). Com isso, a nossa hipótese é de que, para *C. gattii*, mudanças estruturais na cápsula podem ser mais determinantes para a virulência do que sua própria espessura em si. Embora tenham tamanho capsular semelhante, é possível que diferenças estruturais na capsula polissacarídica alterem o reconhecimento imunológico durante a infecção e levem a diferentes padrões de virulência, cepa dependente. Para explorar essa hipótese, ainda serão realizadas análises da estrutura capsular das diferentes linhagens de *C. gattii* e dosagem de citocinas pró e anti-inflamatórias nos diferentes tempos da infecção.

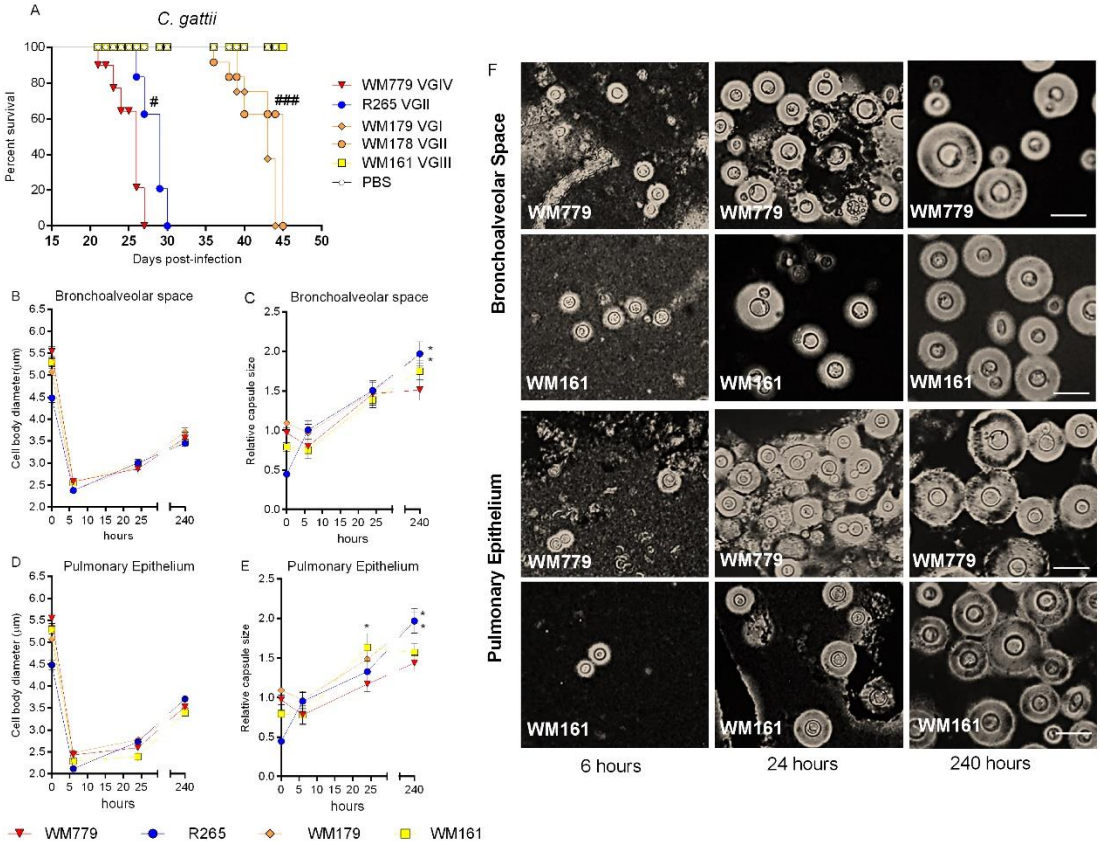

Figure 1: Dinâmica da variação morfológica de *C. gattii in vivo*. A) Curva de mortalidade após infecção intratraqueal com $1x10^5$ células. (B-E) Variação morfológica no espaço broncoalveolar e epitélio pulmonar de quarto cepas de *C. gattii* após 6, 24 e 240 houras de infecção. Média de valores comparados a cepa WM779 (∗p =< 0.05). (F) Coloração com tinta nanquin de leveduras recuparadas do espaço broncoalveolar e epitélio pulmonar após diferentes tempos de infecção. Barra: 5µm.

4. REFERÊNCIAS

1. Byrnes EJ, Heitman J. 2009. *Cryptococcus* gattii outbreak expands into the Northwestern United States with fatal consequences. F1000 Biol Rep 1.

2. Fyfe M, MacDougall L, Romney M, Starr M, Pearce M, Mak S, Mithani S, Kibsey P. 2008. *Cryptococcus* gattii infections on Vancouver Island, British Columbia, Canada: emergence of a tropical fungus in a temperate environment. Can Commun Dis Rep 34:1-12.

3. Stephen C, Lester S, Black W, Fyfe M, Raverty S. 2002. Multispecies outbreak of cryptococcosis on southern Vancouver Island, British Columbia. Can Vet J 43:792-4.

4. Upton A, Fraser JA, Kidd SE, Bretz C, Bartlett KH, Heitman J, Marr KA. 2007. First contemporary case of human infection with *Cryptococcus* gattii in Puget Sound: evidence for spread of the Vancouver Island outbreak. J Clin Microbiol 45:3086-8.

1818 5. Chen SC, Meyer W, Sorrell TC. 2014. *Cryptococcus* gattii infections. Clin Microbiol Rev 27:980-
1819 1024.

1820 6. Barcellos VA, Martins LMS, Fontes ACL, Reuwsaat JCV, Squizani ED, de Sousa Araújo GR, Frases
1821 S, Staats CC, Schrank A, Kmetzsch L, Vainstein MH. 2018. Genotypic and Phenotypic Diversity of.
1822 Front Microbiol 9:132.

1823 7. García-Rodas R, Cordero RJ, Trevijano-Contador N, Janbon G, Moyrand F, Casadevall A,
1824 Zaragoza O. 2014. Capsule growth in *Cryptococcus* neoformans is coordinated with cell cycle
1825 progression. MBio 5:e00945-14.

1826 8. Urai M, Kaneko Y, Ueno K, Okubo Y, Aizawa T, Fukazawa H, Sugita T, Ohno H, Shibuya K, Kinjo
1827 Y, Miyazaki Y. 2015. Evasion of Innate Immune Responses by the Highly Virulent *Cryptococcus*
1828 gattii by Altering Capsule Glucuronoxylomannan Structure. Front Cell Infect Microbiol 5:101.

1829 9. Yauch LE, Lam JS, Levitz SM. 2006. Direct inhibition of T-cell responses by the *Cryptococcus*
1830 capsular polysaccharide glucuronoxylomannan. PLoS Pathog 2:e120.

1831 10. Syme RM, Spurrell JC, Amankwah EK, Green FH, Mody CH. 2002. Primary dendritic cells
1832 phagocytose *Cryptococcus* neoformans via mannose receptors and Fcgamma receptor II for
1833 presentation to T lymphocytes. Infect Immun 70:5972-81.

1834

1835

1836

1837

1838

1839

1840

1841

1842

1843

1844

1845

CAPÍTULO 2

Polysaccharide capsule: An insight on fungal-host interactions and vaccine studies

Gustavo J. C. Freitas; Daniel A. Santos.

ABSTRACT

Cryptococcus neoformans and *C. gattii* complexes are the main causative agents of cryptococcosis, a neglected disease with high lethality. The capsule, composed predominantly of the capsular polysaccharide (CP) GXM, is the main virulence factor of this pathogen. The role of CP is well described for *C. neoformans* and; however, there is a scarcity of studies focused on *C. gattii*, especially in the context of the fungal–host interaction. Understanding how the immune system recognizes *C. gattii* can generate meaningful information for diagnosing, preventing, and treating cryptococcosis. In the current issue of the European Journal of Immunology [Eur. J. Immunol. 2021. 51: 2281–2295], Ueno et al. demonstrate that CP inhibits *C. gattii* recognition by CD11b. In this commentary, we highlight the importance of deeply understanding the role of *C. gattii* CP during infection and how this knowledge would influence the strategies to develop new vaccines against cryptococcosis.

Keywords: *Cryptococcus gattii*, capsular polysaccharide, vaccine, host–pathogen interaction

 DOI: 10.1002/eji.202149349 Eur. J. Immunol. 2021. 51: 2206–2209

Basic

European Journal of Immunology

HIGHLIGHTS

COMMENTARY

Cryptococcus gattii polysaccharide capsule: An insight on fungal-host interactions and vaccine studies

Gustavo J. C. Freitas and Daniel A. Santos

Departament of Microbiology, Institute of Biological Sciences, Universidade Federal de Minas Gerais, Belo Horizonte, Minas Gerais, Brazil

***Cryptococcus neoformans* and *C. gattii* complexes are the main causative agents of cryptococcosis, a neglected disease with high lethality. The capsule, composed predominantlyof the capsular polysaccharide (CP) GXM, is the main virulence factor of this pathogen.The role of CP is well described for *C. neoformans* and; however, there is a scarcity of stud- ies focused on *C. gattii*, especially in the context of the fungal–host interaction. Under- standing how the immune system recognizes *C. gattii* can generate meaningful informa- tion for diagnosing, preventing, and treating cryptococcosis. In the current issue of the *European Journal of Immunology* [Eur. J. Immunol. 2021. 51: 2281–2295], Ueno et al. demon- strate that CP inhibits *C. gattii* recognition by CD11b. In this commentary, we highlight the importance of deeply understanding the role of *C. gattii* CP during infection and how this knowledge would influence the strategies to develop new vaccines against cryptococcosis.**

Keywords: *Cryptococcus gattii* · capsular polysaccharide · vaccine · host–pathogen interaction

See accompanying article by Ueno et al.

Cryptococcosis is a severe fungal infection for humans and animals caused by species from the *Cryptococcus neoformans* and *C. gattii* complexes [1]. The disease initially affects the lungs and can lead to meningitis and meningoencephalitis, the most severe forms of the infection [2]. Neurocriptococcosis affects HIV patients predominantly, with high lethality rates [3, 4].

The description of *C. neoformans* as human pathogen datesmore than 100 years ago and still, the disease is quite challenging [5, 6]. It is a neglected disease with low research support com- pared to other infectious diseases [7]. In addition, current treat- ments have limitations, including toxicity, low blood-brain barrier permeability, high cost, and drug resistance (Fig. 1).

Glucuronoxylomannan (GXM) and galactoxylomannan (GalXM) composes the *Cryptococcus* spp. polysaccharide capsule, its main fungal virulence factor [8–10]. Although its detailed structure has been widely studied for *C. neoformans* (Fig. 1), more studies are still necessary to determine the role of *C. gattii* capsular polysaccharide (CP), especially in the context of the host–pathogen interaction.

In this issue of the *European Journal of Immunology*, Ueno et al. [11] provided new insights about the role of *C. gattii* CP by investigating mechanisms responsible for the low virulence of an acapsular *C. gattii* strain, which they previously described [12, 13]. They proved that *C. gattii* CP is essential for pathogenicity and evasion from the immune system. Acapsular yeasts were quickly recognized by CD11b – SyK and killed by dendritic cells (DC). Otherwise, the treatment of acapsular *C. gattii* with extracellular CP coated cell wall antigens. It hampered fungal recognition by DC, reduced phagocytosis and cytokine production.

During infection, *C. neoformans* and *C. gattii* can alter the polarization of T-helper (Th) cells, which can be orchestrated by DC [14]. However, it is not clear yet which specific *C. gat-tii* molecule binds to CD11b and drives the production of the Th1 and Th17 cytokines (IL-6 and IL-23) presented by Uenoet al. Additionally, previous studies proved that *Cryptococcus* sp.

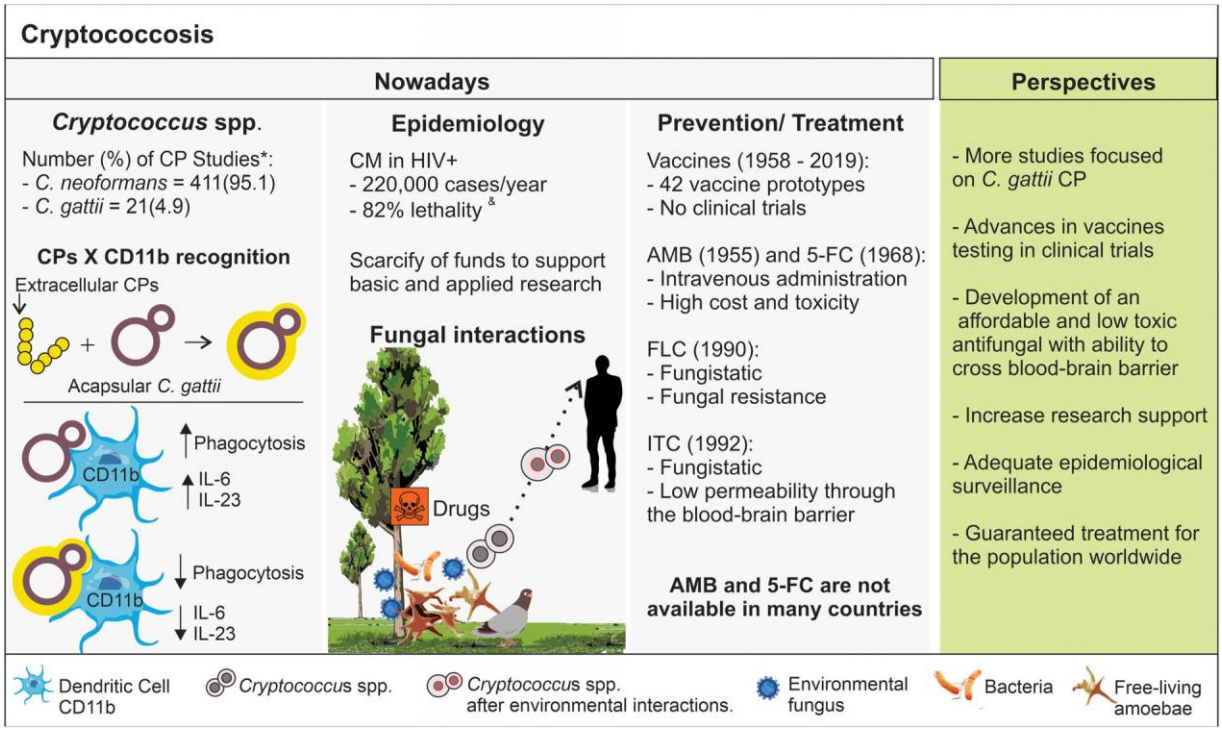

Figure 1. Cryptococcosis: current scenario, challenges, and perspectives. To date, little is known about the role of *C. gattii* capsular polysaccharide (CP) in fungal-host interaction since most of the studies focus on *C. neoformans* CP. Ueno et al. [11] demonstrated that CP mediates the inhibition of the recognition of acapsular *C. gattii* by CD11b. The treatment of acapsular *C. gattii* with extracellular CP coated cell wall antigens. It hampered fungal recognition by DC, reduced phagocytosis and cytokine production. Cryptococcosis has a high mortality rate, but lower budget for basic and applied science to support research is available. *C. gattii* is an environmental pathogen, susceptible to stresses such as drugs (agrochemicals and antibacterial), plants, protozoa, free-living amoebae [24], bacteria [25], and other fungi [26]. However, we still need to know how these stresses influence fungus CP and interfere with the pathogen-host interaction (dashed arrow). Unfortunately, there are severe limitations in anticryptococcal therapy and little progress in the field of fungal vaccines. More studies focusing on *C. gattii* CP are necessary to increase the knowledge about the pathogen to favor the development of prevention and treatment strategies. *Data on vaccines were obtained from Pubmed platform data, considering studies published from 1986 to 2021, except reviews, using the keywords "*Cryptococcus neoformans* and capsular polysaccharide" or "*Cryptococcus gattii* and capsular polysaccharide." &[3] Rajasingham et al., *Lancet Infect Dis* 2017. **17**: 873–881. CP: Capsular Polysaccharide. CM: Cryptococcal meningitis. AMB: Amphotericin B. 5-FC: 5-Flucytosine. FLC: fluconazole. ITC: itraconazole

can bind to DC-CD11b and induce Th2 polarization [14–16]. Thus, unraveling the fungal component that binds DC-CD11b would help to understand how this interaction influences the host response.

One intriguing result presented by Ueno et al. is that the effects mediated by CP occurred when *C. gattii* was cultured in yeast-peptone-dextrose (YPD), but not in synthetic-dextrose (SD). The authors hypothesize that SD medium may interfere with the expression of CD11b ligands and nullify the CP-mediated immune effect. However, cell wall structure was not analyzed for *C. gattii* in each medium to confirm this hypothesis. It is well known that culture conditions (media, temperature), host immune system, and drugs (clinical and environmental antifungals) can influence *C. gattii* morphology and, therefore, the fungal-host interaction [17–19]. Thus, it turns that a profound understanding of CP and cell wall structures in different culture conditions can be essential to define how *C. gattii* drives the host immune system.

The influence of culture conditions described by Ueno et al. reinforces previous information about the phenotypic plasticity of *Cryptococcus* spp. [20, 21], leading to the question: What are the best conditions to study virulence and *C. gattii*–host interaction? Previously published data have already shown that the exposure of *C. gattii* to agrochemicals and antifungals may reduce capsule but not necessarily may reduce virulence [17–19]. Considering that CP synthesis is an energy- and time-consuming process, a reduced capsule may indicate that fungal can save time and energy to other critical functions that can influence how *C. gattii* will behave inside a mammalian host. In this context, it is always important to look at the whole-cell morphology and fungal fitness. For example, the clinical antifungal fluconazole increases cell body diameter and reduces *C. gattii* capsule and fitness. These alterations reduce CP antiphagocytic properties, survival inside macrophages, and production of pro-inflammatory cytokines [19]. Furthermore, the agrochemical benomyl reduces *C. gattii* capsule size, increasing fungal fitness, turning hypervirulent a previously avirulent strain [17]. In this context, CP synthesis is a dynamic process that should be linked to other cellular processes for a better understanding of *C. gattii*–host interaction.

In addition, since *C. gattii* is an environmental fungus, it is practically impossible to reproduce (inside the lab) all the

conditions that influence CP synthesis and fungal pathogenic- ity. Nevertheless, different culture conditions trying to mimic environmental stresses (agrochemicals, antibacterial, plants, soil protozoans, and other microorganisms) would provide more accurate knowledge of CP modifications in the environment and how they interfere in *C. gattii*–host interaction (Fig. 1). The Ueno et al. [11] results demonstrate how the culture condition alters *C. gattii* structure and influences host–immune response. It also shows the importance of choosing different culture conditions when studying fungal pathogenicity.

In another study, acapsular *C. gattii* cells were also used to develop a vaccine against cryptococcosis, by pulsing DC with the heat-killed *C. gattii* ΔCap60 (acapsular mutant) and inoculated in mice [13]. This strategy reduced lethality and fungal burden in the lungs after intratracheal infection with the virulent *C. gattii* (R265) strain [13]. Unfortunately, despite the promising results, this vaccine still has a long way to go before reaching clinical tri- als. In addition, the search for anti-cryptococcosis vaccines is a significant challenge, as the disease affects mainly HIV patients, and most of the studies are still performed using immunocompe- tent models.

To date, 42 anti-cryptococcosis vaccine prototypes have been evaluated in mice, but none of them have been tested in a clinical trial [22]. Furthermore, it is probably a consequence of the reduced financial support to studies focused on cryptococ- cosis [7], which also affects the development of new antifun- gals. Since 1992 (the year at which itraconazole was approved), no new antifungals became available to treat this mycosis [23] and currently, effective treatments are not available in all coun- tries. Only 0.61–1.21% of cases of neurocriptococcosis in sub- Saharan Africa were treated with the gold standard therapy (flucytosine plus amphotericin B) [3,6]. We believe that the search for new strategies (vaccines and new drugs) to control cryptococcosis is necessary; however, access to existing thera- pies must be guaranteed to the population all around the globe (Fig. 1).

In summary, Ueno et al. [11] provided new insights into the immunological effects of CP on *C. gattii*. The study demonstrates that CP can block the interaction between CD11b and *C. gattii*, affecting immune recognition. Overall, the study provides essen- tial information on how CP modulates *C. gattii* recognition, and it reinforces previous data regarding the use of acapsular strains of *C. gattii* as potential vaccines. However, more studies focused on unraveling details on *C. gattii* host–interaction are still necessary. Understanding how the immune system recognizes *C. gattii* can generate meaningful information for diagnosing, preventing, and treating cryptococcosis.

Acknowledgment: DAS (303762/2020-9) is research fellow of the Conselho Nacional de Desenvolvimento Científico e Tec- nológico - CNPq.

Conflict of interest: The authors declare no commercial or finan- cial conflicts of interest.

Author contributions: G.J.C.F. and D.A.S. wrote this paper.

References

1 **Kwon-Chung, K. J., Bennett, J. E., Wickes, B. L., Meyer, W., Cuomo, C. A., Wollenburg, K. R., Bicanic, T. A. et al.**, The case for adopting the "species complex" nomenclature for the etiologic agents of cryptococco- sis. *mSphere* 2017. 2.

2 **Maziarz, E. K. and Perfect, J. R.**, Cryptococcosis. *Infect. Dis. Clin. North Am.* 2016. **30**: 179–206.

3 **Rajasingham, R., Smith, R. M., Park, B. J., Jarvis, J. N., Govender, N. P., Chiller, T. M., Denning, D. W. et al.**, Global burden of disease of HIV- associated cryptococcal meningitis: an updated analysis. *Lancet Infect. Dis.* 2017. **17**: 873–881.

4 **Park, B. J., Wannemuehler, K. A., Marston, B. J., Govender, N., Pappas, P. G. and Chiller, T. M.**, Estimation of the current global burden of cryptococcal meningitis among persons living with HIV/AIDS. *AIDS* 2009. **23**: 525–530.

5 **Giles, S. S., Dagenais, T. R., Botts, M. R., Keller, N. P. and Hull, C. M.**, Eluci- dating the pathogenesis of spores from the human fungal pathogen Cryp- tococcus neoformans. *Infect. Immun.* 2009. **77**: 3491–3500.

6 **Shroufi, A., Chiller, T., Jordan, A., Denning, D. W., Harrison, T. S., Gove- nder, N. P., Loyse, A. et al.**, Ending deaths from HIV-related cryptococcal meningitis by 2030. *Lancet Infect. Dis.* 2021. **21**: 16–18.

7 **Rodrigues, M. L.**, Funding and innovation in diseases of neglected popu- lations: the paradox of *Cryptococcal meningitis*. *PLoS Negl Trop Dis* 2016. **10**: e0004429.

8 **Alspaugh, J. A.**, Virulence mechanisms and Cryptococcus neoformans pathogenesis. *Fungal Genet. Biol.* 2015. **78**: 55–58.

9 **Araujo, G. de. S., Fonseca, F. L., Pontes, B., Torres, A., Cordero, R. J., Zancopé-Oliveira, R. M., Casadevall, A. et al.**, Capsules from pathogenic and non-pathogenic Cryptococcus spp. manifest significant differences in structure and ability to protect against phagocytic cells. *PLoS One* 2012. **7**: e29561.

10 **Zaragoza, O., Rodrigues, M. L., De Jesus, M., Frases, S., Dadachova, E. and Casadevall, A.**, The capsule of the fungal pathogen *Cryptococcus neofor- mans*. *Adv. Appl. Microbiol.* 2009. **68**: 133–216.

11 **Ueno, K., Otani, Y., Yanagihara, N., Urai, M., Nagamori, A., Sato- Fukushima, M., Shimizu, K. et al.**, *Cryptococcus gattii* evades CD11b- mediated fungal recognition by coating itself with capsular polysaccha- rides. *Eur. J. Immunol.* 2021.

12 **Urai, M., Kaneko, Y., Ueno, K., Okubo, Y., Aizawa, T., Fukazawa, H., Sugita, T. et al.**, Evasion of Innate Immune Responses by the Highly Virulent Cryptococcus gattii by Altering Capsule Glucuronoxylomannan Struc- ture. *Front Cell Infect. Microbiol.* 2015. **5**: 101.

13 **Ueno, K., Urai, M., Takatsuka, S., Abe, M., Miyazaki, Y. and Kinjo, Y.**, Immu- nization with antigen-pulsed dendritic cells against highly virulent cryp- tococcus gattii infection: analysis of cytokine-producing T cells. *Methods Mol. Biol.* 2017. **1625**: 327–339.

14 **Xu, J., Flaczyk, A., Neal, L. M., Fa, Z., Cheng, D., Ivey, M., Moore, B. B. et al.**, Exploitation of scavenger receptor, macrophage receptor with col- lagenous structure, by Cryptococcus neoformans promotes alternative activation of pulmonary lymph node CD11b$^+$ conventional dendritic cells and non-protective Th2 bias. *Front. Immunol.* 2017. **8**: 1231.

15 **Wiesner, D. L., Specht, C. A., Lee, C. K., Smith, K. D., Mukaremera, L., Lee, S. T., Lee, C. G. et al.**, Chitin recognition via chitotriosidase promotes

pathologic type-2 helper T cell responses to cryptococcal infection. *PLoS Pathog.* 2015. **11**: e1004701.

16 **Iwasaki, A. and Medzhitov, R.**, Control of adaptive immunity by the innate immune system. *Nat. Immunol.* 2015. **16**: 343–353.

17 **Carneiro, H. C. S.**, **Bastos, R. W.**, **Ribeiro, N. Q.**, **Gouveia-Eufrasio, L.**, **Costa, M. C.**, **Magalhães, T. F. F.**, **Oliveira, L. V. N. et al.**, Hypervirulence and cross-resistance to a clinical antifungal are induced by an environmental fungicide in Cryptococcus gattii. *Sci. Total Environ.* 2020. **740**: 140135.

18 **Bastos, R. W.**, **Carneiro, H. C. S.**, **Oliveira, L. V. N.**, **Rocha, K. M.**, **Freitas, G. J. C.**, **Costa, M. C.**, **Magalhães, T. F. F. et al.**, Environmental triazole induces cross-resistance to clinical drugs and affects morphophysiology and virulence of *Cryptococcus gattii* and *C. neoformans*. *Antimicrob. Agents Chemother.* 2018. 62.

19 **Santos, J. R.**, **Holanda, R. A.**, **Frases, S.**, **Bravim, M.**, **Araujo, G. e. S.**, **Santos, P. C.**, **Costa, M. C. et al.**, Fluconazole alters the polysaccharide capsule of *Cryptococcus gattii* and leads to distinct behaviors in murine Cryptococcosis. *PLoS One* 2014. **9**: e112669.

20 **Barcellos, V. A.**, **Martins, L. M. S.**, **Fontes, A. C. L.**, **Reuwsaat, J. C. V.**, **Squizani, E. D.**, **de Sousa Araújo, G. R.**, **Frases, S. et al.**, Genotypic and phenotypic diversity of Cryptococcus gattii VGII clinical isolates and its impact on virulence. *Front Microbiol* 2018. **9**: 132.

21 **Fernandes, K. E.**, **Brockway, A.**, **Haverkamp, M.**, **Cuomo, C. A.**, **van Ogtrop, F.**, **Perfect, J. R. and Carter, D. A.**, Phenotypic variability correlates with clinical outcome in cryptococcus isolates obtained from Botswanan HIV/AIDS patients. *mBio* 2018. 9.

22 **Ueno, K.**, **Yanagihara, N.**, **Shimizu, K. and Miyazaki, Y.**, Vaccines and protective immune memory against Cryptococcosis. *Biol. Pharm. Bull.* 2020. **43**: 230–239.

23 **Houšť, J.**, **Spížek, J. and Havlíček, V.**, Antifungal drugs. *Metabolites* 2020. **10**:106.

24 **May, R. C.**, **Stone, N. R.**, **Wiesner, D. L.**, **Bicanic, T. and Nielsen, K.**, Cryptococcus: from environmental saprophyte to global pathogen. *Nat. Rev. Microbiol.* 2016. **14**: 106–117.

25 **Rella, A.**, **Yang, M. W.**, **Gruber, J.**, **Montagna, M. T.**, **Luberto, C.**, **Zhang, Y. M. and Del Poeta, M.**, Pseudomonas aeruginosa inhibits the growth of Cryptococcus species. *Mycopathologia* 2012. **173**: 451–461.

26 **Cordero, R. J.**, **Liedke, S. C.**, de S **Araújo, G. R.**, **Martinez, L. R.**, **Nimrichter, L.**, **Frases, S.**, **Peralta, J. M. et al.**, Enhanced virulence of *Histoplasma capsulatum* through transfer and surface incorporation of glycans from *Cryptococcus neoformans* during co-infection. *Sci. Rep.* 2016. **6**: 21765.

Abbreviations: **CP**: capsular polysaccharide · **DC**: dendritic cells

Full correspondence: Dr. Daniel Assis Santos, Departamento de Microbiologia, Instituto de Ciências Biológicas, Universidade Federal de Minas Gerais, Av. Antonio Carlos, 6627, Pampulha, Belo Horizonte, Minas Gerais, 31270–901, Brazil
e-mail: das@ufmg.br, dasufmg@gmail.com

See accompanying article: https://doi.org/10.1002/eji.202049042

Received: 30/5/2021
Accepted: 27/7/2021
Accepted article online: 31/7/2021

CAPÍTULO 3

Antimalarials and amphotericin B interact synergistically and are new options to treat cryptococcosis.

Gustavo J. C. Freitas; Noelly Q. Ribeiro; Ludmila Gouveia-Eufrasio; Elúzia C.P. Emidio; Gabrielle M. Guimarães; Isabela C. César; Tatiane A. Paixão, Jeferson B. S. Oliveira, Melissa Caza, James W. Kronstad, Daniel A. Santos.

ABSTRACT

Cryptococcus gattii and *C. neoformans* are the main etiological agents of cryptococcosis, an invasive mycosis treated with amphotericin B, 5-fluorocytosine, and fluconazole. However, this limited arsenal is toxic and associated with antifungal resistance. Cryptococcosis and malaria pathogens are eukaryotic organisms and have a high incidence in Sub-Saharan Africa. The antimalarials (ATMs) halofantrine (HAL) and amodiaquine (AQ) block *Plasmodium* heme polymerase, while artesunate (ART) induces oxidative stresses. Considering that *Cryptococcus* spp. is susceptible to reactive oxygen species, and that iron is important for metabolism, we tested the repurposing of ATMs for the treatment of cryptococcosis. ATMs reduced fungal growth, induced oxidative and nitrosative stresses, altered ergosterol content, melanin production, and polysaccharide capsule size in *C. neoformans* and *C. gattii*, revealing a dynamic effect on fungal physiology. A comprehensive chemical-genetic analysis using two mutant libraries demonstrated that the deletion of genes involved in synthesizing components of the plasma membrane and cell wall, and oxidative stress responses are essential for fungal susceptibility to ATMs. Interestingly, when ATMs were combined *in vitro* with antifungals, the amphotericin B fungicidal concentrations were ~ 10 times lower, demonstrating a synergistic interaction. Further, the combinations showed reduced toxicity to murine macrophages. Finally, the treatment of murine cryptococcosis with the combinations of amphotericin B with HAL or AQ reduced lethality and fungal burden in the lungs and brain. These findings provide perspectives for further studies with ATMs against cryptococcosis and other fungal infections.

Keywords: Cryptococcosis, drug repurposing, antimalarials, synergism.

Editor: Professor Jian Li

Journal Pre-proof

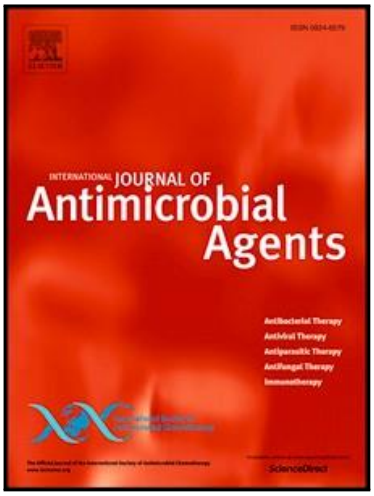

Antimalarials and amphotericin B interact synergistically and are new options to treat cryptococcosis

Gustavo J.C. Freitas , Noelly Q. Ribeiro ,
Ludmila Gouveia-Eufrasio , Elúzia C.P. Emidio ,
Gabrielle M. Guimarães , Isabela C. César , Tatiane A. Paixão ,
Jeferson B.S. Oliveira , Melissa Caza , James W. Kronstad ,
Daniel A. Santos

PII: S0924-8579(23)00086-9
DOI: https://doi.org/10.1016/j.ijantimicag.2023.106807
Reference: ANTAGE 106807

To appear in: *International Journal of Antimicrobial Agents*

Received date: 23 September 2022
Accepted date: 28 March 2023

Please cite this article as: Gustavo J.C. Freitas , Noelly Q. Ribeiro , Ludmila Gouveia-Eufrasio , Elúzia C.P. Emidio , Gabrielle M. Guimarães , Isabela C. César , Tatiane A. Paixão , Jeferson B.S. Oliveira , Melissa Caza , James W. Kronstad , Daniel A. Santos , Antimalarials and amphotericin B interact synergistically and are new options to treat cryptococcosis, *International Journal of Antimicrobial Agents* (2023), doi: https://doi.org/10.1016/j.ijantimicag.2023.106807

HIGHLIGHTS

- Antimalarials (Halofantrine (HAL), amodiaquine (AQ), artesunate (ART)) reduce fungal growth.
- Antimalarials affect *Cryptococcus* virulence factors.
- HAL, AQ and ART interact synergically with amphotericin B (AMB) against *Cryptococcus.*
- HAL+AMB and AQ+AMB increased survival of mice infected with *Cryptococcus.*
- HAL+AMB and AQ+AMB reduced fungal burden during murine cryptococcosis.

Antimalarials and amphotericin B interact synergistically and are new options to treat cryptococcosis

Gustavo J. C. Freitas[1]; Noelly Q. Ribeiro[1]; Ludmila Gouveia-Eufrasio[1]; Elúzia C.P. Emidio[1]; Gabrielle M. Guimarães [2]; Isabela C. César[3]; Tatiane A. Paixão[4], Jeferson B. S. Oliveira [4], Melissa Caza[5], James W. Kronstad[5], Daniel A. Santos[1]*

[1]Universidade Federal de Minas Gerais, Departamento de Microbiologia / Laboratório de Micologia, Belo Horizonte, Brazil.

[2]Universidade Federal de Minas Gerais, Departamento de Microbiologia / Laboratório de Ecologia e Fisiologia de Microrganismos, Belo Horizonte, Brazil.

[3]Universidade Federal de Minas Gerais, Departamento de Produtos Farmacêuticos, Faculdade de Farmácia, Belo Horizonte, Brazil.

[4]Universidade Federal de Minas Gerais, Departamento de Patologia / Laboratório de Patologia Celular e Molecular, Belo Horizonte, Brazil.

[5]University of British Columbia, Michael Smith Labs, Vancouver, BC, Canada.

***Corresponding author:** Daniel Assis Santos, Departamento de Microbiologia, Instituto de Ciências Biológicas, Universidade Federal de Minas Gerais, Av. Antonio Carlos, 6627, Pampulha, Belo Horizonte, Minas Gerais, Brazil, 31270-901. E-mail: das@ufmg.br or dasufmg@gmail.com; Tel: +55 31 3409 2758; Fax: +55 31 3409 2733.

ABSTRACT

Cryptococcus gattii and *C. neoformans* are the main etiological agents of cryptococcosis, an invasive mycosis treated with amphotericin B, 5-fluorocytosine, and fluconazole. However, this limited arsenal is toxic and associated with antifungal resistance. Cryptococcosis and malaria pathogens are eukaryotic organisms and have a high incidence in Sub-Saharan Africa. The antimalarials (ATMs) halofantrine (HAL) and amodiaquine (AQ) block *Plasmodium* heme polymerase, while artesunate (ART) induces oxidative stresses. Considering that *Cryptococcus* spp. is susceptible to reactive oxygen species and that iron is essential for metabolism, we tested the repurposing of ATMs to treat cryptococcosis. ATMs reduced fungal growth, induced oxidative and nitrosative stresses, and altered ergosterol content, melanin production, and polysaccharide capsule size in *C. neoformans* and *C. gattii*, revealing a dynamic effect on fungal physiology. A comprehensive chemical-genetic analysis using two mutant libraries demonstrated that the deletion of genes involved in synthesizing components of the plasma membrane and cell wall, and oxidative stress responses are essential for fungal susceptibility to ATMs. Interestingly, the amphotericin B (AMB) fungicidal concentrations were ~ 10 times lower when combined with ATMs, demonstrating a synergistic interaction. Further, the combinations showed reduced toxicity to murine macrophages. Finally, HAL+AMB and AQ+AMB efficiently reduced lethality and fungal burden in the lungs and brain, in murine cryptococcosis. These findings provide perspectives for further studies with ATMs against cryptococcosis and other fungal infections.

Keywords: Cryptococcosis, drug repurposing, antimalarials, synergism.

1. INTRODUCTION

The invasive medical procedures, AIDS, transplants, and immunosuppressive therapies have contributed to the higher incidence of invasive fungal infections. Among them, cryptococcosis, an infection mainly caused by *Cryptococcus neoformans* and *Cryptococcus gattii*, stands out due to the high lethality rate[1]. Cryptococcosis' treatment is restricted to the use of amphotericin B (AMB), fluconazole (FCZ), and 5-flucytosine (5-FC)[2]. Furthermore, this small therapeutic arsenal is associated with a high cost, toxicity, and drug resistance[3], influencing the mortality due this mycosis.

In the last years, few antifungal (isavuconazole, oteseconazole, ibrexafungerp) has been approved for human use, but they are not currently indicated to treat cryptococcosis [4-6]. Developing new antifungals is an expensive and time-consuming process, and the final result is not always promising[7]. Thus, drug repurposing offers a viable strategy to search for new therapeutic approaches in mycology[4, 8, 9]. This strategy consists of studying available drugs for new therapeutic purposes[3, 8]. Since the pharmacological and toxicological features are already described, the cost and time for its implementation in treating other diseases are reduced[3, 8]. In cryptococcosis, drug repurposing can be used as a single agent or adjuvant in combination with established antifungal therapy[4, 10].

Cryptococcosis and malaria are diseases caused by eukaryotic organisms and have a high incidence in Sub-Saharan Africa[11, 12]. Furthermore, despite the scarce literature, there are reports of patients presenting both diseases[13]. Consequently, it is reasonable to assume that cryptococcosis' agents may be exposed to antimalarials (ATMs). Halofantrine (HAL) and amodiaquine (AQ) block heme polymerase activity, while artesunate (ART) induces oxidative stress in *Plasmodium*[14, 15]. Since *Cryptococcus* spp.

is sensitive to oxidative stress, and iron metabolism is essential for fungal biology, we evaluated the repurposing of HAL, AQ, and ART for treating cryptococcosis. In addition, it has been reported that these antimalarials may influence the control of cancer, diabetes, obesity, and inflammatory diseases[16-20], suggesting a pleiotropic effect on the different eukaryotic cells.

Briefly, we observed that antimalarials inhibited *Cryptococcus* spp. growth, altered fungal physiology and showed synergism with amphotericin B. Interestingly, the combination HAL + AMB and AQ + AMB increased mice survival and reduced fungal burden in a murine model of cryptococcosis. These findings open perspectives for further studies with antimalarials against fungal infections and their use in the treatment of cryptococcosis.

2. MATERIALS AND METHODS

2.1 *In vitro* study

2.1.1 Antimicrobial agents

Fluconazole (FCZ) (Sigma-Aldrich®), amphotericin B (AMB) (Sigma-Aldrich®), and the antimalarials (ATMs) Artesunate (ART) (Sigma-Aldrich®), Halofantrine (HAL) (Sigma-Aldrich®) and Amodiaquine (AQ) (Sigma-Aldrich®) were used. The drugs were solubilized as recommended by the manufacturer.

2.1.2 Organisms

Five *C. gattii* strains (WM161, WM178, WM179, WM779, R265), five *C. neoformans* strains (H99, WM626, WM628, WM629, WM148) and five *Candida* spp. strains (*C. albicans*/ATCCSC51314, *C. glabrata*/ATCC2001, *C. parapsilosis*/ATCC22019 *C.*

krusei/ATCC20298 and *C. tropicalis*/ATCC750) were tested. All strains were maintained at -80ºC and cultured in Yeast extract Peptone Dextrose (YPD) medium at 37°C for each experiment.

2.1.3 Minimum inhibitory concentration (MIC), Fractional inhibitory concentration index (FICI), and Zero Interaction Potency (ZIP) analysis

The *in vitro* susceptibility to ATMs and drug interactions were performed by the broth microdilution method as recommended by the CLSI[21], using the strains described above. AMB, FCZ, and ATMs were tested at concentrations from 0.03 to 8; 0.25 to 64; and 8 to 512 µg/mL, respectively. The drugs were diluted in RPMI 1640, and 100 µL of each dilution was distributed in a 96-well microdilution plate.

Fungal suspensions were prepared, and the transmittance was adjusted to 75 to 77% at 530 nm, followed by dilution in RPMI 1640 to obtain 1.0 x 10^3 to 5 x 10^3 cells/mL. 100 µL were transferred to the 96-well plates containing the antifungals or ATMs. The plates were incubated at 37°C for 72 h for *Cryptococcus* and 48h for *Candida*. For AMB and ATMs, the MIC was defined as the lowest concentration that resulted in 100% inhibition of fungal growth. For FCZ, 50% inhibition was considered.

Antifungals and ATMs were also tested in combination. A checkerboard microdilution method, which provides a matrix of all possible drug combinations in the required concentration range, was used to test the fungal susceptibility. One plate was used to test each strain. The spectrophotometric (600 nm) reading was performed, and the combination that provided 100% of growth inhibition was considered.

FICI and ZIP were used to classify drug interactions as previously described[3, 22]. FICI was defined as: synergistic if FICI was ≤0.5, indifferent if the FICI was >0.5 and ≤4, and antagonistic if the FICI was >4. ZIP analyses were performed using the

SynergyFinder 2.0 (https://synergyfinder.fimm.fi) software [22], and the interactions were defined as antagonistic if the ZIP is < -10, indifferent if the ZIP is > -10 and ≤10, and synergistic if the ZIP is >10[22].

2.1.4 Time–kill studies

1.0 x 10^3 cells/mL of *C. gattii* R265 and *C. neoformans* H99 were transferred to 24-well plates containing ATMs (256 µg/mL or 32 µg/mL), AMB (0.5 µg/mL or 0.06 µg/mL) or FCZ (2 µg/mL) in RPMI medium. The plates were incubated at 37°C, and plating was performed on YPD solid medium after 3, 6, 24, and 48 h. YPD plates were incubated at 37°C, and colony-forming units (CFU) were quantified after 72 h.

2.1.5 Chemical-genetic screening

After determining the ATMs activity against *C. neoformans*, *C. gattii*, and *Candida* spp., we performed a chemical-genetic screening using two *C. neoformans* single-gene mutant libraries. We used the collections of *C. neoformans* KO mutants (2008 and 2015) from the Madhani laboratory (distributed through the Fungal Genetics Stock Center, http://www.fgsc.net) and the transcription factor (TF) mutant library, developed by the Bahn laboratory[23]. The 2008 and 2015 CNKO libraries contain 1,180 and 2,111 mutants, respectively[24]. The TF mutant library consists of 322 mutants with deletions in 155 different TFs (with at least two independent deletion strains per TF)[23, 25].

Initially, the mutants were cultured in a liquid YPD medium at 30°C. Then, 5 µL of each culture were inoculated with the Biomek 4000 equipment into 96-well, flat-bottomed plates containing 100 µL of YPD supplemented with one of the drugs (ART - 4.0 µg/mL or HAL - 2 µg/mL or AQ - 16 µg/mL). The plates were incubated at 37°C for 48h and were read visually. A mutant was considered susceptible when it was unable to grow (100% inhibition compared to ATMs-free control) [25].

2.1.6 *In silico* analysis

For each susceptible mutant, the product and function of the deleted gene were consulted. Then, the gene ontology (GO) analysis was carried out using the FungiDB platform (http://fungidb.org/)[26]. The genes were analyzed for enrichment of GO in molecular functions, cellular components, and biological processes, considering $p<0.05$ as significant.

2.1.7 Stress susceptibility tests

1.0 x 10^4 cells/mL of *C. gattii* R265 and *C. neoformans* H99 strains were spotted in YPD medium supplemented with subinhibitory concentrations of ATMs (32 µg/mL), FCZ (1.0 µg/mL) or AMB (0.25µg/mL), and incubated at 37°C for 48h. After exposure to the drugs, a new inoculum was prepared to obtain 1.0 x 10^6 cells/mL. Then, four 1:10 serial dilutions were carried out, and 5µL of each were spotted in YPD medium supplemented with one of the following agents: 0.025% triton (cell wall and membrane stresses), 1.5M Sodium Chloride (osmotic stress), 1.5M potassium chloride (osmotic stress) and 17.5mM Dithiothreitol (endoplasmic reticulum stress). The plates were incubated at 37°C for 72 h, photographed and analyzed visually.

2.1.8 Ergosterol quantification

1.0 x 10^8 cells/ml of *C. gattii* R265 and *C. neoformans* H99 were treated with FCZ (1.0 µg/mL) or ATMs (32 µg/mL) overnight. A drug-free control was performed. After treatment, 3 ml of 25% potassium hydroxide ethanolic solution was added to each cell mass, followed by stirring for 1 min. Next, the tubes were incubated in a water bath at 85°C for 1 hour and then cooled. Then, 1 ml of sterile water and 3 ml of n-heptane (Sigma-Aldrich) were added, followed by stirring for 3 min. Finally, the supernatant

was removed, and the reading was performed in a spectrophotometer at 282 and 230 nm [27].

2.1.9 Laccase, melanin, and capsule analysis

1.0 x 10^8 cells/ml of *C. gattii* R265 and *C. neoformans* H99 were treated with ATMs (32 µg/mL) and FCZ (1.0 µg/mL) overnight at 37°C. After incubation, the tubes were centrifuged at 1200 r.p.m. and the supernatant was discharged. Laccase quantification was performed by the Azino-bis(3-ethylbenzothiazoline-6-sulfonic acid) diammonium salt (ABTS) oxidation method. Briefly, a mixture containing 1 mM substrate (ABTS), and 2.8 mL of 0.1 M sodium acetate buffer, pH 4.0, were added to the cultures and incubated at 30 ºC for 2 h. The absorbance at 420 nm was determined. A cell suspension without ABTS was used as a control [28].

Melanin production was evaluated in solid minimal medium (MM) (15 mM glucose, 10mM $MgSO_4$, 29.4mM $KHPO_4$, 13mM glycine, and 18g/L agar, pH 5.5) supplemented with 1mM L-dopa ATMs (32 µg/mL) or FCZ (1.0 µg/mL) [29].

For the polysaccharide capsule analysis, H99 and R265 were cultured in liquid MM supplemented with ATMs (32µg/mL) or FCZ (1.0 µg/mL) for 72 h at 37 ºC. The capsule size was determined using ImageJ software [30] under India ink dye.

2.1.10 Quantification of reactive oxygen species (ROS) and peroxynitrite (PRN) production

1.0 x10^4 cells/mL of *C. gattii* R265 and *C. neoformans* H99 were treated with ATMs (32 and 256 µg/mL), AMB (0.25 µg/mL) or N-acetylcysteine (16 µg/mL) (antioxidant) in RPMI 1640 without phenol red. Then, suspensions were incubated for 3h with 10 mM 2,7'-dichlorofluorescein diacetate (Invitrogen, Life Technologies, Carlsbad, CA, USA) to quantify ROS; or 1,2,3 dihydrorhodamine (Invitrogen) to quantify PRN. After

incubation, the fluorescence was measured with a fluorometer (Synergy 2 SL Luminescence Microplate Reader; Biotek) using excitation and emission wavelengths of 500nm. Data are expressed as arbitrary units of fluorescence ± SE [31].

2.2. *Ex vivo* and *in vivo* studies

2.2.1 Ethics

This study was approved (protocol 237/2021) by the Ethics Committee in the Use of Animals (CEUA) from Universidade Federal de Minas Gerais. We followed the Brazilian Society of Zootechnics/Brazilian College of Animal Experimentation guidelines (available at http://www.cobea.org.br/) and Federal Law 11,794. Water and food were provided *ad libitum*, and light/dark cycles were maintained. All efforts to minimize the suffering of the animals were carried out.

2.2.2 Toxicity assays in murine macrophages

Bone marrow macrophages were obtained from C57BL/6 mice[32]. 1×10^5 cells/mL (in RPMI supplemented with 10% bovine fetal serum) were distributed in 96-well plates and incubated overnight at 37°C (with 5% CO_2). Then, macrophages were treated with ATMs (16 and 256µg/mL) and AMB (0.03 and 32 µg/mL), alone or in combination, for 3 h. The cell viability was determined by the MTT assay[33]. DMSO 50% was used as a control.

2.2.3 Murine model of cryptococcosis

1.0 x 10^5 CFU/30 µL of *C. neoformans* (H99 strain) was used to infect C57/BL6 male mice (6 – 8 weeks-old). The inoculum was counted on the Neubauer chamber under Trypan Blue staining. Animals were infected intratracheally (i.t.) under anesthesia with ketamine (100 mg/kg) and xylazine (16 mg/kg) [3].

2.2.4 Survival experiment

Mice were divided into nine groups according to the treatments, which started 24 h after infection (i.p. injections once daily): (1) HAL (8 mg/kg); (2) AQ (20 mg/kg); (3) ART (25 mg/kg); (4) AMB (0.5 mg/kg); (5) HAL (8 mg/kg) + AMB (0.5 mg/kg); (6) AQ (20 mg/kg) + AMB (0.5 mg/kg); (7) ART (25 mg/kg) + AMB (0.5 mg/kg) (8) non-treated (NT); and (9) Non-infected (NI). Mice were monitored daily for survival, and animals that showed weight loss greater than 20%, tremors, and immobility, were euthanized (following the Euthanasia Practice Guidelines of the National Council for Control of Animal Experimentation). ATMs' human equivalent doses for mice were calculated as previously described[34].

2.2.5 Determination of fungal burden in bronchoalveolar lavage fluid (BALF), lungs, and brain

After the survival experiment, other groups were infected and treated. Animals were euthanized 15 days post-infection (d.p.i.) to collect the bronchoalveolar lavage fluid (BALF), lungs, and brain. The organ homogenates were plated onto YPD and incubated for 48 h at 37 °C to determine the fungal burden, expressed as CFU/g or CFU/mL.

2.2.6 Statistical analyses

Statistical analysis of all data was performed using GraphPad Prism version 5.0 (GrapPad Inc., San Diego, CA, USA), with $p<0.05$ considered to be significant. The time-kill curves were analyzed by the area under the curve. Results of ROS, PRN, ergosterol, capsule size, laccase and CFU were analyzed by analysis of variance (ANOVA), followed by the non-parametric Friedman post-test. Survival curve was plotted by the Kaplan–Meier method, and the results were analyzed using the log-rank test. The experiments were repeated at least twice, and reproducible results were found.

3. RESULTS

3.1 ATMs have fungistatic effect against *C. neoformans* and *C. gattii*

Initially, we evaluated the susceptibility of ten strains of *C. gattii* and *C. neoformans* to the ATMs. The inhibition ranged from 20.34 – 34.16% for HAL, 5.83 – 35.77% for AQ, and 20.94 – 42.67% for ART, according to the concentration tested (Fig. 1A).

Then we performed a time-kill curve in the presence of ATMs with the strains H99 and R265. For all the ATMs, there was a reduction in growth, similar to FCZ (Fig. 1B - G). In addition, there was a significant reduction in growth for HAL and AQ compared to the untreated control, while concentration and strain-dependent effects were obtained for ART (Fig. 1B - G).

3.2 Different cellular processes contribute to the *C. neoformans* response to antimalarials

Preliminary data from the chemical-genetic screening revealed different susceptible mutants to antimalarials. Sixteen mutants were susceptible to HAL (Table 1), 20 to AQ (Table 2), and 29 to ART (Table 3). Briefly, HAL inhibited the growth of mutants associated with responses to oxidative damage, membrane destabilizing and osmotic fluctuations (*CFO1Δ*), nutritional limitation (*STL1Δ*), and calcium/manganese transport (*PMR1Δ*) (Table 1). AQ inhibited the growth of mutants for membrane transporters (PMR5Δ and MSFΔ) and alternative transport of carbon (STL1Δ) (Table 2). ART inhibited the growth of mutants associated with cell wall integrity (*VPS22Δ, GS1Δ,* and *LGR1Δ*), polysaccharide capsule synthesis (*CAP60Δ*), and antioxidant response (*HXT2Δ* and *GPX2Δ*) (Table 3).

We performed an ontology analysis to obtain a detailed view of the processes affected by ATMs. Eight cellular components and 15 enriched biological processes (Fig. 2A),

including metabolism of nucleotides, and iron and biological processes involved in melanin biosynthesis, pathogenesis, and cell growth were enriched for HAL. Five cellular components, 15 molecular functions, and 14 biological processes (Fig. 2B), including membrane-related cellular components, transport and movement of substances, transport of molecules, were enriched for AQ. Finally, 16 biological processes, three cellular components, and seven molecular functions (Fig. 2C), including antioxidant activity and pathogenesis were enriched for ART.

Based on these findings, we characterized the effect of ATMs in different aspects: growth under stress agents, induction of oxidative and nitrosative stresses, and synthesis of ergosterol, melanin, and polysaccharide capsule.

3.3 Exposure to ATMs increases fungal growth under stressing conditions

The exposure to ATMs and AMB increased the fungal growth in membrane stressors (potassium chloride, sodium chloride) and endoplasmic reticulum stressor (DTT) (Fig. 3A - C). However, only *C. gattii* R265 exposed to ART increased growth in triton (Fig. 3D). The exposure to ATMs did not alter the fungal viability (Fig. S1). These findings suggest possible effects of antimalarials on *Cryptococcus*. The exposure to AMB increased fungal growth under osmotic stressors, corroborating previous data[35].

3.4* ATMs induce oxidative and nitrosative bursts in *C. neoformans* e *C. gattii

Treatment with HAL, ART and AQ increased ROS production compared to untreated control (Fig. 4A). Interestingly, AQ increased ROS levels higher than AMB (Fig. 4A). Increased production of PRN were also observed after HAL, ART, and AQ treatments (Fig. 4B). Furthermore, PRN production was higher than AMB for AQ and ART (Fig. 4B).

3.5 ATMs alter the synthesis of ergosterol, melanin, and polysaccharide capsule

The treatment with ART and AQ reduced the ergosterol content. However, an opposite profile was observed for HAL (Fig. 4C - D). As expected, FCZ significantly reduced the sterol content.

Laccase is an important enzyme involved in melanin synthesis. ATMs reduced laccase activity in both *C. gattii* and *C. neoformans* (Fig. 4E - F). This reduction was also associated with the lower melanin production (Fig. 4I). ATMs also inhibited polysaccharide capsule synthesis (Fig. 4G - I).

3.6 The ATMs + AMB combinations were synergistic against *Cryptococcus* and *Candida*

The combination ATMs+AMB was a synergistic in a dose-dependent manner (CIF <0.5 and ZIP > 10) (Table 4) (Fig. 5A – F). The interaction curves (Fig. 5A, C, and E) show that ATMs reduced the AMB MIC at least 10-fold compared to AMB MIC alone (Fig. 5). The AMB mean MIC was 0.054 µg/mL for *C. gattii* and 0.042 µg/mL for *C. neoformans*, when combined with HAL (Fig. 5A). Similar, lower AMB MICs were obtained when it was combined with AQ and ART (Fig. 5C and E). A synergistic interaction was also observed against *Candida* strains (Table 4). The interaction between ATMs and Fluconazole (FCZ) was indifferent (data not shown). The heatmaps shown in Fig. 5 (B, D, and F) reinforce the synergism between the tested drugs. The ZIP synergy scores were 54.28 for HAL, 58.35 for AQ, and 31.23 for ART.

We then tested if the combinations were toxic to murine macrophages. Fig. 6 (A-C) shows that cell viability was higher than 50% when AMB was combined with low and high ATMs doses. Conversely, low viability was verified when a higher dose (128 µg/mL) of HAL was combined with high AMB concentration. Furthermore, the combination of ATMs/AMB does not change the pH of the RPMI medium (data not shown).

3.7 The combinations of ATMs + AMB reduce lethality and fungal burden in murine cryptococcosis

Considering the effects of ATMs on fungal cells, the synergistic interaction with AMB, and the low toxicity of ATMs+AMB, we evaluated the effects of ATMs on murine cryptococcosis. The median survival of untreated mice was 20 days, while it was 28 days for those treated with AMB alone. In addition, the HAL+AMB and AQ+AMB groups survived longer ($p<0.05$), with a median of 34 and 36 days, respectively (Fig. 6D). The ART+AMB combination did not reduce mice lethality (Fig. 6D). The treatment with AMB alone reduced fungal burden in BALF, lungs, and brain compared to the untreated groups. On the other hand, the monotherapy with HAL or AQ did not alter the fungal burden in those organs. However, the combinations of HAL+AMB and AQ+AMB reduced fungal burden in the BALF, lungs, and brain compared to the AMB group (Fig. 6E - G).

4. DISCUSSION

Cryptococcus spp. causes 152,000 new cases of meningitis annually, leading to 112,000 deaths[1]. In this study, we evaluated the repurposing of antimalarials: HAL, AQ, and ART for treating this mycosis. In addition, this is the first study to assess the effects of those ATMs, alone and combined with AMB, against *Cryptococcus* spp.

ATMs inhibits *C. neoformans* and *C. gattii* growth in a dose-dependent manner. We then performed a chemical-genetic screening to understand the effects of ATMs on fungal cells. Several cellular processes are important for the susceptibility to ATMs, including membrane transport, pigment biosynthesis, xenobiotic responses, iron and potassium responses, cellular growth, and peroxidase activity. Interestingly, the

exposure of H99 and R265 strains to ATMs, increased fungal resistance to osmotic stress, reinforcing the role of the membrane in the susceptibility to ATMs. In addition, ATMs reduced melanin and polysaccharide capsule, altered ergosterol synthesis, and induced oxidative and nitrosative stresses. These findings revealed an unprecedented and multifaceted potential for the action of ATMs on *Cryptococcus* spp.

Considering that ATMs reduced the synthesis of virulence factors, these drugs may be acting by disarming pathogens and influencing host-pathogen interaction. Melanin and polysaccharide capsule, both reduced by ATMs, are essential to protect *Cryptocuccus* cells from immune response[30, 36]. This could be a consequence of the whole metabolism reduction (evidenced as the reduced growth caused by ATMs), which may affect melanin and polysaccharide capsule synthesis. Otherwise, we assume that ATMs can directly act on fungal virulence-related pathways. This hypothesis is corroborated by the susceptibility to HAL and ART of the knockout strains for the genes important for the synthesis of melanin (*CFO1*) and polysaccharide capsule (*CAP60*), respectively.

In cryptococcosis, drug repurposing can be used as a single agent or an adjuvant in combined with the standard antifungal therapy[4]. Unprecedently, the combination of ATMs with AMB are synergistic. AMB binds to ergosterol in the fungal cell membrane, inducing cell leakage, and recent studies have shown that AMB also induces oxidative and nitrosative stresses[31, 35, 37-40]. Although ergosterol is the main AMB target, small reductions in sterol in the fungal membrane may improve the activity of the polyene[27]. This effect can also be observed when synergism occurs between FCZ and AMB[27]. This is consistent with the synergism of AQ+AMB and ART+AMB. AQ and ART reduced the ergosterol content and increased ROS and PRN. These data suggest that ergosterol reduction may increase membrane permeability, with further AMB passive diffusion, accelerating fungal inhibition through oxidative and nitrosative stresses. On the other

hand, HAL increased the ergosterol content, ROS, and PRN. The increase in oxidative and nitrosative stresses and other non-addressed targets may improve the fungicidal AMB activity.

Interestingly, the combinations HAL+AMB and AQ+AMB reduced mice lethality, probably because of the efficient fungal killing during infection, as attested by the lower fungal burden in organs. On the other hand, monotherapy with ATMs and the ART+AMB combination did not reduce lethality with the tested doses. Therefore, we hypothesize that the ART pharmacokinetics and pharmacodynamics may have contributed to the lack of *in vivo* synergism. However, further studies are needed to evaluate other therapeutic regimens for ART+AMB.

In conclusion, HAL+AMB and AQ+AMB combinations may be promising in treating cryptococcosis.

Declarations

Funding: This study was supported by Fundação de Amparo a Pesquisa do Estado de Minas Gerais - FAPEMIG (PPM-00061-18), Coordenação de Aperfeiçoamento de Pessoal de Nível Superior (CAPES), Conselho Nacional de Desenvolvimento Científico e Tecnológico - CNPq (402200/2021-7, 408540/2022-2) Brazilian Ministry of Health (440010/2018-7), and the Canadian Institutes for Health Research (to JWK). DAS (303762/2020-9) is a research fellow of the CNPq.

Competing Interests: None declared.

Ethical Approval: This study was approved (protocol 237/2021) by the Ethics Committee in the Use of Animals (CEUA) from Universidade Federal de Minas Gerais.

Sequence Information: Not applicable

LEGENDS

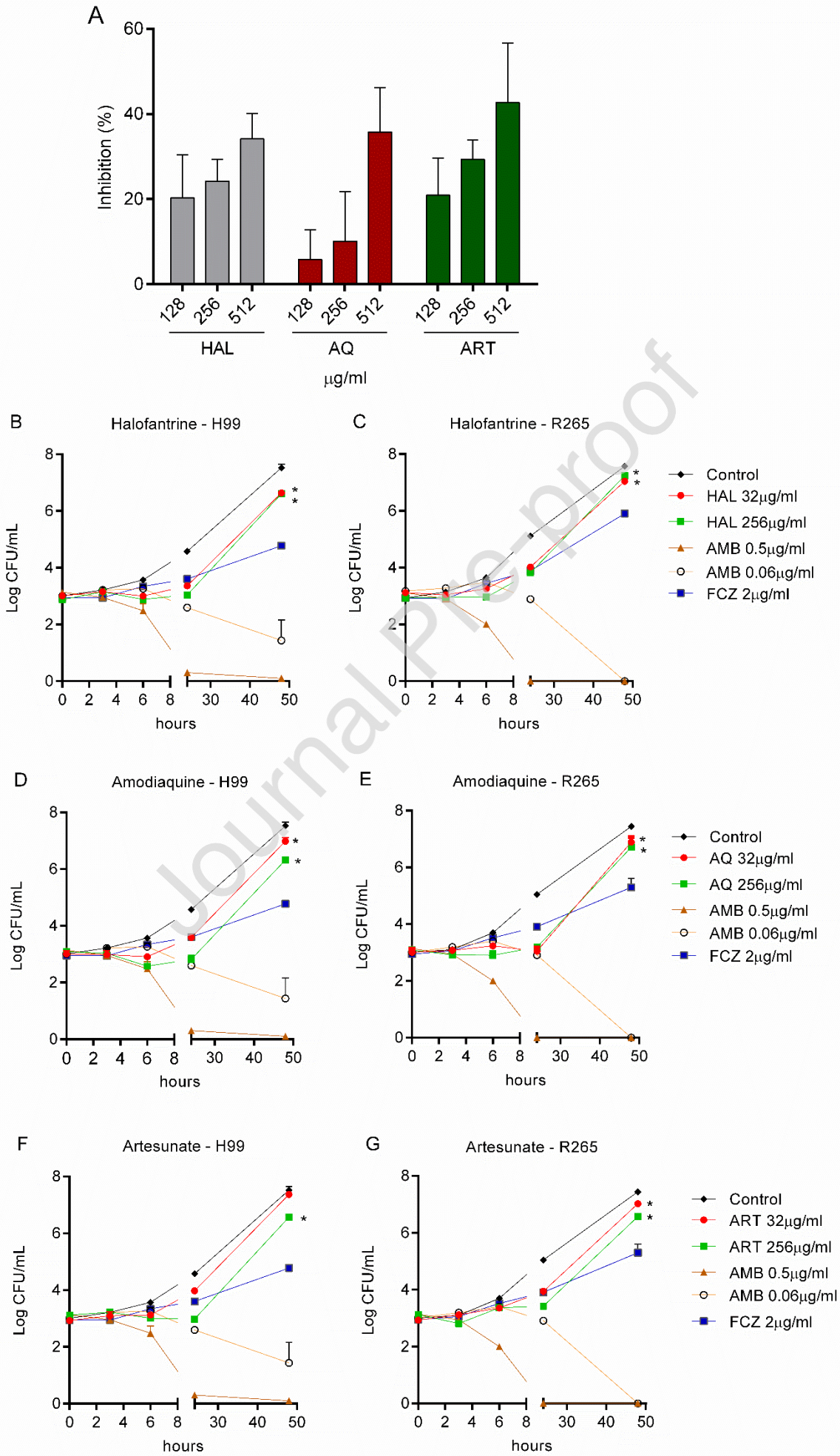

Figure 1: Antimalarials (ATMs) inhibit *Cryptococcus neoformans* and *C. gattii* growth.A) Percentage of inhibition of fungal growth at different ATMs concentration for ten strains of *C. neoformans* e *C. gattii*. B-C) Effect of different halofantrine (HAL) concentrations on the growth of H99 and R265 strains. D-E) Effect of different amodiaquine (AQ) concentrations on the growth of H99 and R265 strains. F-G) Effect of different artesunate (ART) concentrations on the growth of H99 and R265 strains. Statistical analysis: Area under the curve, * $p < 0.05$ compared to untreated control.

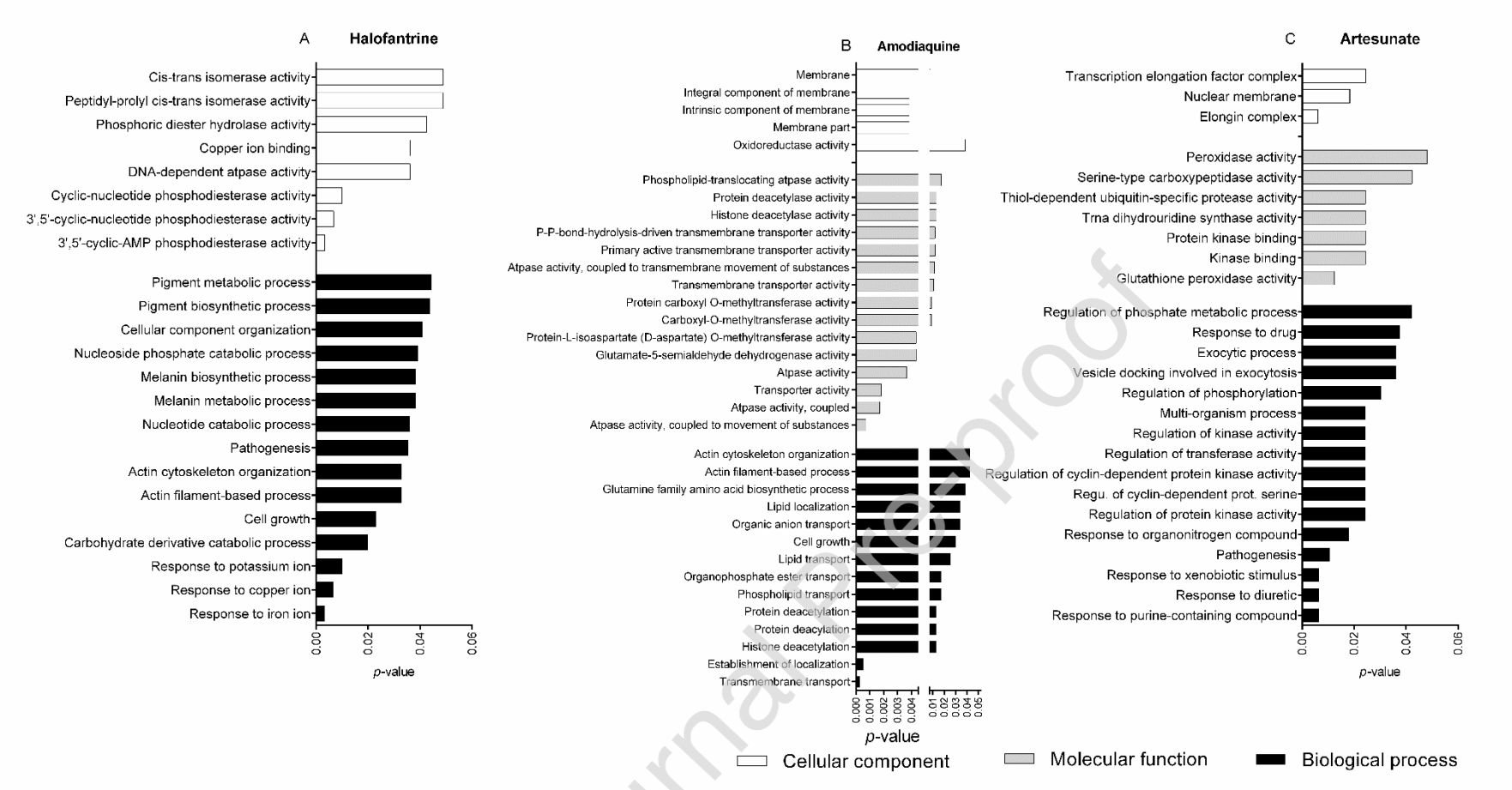

Figure 2: Different cellular processes are important for the susceptibility of *Cryptococcus* to antimalarials. A) Cellular components, molecular functions, and biological processes enriched for halofantrine (HAL) susceptible *C. neoformans* mutants. B) Cellular components, molecular mutants functions, and biological processes enriched for amodiaquine (AQ) susceptible *C. neoformans* mutants. C) Cellular components, molecular functions, and biological processes enriched for artesunate (ART) susceptible *C. neoformans* mutants.

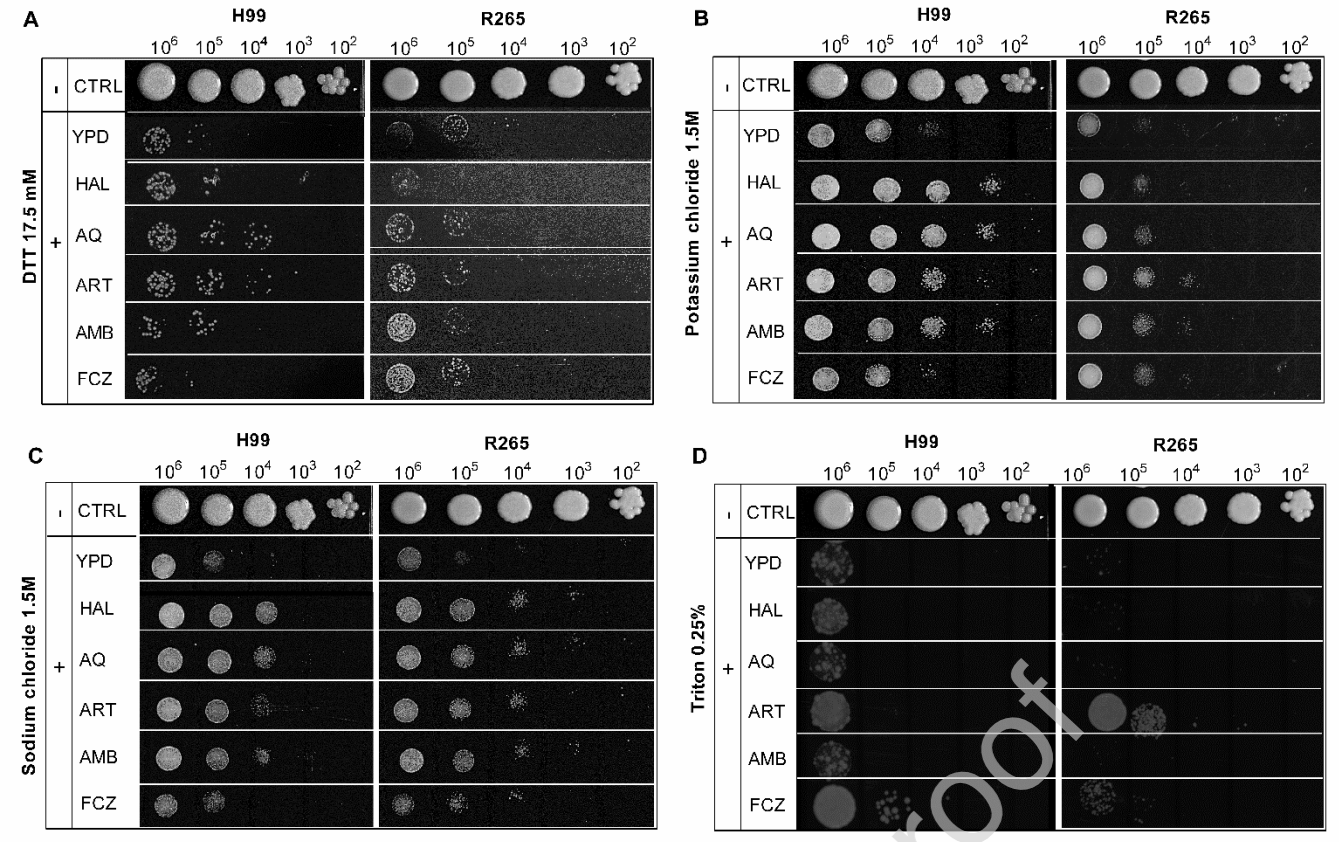

Figure 3: Exposure to antimalarials (ATMs) increases fungal growth under stressing conditions. A) Growth of H99 and R265 strains in DTT after exposure to ATMs. B) Growth of strains H99 and R265 in potassium chloride after exposure to ATMs. C) Growth of strains H99 and R265 in sodium chloride after exposure to ATMs. D) Growth of strains H99 and R265 in triton after exposure to ATMs. CTRL: growth control in YPD; HAL: Halofantrine; AQ: Amodiaquine; ART: Artesunate; AMB: Amphotericin b; FCZ: Fluconazole. + presence of xenobiotic; - absence of xenobiotic.

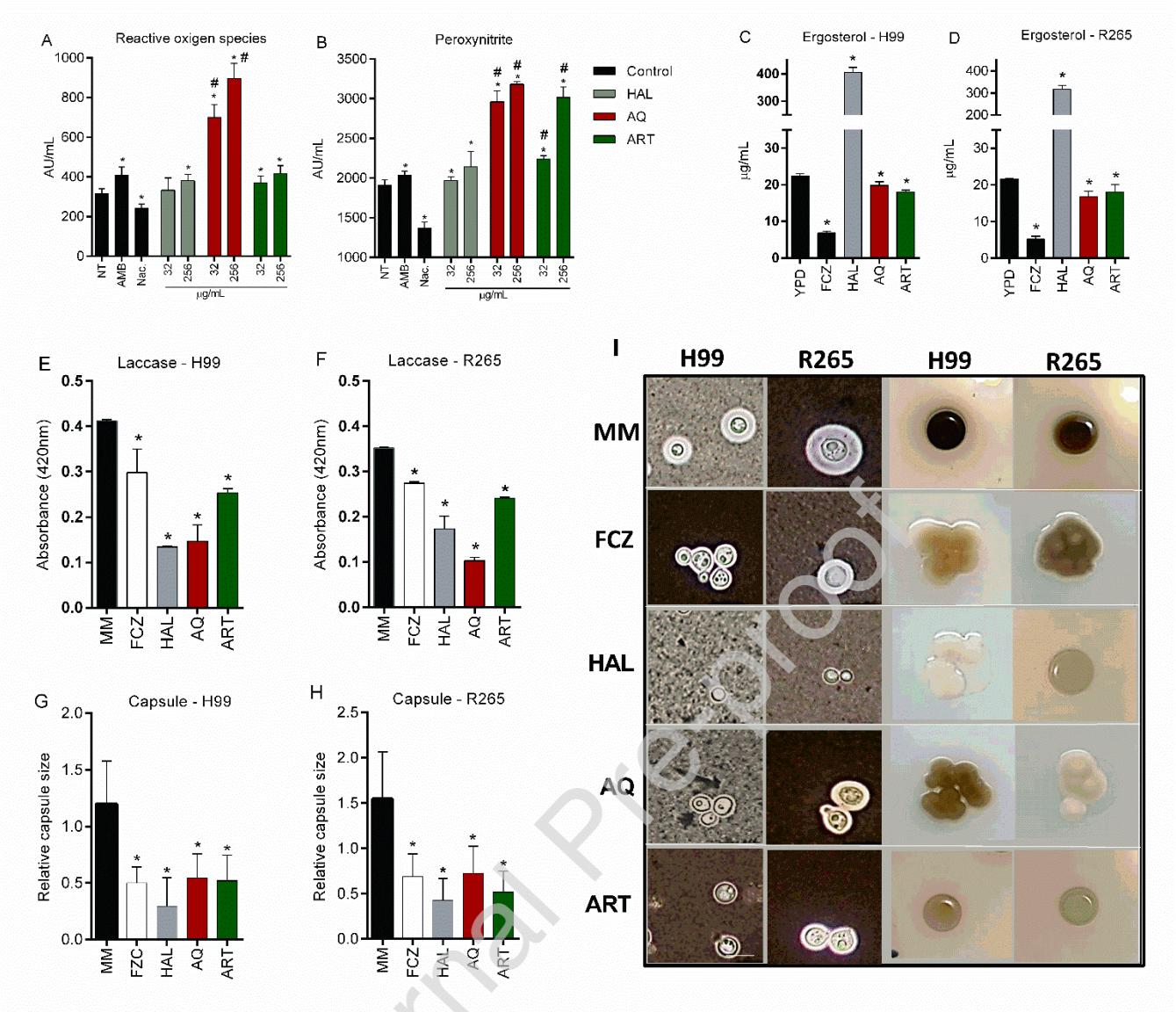

Figure 4: Antimalarials (ATMs) induce oxidative/nitrosative stresses and alter the synthesis of *Cryptococcus*'s ergosterol, melanin, and the polysaccharide capsule. A) Reactive oxygen species for the R265 and H99 strains. B) Peroxynitrite for the R265 and H99 strains. C-D) Quantification of ergosterol for strains H99 and R265 after treatment with ATMs. E-F) Laccase activity for strains H99 and R265 after exposure to ATMs. G-H) Relative capsule size for strains H99 and R265 after exposure to ATMs. I) India ink preparations and melanin phenotype of strains R265 and H99 after exposure to ATMs. The bar represents a length of 5µm. Statistical analysis: ANOVA followed by non-parametric Friedman post-test, * $p < 0.05$ compared to untreated control, # $p < 0.05$compared to AMB or FCZ.

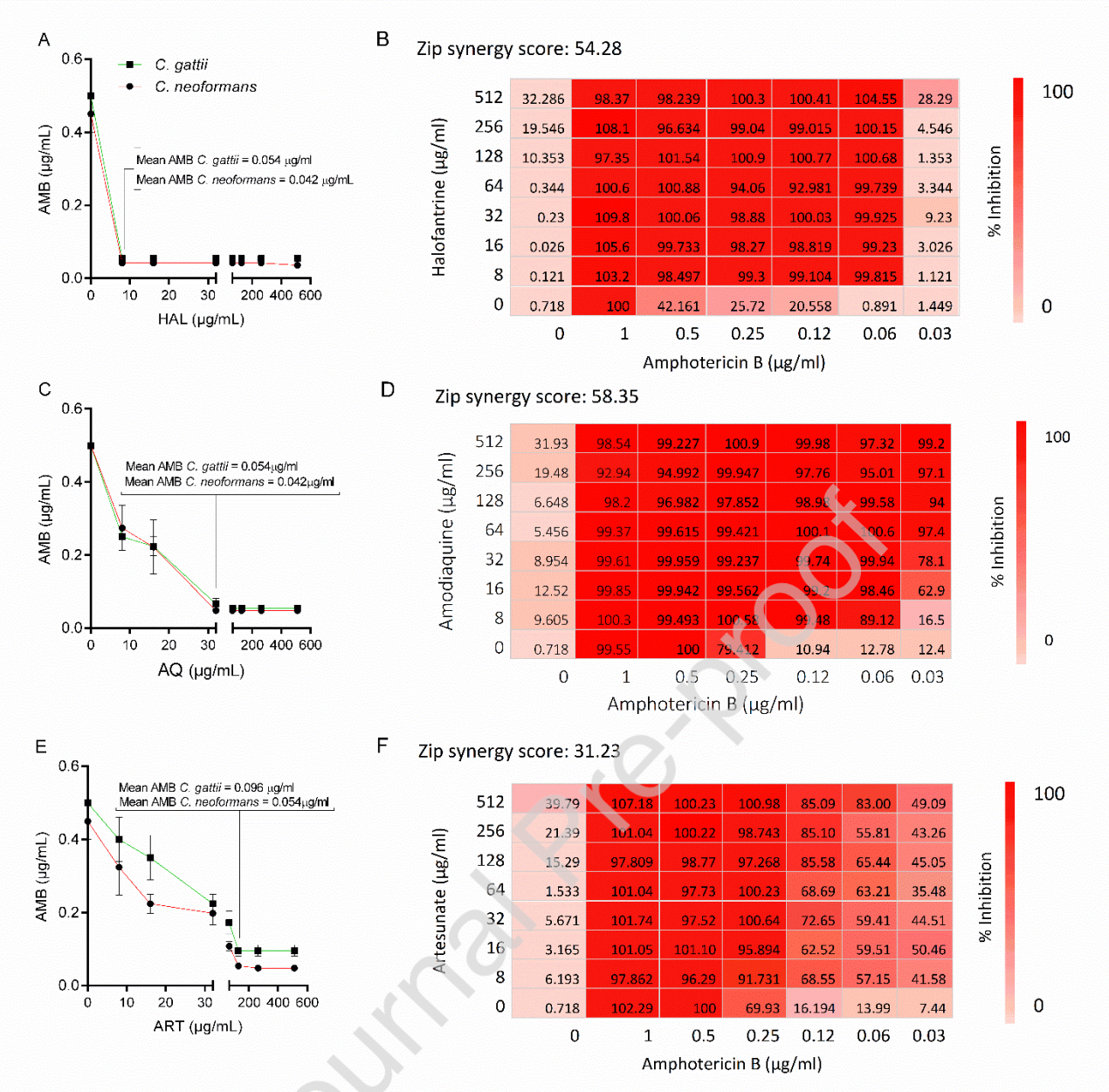

Figure 5: Antimalarials (ATMs) + Amphotericin B (AMB) is synergistic against *Cryptococcus* strains. A) Interaction curve between Amphotericin/Halofantrine against *Cryptococcus* strains. B) Heatmap of the interaction between Amphotericin/Halofantrine against the H99 strain. C) Interaction curve between Amphotericin/Amodiaquine against *Cryptococcus* strains. D) Heatmap of the interaction between Amphotericin/Amodiaquine against the H99 strain. E) Interaction curve between Amphotericin/Artesunate against *Cryptococcus* strains. F) Heatmap of the interaction between Amphotericin/Artesunate against the H99 strain.

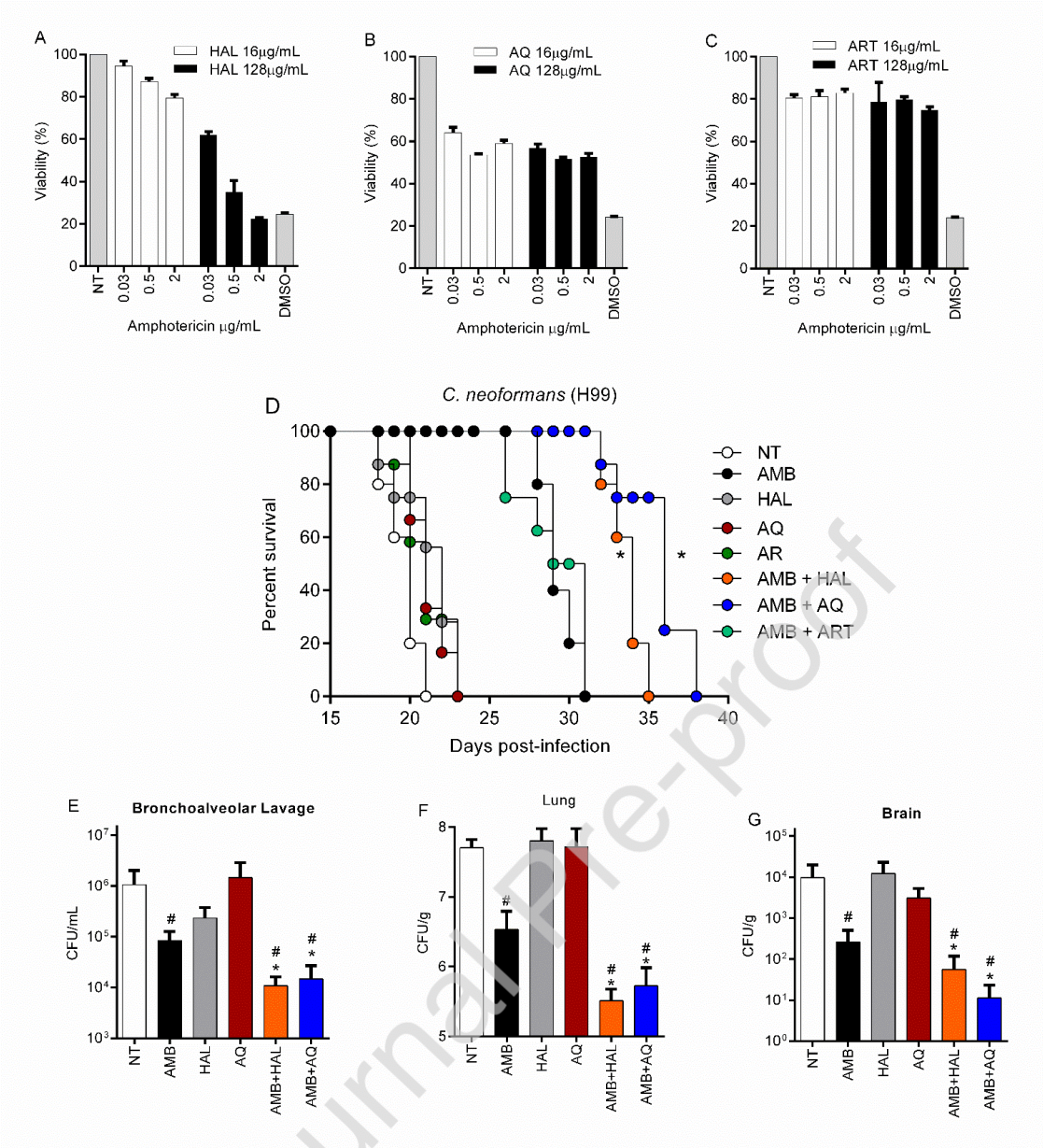

Figure 6: Antimalarials (ATMs) + Amphotercin b (AMB) have low toxicity to murine macrophages and reduce lethality and fungal burden in the lungs and brain. A-B) Viability of murine macrophages after exposure to ATMs + AMB. D) Lethality curve of mice infected with the H99 strain after treatment with ATMs, alone or in combination with AMB. E – G) Fungal burden recovered from BALF, lung, and brain. Statistical analysis: Survival curve was plotted by the Kaplan–Meier method, and the results were analyzed using the log rank test, # $p < 0.05$ compared to NT, * $p < 0.05$ compared to AMB alone.

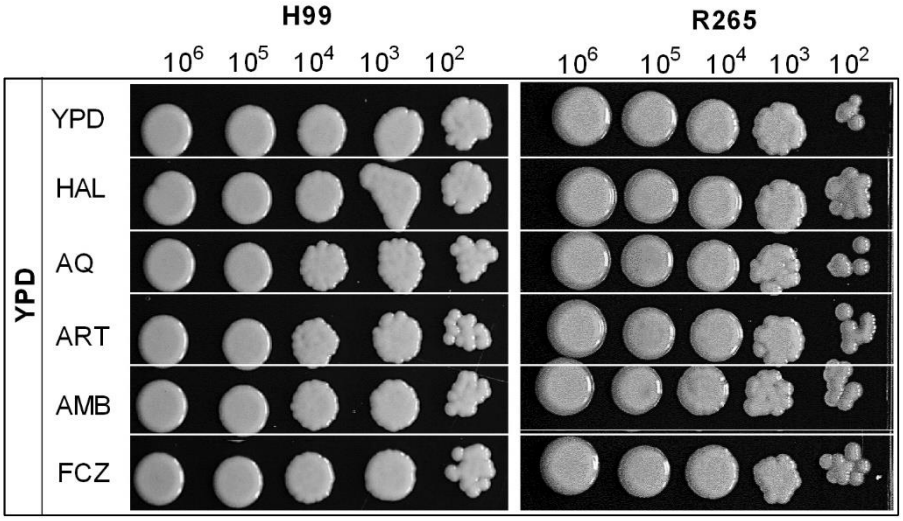

Figure S1: Exposure to antimalarials (ATMs) does not alter fungal viability. Growth ofH99 and R265 strains in YPD after exposure to ATMs.

Table 1: *C. neoformans* deletion mutants susceptible to halofantrine*.

CNAG	Symbol[a]	Function/ Predicted function[a]
CNAG_06241	CFO1	Acidic laccase
CNAG_04650	ARP6	Actin-like protein
CNAG_05135	PMR1	Ca2 -transporting ATPase
CNAG_06551		Carnitine O-acetyltransferase
CNAG_05109	CBD1	CBS and PB1 domain-containing protein
CNAG_04243	CDC24	Cell division control protein 24
CNAG_03621	CPA2	Cyclophilin A
CNAG_03652		Dynactin 6
CNAG_02449		Long-chain fatty acid Coa ligase
CNAG_01683	STL1	Monosaccharide transporter
CNAG_00445	NHPSO1	Nonhistone chromosomal protein
CNAG_03183	FZC24	Nuclear protein
CNAG_05081	PDE1	Phosphodiesterase, phosphodiesterase, variant
CNAG_04320	CPS1P	Polysaccharide synthase
CNAG_02006		Protein N-terminal amidase
CNAG_00384		RAD51-like protein 2

[a] Symbol and Predicted functions are based on data retrieved from FungiDB

* As described in materials and methods, a collection of single-gene deletion mutants were screened for alteration in growth in liquid medium containing 16 µg/mL amodiaquine. The table represents the deleted genes in each mutant that showed 100% growth inhibition compared to the drug-free growth control.

Table 2: *C. neoformans* deletion mutants susceptible to Amodiaquine*.

CNAG	Symbol[a]	Function/ Predicted function[a]
CNAG_06348	PMR5	ABC transporter PMR5
CNAG_00749		alternative sulfate transporter
CNAG_05282	APT4	Aminophospholipid translocase, putative apt4
CNAG_04159		ariadne-1
CNAG_04243	CDC24	cell division control protein 24
CNAG_04662	CTF4	chromosome transmission fidelity protein 4
CNAG_03100		cytoplasmic protein
CNAG_01870		electron transfer flavoprotein beta subunit
CNAG_02790		galactinol synthase
CNAG_04990	PRO2	glutamate-5-semialdehyde dehydrogenase
CNAG_04947		high-affinity nicotinic acid transporter
CNAG_05563	HOS2	histone deacetylase HOS2
CNAG_04898	MSF	MFS transporter
CNAG_04783	STL1	Monosaccharide transporter STL1
CNAG_04784	STL1	Monosaccharide transporter STL1
CNAG_00701	CAS31	protein involved in gxm O-acetylation CAS31
CNAG_03837		protein-L-isoaspartate O-methyltransferase
CNAG_07679	DST1	transcription elongation factor S-II
CNAG_07730		tricarboxylate transporter
CNAG_00560		V-type H -transporting ATPase subunit E

[a] Symbol and Predicted functions are based on data retrieved from FungiDB

* As described in materials and methods, a collection of single-gene deletion mutants were screened for alteration in growth in liquid medium containing 2 µg/mL halofantrine. The table represents the deleted genes in each mutant that showed 100% growth inhibition compared to the drug-free growth control.

Table 3: *C. neoformans* deletion mutants susceptible to artesunate*.

CNAG	Symbol[a]	Function/ Predicted function[a]
CNAG_03919		Acetate non-utilizing protein 9
CNAG_04208		Ataxin-3
CNAG_02373		ATP-binding protein
CNAG_03665	DDX35	ATP-dependent RNA helicase
CNAG_00600	CAP60	Capsular associated protein
CNAG_01040		Carboxypeptidase D
CNAG_05583	GCS1	Ceramide glucosyltransferase GCS1
CNAG_00415	CDC2801	CMGC/CDK protein kinase CDC2801
CNAG_01828	SWD1	Compass component swd1
CNAG_06365		Derlin-2/3
CNAG_05447		Elongin-A
CNAG_05704	VPS22	ESCRT-II complex subunit VPS22
CNAG_05280	GRR1	F-box and leucine-rich repeat protein
CNAG_02225	EXG104	Glucan 1,3-beta-glucosidase EXG104
CNAG_06287	GPX2	Glutathione peroxidase GPX2
CNAG_05524		Glycogen storage control protein
CNAG_02458		GTPase activating protein
CNAG_03069		Hydrolase
CNAG_06087		Kinetochore protein Spc7/SPC105
CNAG_06290	HXT2	Low-affinity glucose transporter HXT2
CNAG_00165		Methylthioadenosine phosphorylase
CNAG_05437		Nascent polypeptide-associated complex
CNAG_03584		Prp8 binding protein
CNAG_05703	LRG1	Rho GTPase activator LRG1
CNAG_02898		RNA-binding protein 8[a]
CNAG_01740	CDC12	Septin CDC12
CNAG_02259		Trna-dihydrouridine synthase 2
CNAG_01016		Vacuolar membrane protein
CNAG_02260	CRG1	Xap5-domain-containing protein CRG1

[a] Symbol and Predicted functions are based on data retrieved from FungiDB

* As described in materials and methods, a collection of single-gene deletion mutants were screened for alteration in growth in liquid medium containing 4 µg/mL artesunate. The table represents the deleted genes in each mutant that showed 100% growth inhibition compared to the drug-free growth control.

Table 4: Minimum inhibitory concentration (MIC) of antifungals and antimalarials (ATMs) against *C. neoformans*, *C. gattii* and *Candida* spp. strains. Mean fractional inhibitory concentration index (FICI) for Amphotericin B (AMB)/ (ATMs) interaction against *C. neoformans*, *C. gattii* and *Candida* spp. strains.

		MIC (µg/mL)					**Mean FICI interaction AMB/ATMs**		
	Strains	AMB[a]	FCZ[b]	HAL[a]	AQ[a]	ART[a]	HAL	AQ	ART
C. neoformans	H99	0.5	2	>512	>512	>512	0.33	0.33	0.31
	WM148	0.25	4	>512	>512	>512	0.39	0.39	0.36
	WM626	0.5	4	>512	>512	>512	0.29	0.29	0.38
	WM628	0.5	4	>512	>512	>512	0.35	0.35	0.36
	WM629	0.5	2	512	>512	>512	0.38	0.38	0.39
C. gattii	R265	0.5	4	>512	>512	>512	0.39	0.39	0.24
	WM179	0.5	1	>512	>512	>512	0.39	0.39	0.36
	WM178	0.5	4	>512	>512	>512	0.34	0.34	0.35
	WM161	0.25	2	>512	>512	>512	0.36	0.36	0.39
	WM779	0.5	8	>512	>512	>512	0.33	0.33	0.35
***C. albicans* (ATCCSC51314)**		1	4	>512	>512	>512	0,42	0.37	0.24
***C. glabrata* (ATCC2001)**		1	4	>512	>512	>512	0,38	0.38	0.42
***C. parapsilosis* (ATCC22019)**		1	8	>512	>512	>512	0,31	0.37	0.37
***C. krusei* (ATCC20298)**		1	8	>512	>512	>512	0,32	0.42	0.37
***C. tropicalis* (ATCC750)**		1	4	>512	>512	>512	0.38	0.37	0.42

[a] 100% growth inhibition. [b] 50% growth inhibition. Amphotericin B (AMB); Fluconazole (FCZ); Halofantrine (HAL); Amodiaquine (AQ); Artesunate (ART).

REFERENCES

1. Rajasingham R, Govender NP, Jordan A et al. The global burden of HIV-associated cryptococcal infection in adults in 2020: a modelling analysis. *Lancet Infect Dis* 2022.

2. Perfect JR, Bicanic T. Cryptococcosis diagnosis and treatment: What do we know now. *Fungal Genet Biol* 2015; **78**: 49-54.

3. Ribeiro NQ, Santos APN, Emídio ECP et al. Pioglitazone as an adjuvant of

amphotericin B for the treatment of cryptococcosis. *Int J Antimicrob Agents* 2019; **54**: 301-8.

4. Rossi SA, de Oliveira HC, Agreda-Mellon D et al. Identification of Off-Patent Drugs That Show Synergism with Amphotericin B or That Present Antifungal Action against Cryptococcus neoformans and. *Antimicrob Agents Chemother* 2020; **64**.

5. McCarty TP, Pappas PG. Antifungal Pipeline. *Front Cell Infect Microbiol* 2021; **11**: 732223.

6. Hoy SM. Oteseconazole: First Approval. *Drugs* 2022; **82**: 1017-23.

7. Cassetta MI, Marzo T, Fallani S et al. Drug repositioning: auranofin as a prospective antimicrobial agent for the treatment of severe staphylococcal infections. *Biometals* 2014; **27**: 787-91.

8. Oprea TI, Mestres J. Drug repurposing: far beyond new targets for old drugs. *AAPS J* 2012; **14**: 759-63.

9. Pushpakom S, Iorio F, Eyers PA et al. Drug repurposing: progress, challenges and recommendations. *Nat Rev Drug Discov* 2019; **18**: 41-58.

10. Delattin N, De Brucker K, Vandamme K et al. Repurposing as a means to increase the activity of amphotericin B and caspofungin against Candida albicans biofilms. *J Antimicrob Chemother* 2014; **69**: 1035-44.

11. Monroe A, Williams NA, Ogoma S et al. Reflections on the 2021 World Malaria Report and the future of malaria control. *Malar J* 2022; **21**: 154.

12. Akaihe CL, Nweze EI. Epidemiology of Cryptococcus and cryptococcosis in Western Africa. *Mycoses* 2021; **64**: 4-17.

13. Ashiru JO, Akang EE. Cryptococcal meningitis with malaria. A case report. *Mycopathologia* 1994; **127**: 15-7.

14. Gopalakrishnan AM, Kumar N. Antimalarial action of artesunate involves DNA damage mediated by reactive oxygen species. *Antimicrob Agents Chemother* 2015; **59**: 317-25.

15. Meshnick SR. Artemisinin: mechanisms of action, resistance and toxicity. *Int J*

Parasitol 2002; **32**: 1655-60.

16. Jung HY, Kim B, Ryu HG et al. Amodiaquine improves insulin resistance and lipid metabolism in diabetic model mice. *Diabetes Obes Metab* 2018; **20**: 1688-701.

17. Kaptein SJ, Efferth T, Leis M et al. The anti-malaria drug artesunate inhibits replication of cytomegalovirus in vitro and in vivo. *Antiviral Res* 2006; **69**: 60-9.

18. Qiao S, Tao S, Rojo de la Vega M et al. The antimalarial amodiaquine causes autophagic-lysosomal and proliferative blockade sensitizing human melanoma cells to starvation- and chemotherapy-induced cell death. *Autophagy* 2013; **9**: 2087-102.

19. Efferth T, Dunstan H, Sauerbrey A et al. The anti-malarial artesunate is also active against cancer. *Int J Oncol* 2001; **18**: 767-73.

20. Efferth T, Giaisi M, Merling A et al. Artesunate induces ROS-mediated apoptosis in doxorubicin-resistant T leukemia cells. *PLoS One* 2007; **2**: e693.

21. (CLSI) CaLSI. *Method for Broth Dilution antifungal Susceptibility Testing of Yeasts; Approved Standard*: Wayne, Pennsylvania, USA, 2012.

22. Correction to 'SynergyFinder 2.0: visual analytics of multi-drug combination synergies'. *Nucleic Acids Res* 2022.

23. Jung KW, Yang DH, Maeng S et al. Systematic functional profiling of transcription factor networks in Cryptococcus neoformans. *Nat Commun* 2015; **6**: 6757.

24. Liu OW, Chun CD, Chow ED et al. Systematic genetic analysis of virulence in the human fungal pathogen Cryptococcus neoformans. *Cell* 2008; **135**: 174-88.

25. Mayer FL, Sánchez-León E, Kronstad JW. A chemical genetic screen reveals a role for proteostasis in capsule and biofilm formation by. *Microb Cell* 2018; **5**: 495-510.

26. Basenko EY, Pulman JA, Shanmugasundram A et al. FungiDB: An Integrated Bioinformatic Resource for Fungi and Oomycetes. *J Fungi (Basel)* 2018; **4**.

27. Santos JR, Gouveia LF, Taylor EL et al. Dynamic interaction between fluconazole and amphotericin B against Cryptococcus gattii. *Antimicrob Agents Chemother* 2012; **56**: 2553-8.

28. Martinez LR, Ntiamoah P, Gácser A et al. Voriconazole inhibits melanization in

Cryptococcus neoformans. *Antimicrob Agents Chemother* 2007; **51**: 4396-400.

29. García-Rodas R, Trevijano-Contador N, Román E et al. Role of Cln1 during melanization of Cryptococcus neoformans. *Front Microbiol* 2015; **6**: 798.

30. Araujo GeS, Fonseca FL, Pontes B et al. Capsules from pathogenic and non-pathogenic Cryptococcus spp. manifest significant differences in structure and ability to protect against phagocytic cells. *PLoS One* 2012; **7**: e29561.

31. Ferreira GF, Baltazar LeM, Santos JR et al. The role of oxidative and nitrosative bursts caused by azoles and amphotericin B against the fungal pathogen Cryptococcus gattii. *J Antimicrob Chemother* 2013; **68**: 1801-11.

32. Ferreira GF, Santos JR, Costa MC et al. Heteroresistance to Itraconazole Alters the Morphology and Increases the Virulence of Cryptococcus gattii. *Antimicrob Agents Chemother* 2015; **59**: 4600-9.

33. Peres-Emidio EC, Freitas GJC, Costa MC et al. Infection Modulates the Immune Response and Increases Mice Resistance to. *Front Cell Infect Microbiol* 2022; **12**: 811474.

34. Reagan-Shaw S, Nihal M, Ahmad N. Dose translation from animal to human studies revisited. *FASEB J* 2008; **22**: 659-61.

35. Mesa-Arango AC, Scorzoni L, Zaragoza O. It only takes one to do many jobs: Amphotericin B as antifungal and immunomodulatory drug. *Front Microbiol* 2012; **3**: 286.

36. Casadevall A, Rosas AL, Nosanchuk JD. Melanin and virulence in Cryptococcus neoformans. *Curr Opin Microbiol* 2000; **3**: 354-8.

37. Coelho C, Casadevall A. Cryptococcal therapies and drug targets: the old, the new and the promising. *Cell Microbiol* 2016; **18**: 792-9.

38. Sangalli-Leite F, Scorzoni L, Mesa-Arango AC et al. Amphotericin B mediates killing in Cryptococcus neoformans through the induction of a strong oxidative burst. *Microbes Infect* 2011; **13**: 457-67.

39. Sokol-Anderson ML, Brajtburg J, Medoff G. Amphotericin B-induced oxidative damage and killing of Candida albicans. *J Infect Dis* 1986; **154**: 76-83.

40. Belenky P, Camacho D, Collins JJ. Fungicidal drugs induce a common oxidative-damage cellular death pathway. *Cell Rep* 2013; **3**: 350-8.

PEDIDO DE PATENTE

Os achados desse estudo resultaram no pedido de patente intitulado "Composições farmacêuticas antifúngicas contendo halofantrina, artesunato e amodiaquina, e uso" número BR1020190271418.

INPI INSTITUTO NACIONAL DA PROPRIEDADE INDUSTRIAL

18/12/2019 870190135954 16:38

29409161911877916

Pedido nacional de Invenção, Modelo de Utilidade, Certificado de Adição de Invenção e entrada na fase nacional do PCT

Número do Processo: BR 10 2019 027141 8

Dados do Depositante (71)

Dados do Pedido

Natureza Patente: 10 - Patente de Invenção (PI)

Título da Invenção ou Modelo de Utilidade (54): COMPOSIÇÕES FARMACÊUTICAS ANTIFÚNGICAS CONTENDO HALOFANTRINA, ARTESUNATO E AMODIAQUINA, E USO

Resumo: A presente tecnologia trata de composições farmacêuticas contendo os compostos halofantrina, artesunato e amodiaquina isoladamente ou em combinação, como adjuvantes em associação com Anfotericina B para produção de medicamentos para tratamento de infecções fúngicas, preferencialmente causadas por Cryptococcus sp. e Candida sp.

Figura a publicar: 2

CERTIFICADO COMISSÃO DE ÉTICA NO USO DE ANIMAIS (CEUA)

UFMG

UNIVERSIDADE FEDERAL DE MINAS GERAIS

CEUA

COMISSÃO DE ÉTICA NO USO DE ANIMAIS

CERTIFICADO

Certificamos que o projeto intitulado "Reposicionamento de antimaláricos para o tratamento da Criptococose em modelo murino", protocolo do CEUA: 237/2021 sob a responsabilidade de Daniel de Assis Santos que envolve a produção, manutenção e/ou utilização de animais pertencentes ao filo Chordata, subfilo Vertebrata (exceto o homem) para fins de pesquisa científica (ou ensino) - encontra-se de acordo com os preceitos da Lei nº 11.794, de 8 de outubro de 2008, do Decreto nº 6.899 de 15 de julho de 2009, e com as normas editadas pelo Conselho Nacional de Controle da Experimentação Animal (CONCEA), e foi aprovado pela COMISSÃO DE ÉTICA NO USO DE ANIMAIS (CEUA) DA UNIVERSIDADE FEDERAL DE MINAS GERAIS, em reunião de 10/01/2022.

Vigência da Autorização	10/01/2022 a 09/01/2027
Finalidade	Pesquisa
***Espécie/linhagem**	Camundongo isogênico / C57/BL6
Nº de animais	6
Peso/Idade	20g / 8(semanas)
Sexo	masculino
Origem	biotério central
***Espécie/linhagem**	Camundongo isogênico / C57/BL6

CAPÍTULO 4
Testosterona e estradiol apresentam sinergismo com anfotericina B contra *Cryptococcus* spp.

Gustavo J. C. Freitas; Junya D. L. Singulani, Daniel A. Santos.

RESUMO

A ocorrência e frequência de algumas infecções fúngicas pode ser influenciada por hormônios sexuais. Esses compostos podem modular a reposta imune durante a infecção e alterar a morfofiologia do patógeno, o tornando potencialmente infeccioso ou não. No contexto da criptococcose, uma infecção fúngica invasiva, camundongos fêmeos apresentam uma mortalidade tardia devido ao aumento do recrutamento de neutrófilos e redução da carga fúngica no início da infecção, comparado a camundongos machos. Apesar dessas evidências, a influência de hormônios sexuais (HSs) na terapia antifúngica permanece inexplorada. Nesse sentido, objetivamos avaliar a interação entre HSs e antifúngicos clínicos frente a diferentes linhagens de *C. neoformans* e *C. gattii*. Demonstramos que, embora não tenha ação antifúngica, a combinação entre os HSs (estradiol e testosterona) e anfotericina B (AMB) resultou em uma interação sinérgica, com redução de até 10x na concentração inibitória mínima da AMB. Por outro lado, a combinação HSs + Fluconazol foi indiferente, não afetando a ação do azólico. Interessantemente, os HSs apresentaram ação antioxidante em contato com a célula fúngica, sugerindo um mecanismo independente de estresse oxidativo e nitrosativo na potencialização fungicida da AMB. Nossos resultados ainda são preliminares e novas análises ainda serão realizadas para a melhor compreensão dos mecanismos envolvidos na interação sinérgica de HSs + AMB.

Palavras-chave: Hormônios sexuais, testosterona, estradiol, criptococose, antifúngicos.

1. Introdução

Muitas doenças infecciosas apresentam frequência e gravidade que podem ser influenciadas por hormônios sexuais (HSs) (testosterona e estradiol)(VOM STEEG; KLEIN, 2016). As células imunes expressam receptores de estrogênio e andrógeno e, portanto, os hormônios sexuais podem desempenhar um papel importante na regulação da resposta imune frente a patógenos (GIEFING-KRÖLL; BERGER; LEPPERDINGER; GRUBECK-LOEBENSTEIN, 2015; KOVATS, 2015). Além disso, HSs também podem alterar a morfofiologia do patógeno e torna-lo potencialmente infeccioso ou não (KUMWENDA; COTTIER; HENDRY; KNEAFSEY *et al.*, 2022; SHANKAR; RESTREPO; CLEMONS; STEVENS, 2011).

A paracoccidioidomicose, por exemplo, infecção causada por *Paracoccidioides brasilienses*, ocorre principalmente em homens na idade reprodutiva, com uma proporção infecciosa de 70,6 homens para cada uma mulher, dependendo da região (SHANKAR; RESTREPO; CLEMONS; STEVENS, 2011). Acredita-se que o estradiol, hormônio sexual feminino, impede a conversão de *P. brasiliensis* de esporo para levedura, interferindo na sua capacidade de causar doença (SHANKAR; RESTREPO; CLEMONS; STEVENS, 2011). De modo oposto, fatores que aumentam os níveis circulatórios de estrogênio, como gravidez, uso de contraceptivos orais e terapia de reposição hormonal, predispõem as mulheres à candidíase vulvovaginal (KUMWENDA; COTTIER; HENDRY; KNEAFSEY *et al.*, 2022). Sabe-se que o estradiol reduz a opsonização de *C. albicans* durante a infecção e diminui a fagocitose, resultando na evasão da resposta imune e eliminação fúngica ineficiente (KUMWENDA; COTTIER; HENDRY; KNEAFSEY *et al.*, 2022). Estudo recente também demonstrou que camundongos fêmeos apresentam uma mortalidade tardia após infecção com *C. gattii* em relação a camundongos machos (COSTA; DE BARROS FERNANDES; GONÇALVES; SANTOS *et al.*, 2020). Entretanto, apesar dessas evidências, a influência de hormônios sexuais na terapia antifúngica permanece inexplorada. Nesse sentido, objetivamos avaliar a interação entre hormônios sexuais e antifúngicos clínicos frente a diferentes linhagens de *C. neoformans* e *C. gattii*.

Em geral, vimos que a combinação entre os hormônios sexuais (HS) (estradiol e testosterona) e anfotericina B (AMB) resultou em uma interação sinérgica. A combinação com fluconazol foi indiferente, não afetando a ação do azólico. Interessantemente, os hormônios apresentaram ação antioxidante em contato com a célula fúngica, sugerindo um mecanismo independente de estresse oxidativo e nitrosativo na potencialização fungicida da AMB.

2. Materiais e métodos

Para o desenvolvimento deste estudo, utilizamos a mesma metodologia descrita no artigo anterior “Antimalarials and amphotericin B interact synergistically and are new options to treat cryptococcosis”. Nesse estudo, foram utilizados os antifúngicos clínicos fluconazol (Sigma-Aldrich®), anfotericina B (Sigma-Aldrich®) e os hormônios sexuais estradiol e testosterona.

3. Resultados e discussão

Inicialmente vimos que o estradiol e a testosterona não foram capazes de inibir o crescimento de *C. neoformans* e *C. gattii*. Como apresentado nas tabelas 1 e 2, a CIM dos HSs foi superior a 512µg/ml. Em seguida, nós decidimos avaliar se a interação entre os HSs e os antifúngicos anfotericina B e Fluconazol poderia alterar o perfil de susceptibilidade. Interessantemente, a combinação entre os HSs + AMB resultou em uma interação sinérgica dose-dependente (CIF <0,5 e ZIP > 10) (Tabela 1 e 2) (Fig. 1A – D*) in vitro*. Para o fluconazol, a interação com os HSs foi indiferente (Tabela 1 e 2). Os mapas de calor mostrados na Fig. 1A - D reforçam o sinergismo entre as drogas testadas. As pontuações de sinergia ZIP foram 32,03 (H99) e 29,03 (R265) para a interação ES + AMB e 27,08 (H99) e 33,09 (R265) para a interação TE + AMB**.**

Posteriormente, decidimos avaliar se o sinergismo observado entre HSs + AMB poderia ser resultante de uma potencialização do estresse oxidativo e nitrosativo induzido pela anfotericina B. Nossos achados demonstraram que a combinação HSs + AMB não foi capaz de aumentar os níveis de ROS e PRN em relação a AMB, pelo contrário, observamos uma redução desses parâmetros, sugerindo um papel antioxidante dos HSs durante o contato com a célula fúngica (Figura 2). Isso reforça evidências anteriores sobre o papel antioxidante de HSs por meio da regulação de diferentes enzimas antioxidantes (CRUZ-TOPETE; DOMINIC; STOKES, 2020; KANDER; CUI; LIU, 2017; MANCINI; LEONE; FESTA; GRANDE *et al.*, 2008), porém, para fungos isso ainda não havia sido explorado.

Especulamos que o sinergismo observado entre os HSs + AMB pode ser consequência de um aumento da fluidez de membrana induzido pelos HSs favorecendo a ação da AMB. Análises do conteúdo de ergosterol, parede celular, permeabilidade de membrana e microscopia de transmissão ainda serão realizadas para investigarmos esta hipótese. Além disso, a fim de aprimorar as nossas análises, também avaliaremos a interação com a anfotericina B, de drogas que apresentam estrutura química semelhante a hormônios sexuais, tais como: espironolactona, isoflavona e eplerenona.

Tabela 1. Valores da concentração inibitória fracionária (CIF) para *C. gattii* e *C. neoformans* obtidos da interação entre anfotericina B (AMB) e fluconazol (FCZ) com estradiol.

		MIC (mg/L)			CIF da interação AMB/EST para diferentes conc. de Estradiol (mg/L):							CIF da interação FLUC/EST para diferentes conc. de Estradiol (mg/L):						
	Linhagem	FLUC[a]	AMB[b]	Estradiol[b]	16	8	4	2	1	0,5	0,25	16	8	4	2	1	0,5	0,25
Cryptococcus gattii	R265	4	0,5	>512	**0,15**	**0,13**	**0,24**	1,00	1,00	1,00	1,00	1,03	1,01	1,00	1,00	1,00	1,00	1,00
	WM179	4	0,5	>512	**0,15**	**0,13**	**0,24**	**0,24**	**0,24**	**0,24**	**0,24**	1,03	1,01	1,00	1,00	1,00	1,00	1,00
	WM178	4	0,5	>512	**0,15**	**0,25**	**0,24**	0,50	0,50	0,50	1,00	1,09	1,07	1,08	1,04	1,02	1,06	0,06
	WM161	2	0,5	>512	**0,15**	**0,13**	**0,24**	0,50	0,50	1,00	1,00	1,03	1,01	1,00	1,00	1,00	1,00	1,00
	WM779	4	0,5	>512	**0,09**	**0,07**	**0,06**	**0,06**	**0,24**	0,50	0,50	1,03	1,01	1,00	1,00	1,00	1,00	1,00
	MIC50*	8	0,5	-														
	MIC90**	8	0,5	-														
	MIC range	2 – 4	0,5	-														
	Geom. mean	8	0,5															
Cryptococcus neoformans	H99	4	0,5	>512	**0,27**	**0,25**	**0,24**	**0,24**	**0,24**	**0,24**	**0,24**	1,03	1,13	1,00	1,09	1,03	1,09	1,08
	WM148	8	0,5	>512	**0,15**	**0,13**	**0,24**	**0,24**	0,50	0,50	0,50	1,02	1,12	1,00	1,03	1,01	1,07	1,04
	WM626	1	0,5	>512	**0,15**	**0,13**	**0,24**	0,50	0,50	0,50	0,50	1,03	1,44	1,00	1,39	1,53	1,97	1,08
	WM628	4	0,5	>512	**0,15**	**0,13**	**0,12**	**0,12**	**0,12**	**0,12**	0,24	1,07	1,02	1,00	1,03	1,19	1,77	1,78
	WM629	2	0,25	>512	**0,15**	**0,13**	**0,12**	**0,12**	**0,12**	**0,12**	0,24	1,08	1,21	1,30	1,06	1,53	1,00	1,88
	MIC50*	4	0,5	-														
	MIC90**	4	0,5	-														
	MIC range	1 – 8	0,25 – 0,5	-														
	Geom. mean	3,03	0,435															

a: CIM (80%) - endpoint considerando 80 % da inibição de crescimento
b: CIM (100%) - endpoint considerando 100 % da inibição de crescimento
*CIM50: valor de CIM que inibiu 50% dos isolados.
**CIM90: valor de CIM que inibiu 90% dos isolados.
CIF em Negrito: sinergismo

Tabela 2. Valores da concentração inibitória fracionária (CIF) para *C. gattii* e *C. neoformans* obtidos da interação entre anfotericina B (AMB) e fluconazol (FCZ) com testosterona.

		MIC (mg/L)			CIF da interação AMB/Tes para diferentes conc. de Testosterona (mg/L):							CIF da interação FLUC/Tes para diferentes conc. de Testosterona (mg/L):						
	Linhagem	FLUC[a]	AMB[b]	TES[b]	16	8	4	2	1	0,5	0,25	16	8	4	2	1	0,5	0,25
Cryptococcus gattii	R265		0,5	>512	**0,13**	**0,24**	**0,24**	**0,24**	1,00	1,00	1,00	1,01	1,00	1,00	1,03	1,97	1,88	1,23
	WM179	4	0,5	>512	**0,13**	**0,24**	**0,24**	**0,24**	0,50	1,00	1,00	1,01	1,00	1,00	1,93	1,07	1,88	1,00
	WM178	8	0,5	>512	**0,25**	**0,24**	0,50	0,50	1,00	1,00	1,00	1,01	1,00	1,00	1,53	1,07	1,08	1,00
	WM161	2	0,5	>512	**0,13**	**0,12**	**0,12**	**0,11**	0,24	0,50	0,50	1,01	1,00	1,00	1,95	1,47	1,04	1,23
	WM779	4	0,5	>512	**0,25**	**0,24**	**0,48**	**0,48**	**0,48**	**0,48**	1,00	1,01	1,00	1,00	1,53	1,77	1,00	1,03
	MIC50*	8	0,5	-														
	MIC90**	8	0,5	-														
	MIC range	4 – 16	0,5	-														
	Geom. mean	8	0,5															
Cryptococcus neoformans	H99	4	0,5	>512	**0,13**	**0,12**	**0,12**	**0,12**	**0,12**	**0,12**	**0,12**	1,01	1,05	1,00	1,03	1,97	1,88	1,23
	WM148	8	0,5	>512	**0,13**	**0,12**	**0,24**	**0,24**	0,50	0,50	1,00	1,01	1,20	1,00	1,93	1,07	1,99	1,00
	WM626	1	0,5	>512	**0,13**	**0,12**	**0,24**	0,50	0,50	1,00	1,00	1,01	1,00	1,00	1,57	1,07	1,78	1,00
	WM628	4	0,5	>512	**0,13**	**0,12**	**0,12**	**0,12**	**0,12**	**0,24**	**0,24**	1,01	1,00	1,00	1,04	1,47	1,04	1,23
	WM629	2	0,25	>512	**0,13**	**0,12**	**0,12**	**0,24**	**0,24**	**0,24**	**0,24**	1,01	1,05	1,00	1,53	1,77	1,00	1,03
	MIC50*	4	0,5	-														
	MIC90**	4	0,5	-														
	MIC range	1 – 8	0,25 – 0,5	-														
	Geom. mean	3,03	0,435															

a: CIM (80%) - endpoint considerando 80 % da inibição de crescimento
b: CIM (100%) - endpoint considerando 100 % da inibição de crescimento
*CIM50: valor de CIM que inibiu 50% dos isolados.
**CIM90: valor de CIM que inibiu 90% dos isolados.
CIF em Negrito: sinergismo

A H99 Strain Zip synergy score: 32,03

Estradiol (µg/ml)	0	0,07	0,015	0,03	0,06	0,12	0,25	0,5	1
16	0,50	52,41	49,56	51,96	104,75	104,48	104,75	104,64	104,40
8	0,38	45,82	42,33	59,93	108,75	107,98	101,03	103,59	102,44
4	0,86	44,68	47,53	58,77	93,92	98,46	100,52	102,08	97,55
2	0,64	44,38	45,57	51,28	112,88	99,19	102,92	102,17	100,13
1	0,34	49,12	35,54	53,97	101,96	103,26	102,02	100,63	104,00
0,5	0,67	47,4	36,27	41,21	100,02	102,00	101,67	104,98	98,53
0,25	0,70	20,79	41,13	48,06	106,30	100,12	102,74	100,66	100,24
0	0,42	4,30	3,19	17,47	38,89	50,00	45,17	100	102,56

Amphotericin B (µg/ml)

Inibition %

B R265 Strain Zip synergy score: 29,03

Estradiol (µg/ml)	0	0,007	0,015	0,03	0,06	0,12	0,25	0,5	1
16	3,21	55,50	57,00	69,45	70,35	107,95	106,76	107,64	103,82
8	1,00	54,74	55,57	50,55	70,82	115,74	106,29	107,80	106,45
4	2,51	54,15	52,54	57,62	64,65	106,26	104,11	102,00	101,83
2	1,42	52,40	51,72	51,91	66,42	100,55	106,33	100,54	99,04
1	2,24	51,63	59,76	56,67	69,24	111,63	108,55	101,24	106,88
0,5	1,66	55,60	51,18	50,15	72,45	102,75	103,89	104,80	102,34
0,25	1,67	52,70	53,16	46,95	68,70	102,78	104,69	105,00	103,04
0	0,66	12,71	14,86	21,30	24,43	31,70	41,44	100	103,35

Amphotericin B (µg/ml)

C H99 Strain Zip synergy score: 27,08

Testosterone (µg/ml)	0	0,007	0,015	0,03	0,06	0,12	0,25	0,5	1
16	0,00	53,63	60,60	73,40	74,66	102,31	106,83	107,72	102,86
8	2,07	47,61	55,26	68,07	74,63	106,75	102,82	107,07	103,75
4	3,11	54,56	55,01	65,59	75,54	100,83	100,94	107,03	102,96
2	0,85	51,18	50,73	65,60	74,96	100,26	105,08	104,55	100,46
1	4,71	54,76	53,38	56,30	73,45	106,89	108,15	107,30	110,14
0,5	2,70	51,48	50,25	47,73	74,52	103,95	104,61	106,93	109,16
0,25	2,15	34,22	45,09	48,19	72,85	104,25	104,92	107,45	104,90
0	0,86	0,76	12,70	12,14	15,43	22,94	45,27	100	102,54

Amphotericin B (µg/ml)

D R265 Strain Zip synergy score: 33,09

Testosterone (µg/ml)	0	0,007	0,015	0,03	0,06	0,12	0,25	0,5	1
16	1,86	69,04	57,69	68,53	100,12	100,38	100,30	104,39	103,99
8	3,55	69,10	60,97	53,30	103,24	101,95	101,48	104,48	101,21
4	2,7	67,00	63,22	72,63	106,38	103,59	101,57	99,51	97,70
2	3,32	65,85	67,02	65,37	95,14	100,57	100,86	99,57	96,83
1	1,18	32,40	63,38	61,40	92,02	99,25	100,49	99,57	95,95
0,5	2,43	32,90	67,53	59,11	74,46	95,41	99,10	100,33	97,79
0,25	3,83	39,17	61,39	55,36	83,12	98,95	100,83	99,15	98,05
0	0,86	13,28	22,13	43,04	33,54	43,53	49,90	100	102,62

Amphotericin B (µg/ml)

Figura 1: A - B) *Heatmap* da interação entre Estradiol/Anfotercicina B frente às linhagens H99 e R265. C - D) *Heatmap* da interação entre Testosterona/Anfotercicina B frente às linhagens H99 e R265.

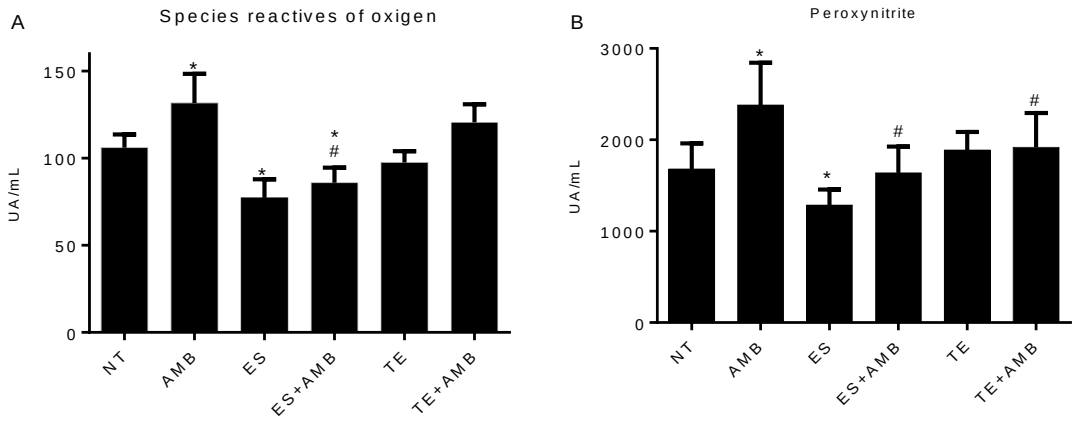

Figura 2: A) Espécies reativas de oxigênio para as linhagens R265 e H99 após tratamento com anfotericina B (AMB), estradiol (ES) e testosterona (TE). B) Peroxinitrito para as linhagens R265 e H99 após tratamento com AMB, ES e TE.

4. REFERÊNCIAS

1. Vom Steeg LG, Klein SL. 2016. SeXX Matters in Infectious Disease Pathogenesis. PLoS Pathog 12:e1005374.

2. Giefing-Kröll C, Berger P, Lepperdinger G, Grubeck-Loebenstein B. 2015. How sex and age affect immune responses, susceptibility to infections, and response to vaccination. Aging Cell 14:309-21.

3. Kovats S. 2015. Estrogen receptors regulate innate immune cells and signaling pathways. Cell Immunol 294:63-9.

4. Kumwenda P, Cottier F, Hendry AC, Kneafsey D, Keevan B, Gallagher H, Tsai HJ, Hall RA. 2022. Estrogen promotes innate immune evasion of Candida albicans through inactivation of the alternative complement system. Cell Rep 38:110183.

5. Shankar J, Restrepo A, Clemons KV, Stevens DA. 2011. Hormones and the resistance of women to paracoccidioidomycosis. Clin Microbiol Rev 24:296-313.

6. Costa MC, de Barros Fernandes H, Gonçalves GKN, Santos APN, Ferreira GF, de Freitas GJC, do Carmo PHF, Hubner J, Emídio ECP, Santos JRA, Dos Santos JL, Dos Reis AM, Fagundes CT, da Silva AM, Santos DA. 2020. 17-β-Estradiol increases macrophage activity through activation of the G-protein-coupled estrogen receptor and improves the response of female mice to *Cryptococcus* gattii. Cell Microbiol 22:e13179.

7. Mancini A, Leone E, Festa R, Grande G, Silvestrini A, de Marinis L, Pontecorvi A, Maira G, Littarru GP, Meucci E. 2008. Effects of testosterone on antioxidant systems in male secondary hypogonadism. J Androl 29:622-9.

8. Kander MC, Cui Y, Liu Z. 2017. Gender difference in oxidative stress: a new look at the mechanisms for cardiovascular diseases. J Cell Mol Med 21:1024-1032.

9. Cruz-Topete D, Dominic P, Stokes KY. 2020. Uncovering sex-specific mechanisms of action of testosterone and redox balance. Redox Biol 31:101490.

6. DISCUSSÃO GERAL

Nesta tese demonstramos a dinâmica do remodelamento celular e transcricional de *C. neoformans* em tempo precoce e tardio da infecção, e em seguida abordamos novas estratégias para o tratamento da criptococose. Estabelecemos uma linha translacional envolvendo a compreensão da patogênese dessa infecção e a busca de novas alternativas terapêuticas.

A mudança morfológica durante a infecção é uma estratégia comum para vários fungos, como *Candida albicans*, *Sporotrix* spp. e *Paracocidiodes* spp(KLEIN; TEBBETS, 2007; KUMWENDA; COTTIER; HENDRY; KNEAFSEY *et al.*, 2022; SHANKAR; RESTREPO; CLEMONS; STEVENS, 2011). Entretanto, para a *Cryptococcus*, apesar de todo o conhecimento da sua plasticidade fenotípica(ZARAGOZA, 2011), a compreensão sobre o remodelamento celular durante a infecção e impacto na virulência permanecia pouco explorado, principalmente em tempos precoces de infecção. Nesta tese, vimos que *Cryptococcus* apresenta alterações morfológicas e transcricionais marcantes durante a infecção, como apresentado no Capítulo I. Inicialmente o fungo utiliza estratégias voltadas para a reprodução, otimização do metabolismo celular, colonização e disseminação tecidual. Logo após 6 horas de infecção, observamos redução no tamanho celular, aumento do *fitness* reprodutivo e energético. Consequentemente esses eventos celulares propiciaram uma maior capacidade de sobreviver ao ambiente pulmonar e ultrapassar as barreiras biológicas do trato respiratório. Tardiamente, observamos alterações mais voltadas para a virulência e resistência a resposta imune, como o aumento da capsula polissacarídica e metabolismo energético. Os nossos resultados preenchem lacunas da literatura e trazem repostas importantes sobre a adaptação do fungo durante o primo contato com o hospedeiro.

Em continuidade ao capítulo 1 e de maneira complementar ao estudo de *C. neoformans,* também apresentamos a dinâmica do remodelamento celular para *C.*

gattii nos diferentes estágios da infecção. Nesse contexto, nós vimos que as alterações morfológicas no início da infecção (6 e 24 horas) se assemelham aos achados de *C. neoformans*. Porém, o aumento da cápsula polissacarídica ao longo da infecção não foi suficiente para predizer a virulência de *C. gattii*, como visto para *C. neoformans*. Dessa forma, outras análises ainda serão realizadas para a melhor compreensão da relação entre a dinâmica morfológica de *C. gattii* durante a infecção e a virulência.

O desenvolvimento desta tese também trouxe perguntas importantes a serem exploradas no aspecto da dinâmica morfológica de *Cryptococcus* durante a infecção, tais como: células pequenas são mais facilmente reconhecidas e fagocitadas por macrófagos no início da infecção do que células de tamanho normal? Após a fagocitose, essas células têm maior capacidade de proliferação intracelular? Uma vez que essas células apresentam maior replicação, isso pode interferir na susceptibilidade a antifúngicos? Drogas que alteram a progressão do ciclo celular, podem alterar a dinâmica do remodelamento celular durante a infecção e atenuar a virulência de *Cryptococccus*? Essas perguntas abrem uma gama de possibilidades para o estudo desse patógeno e podem trazer resultados importantes para a compreensão da biologia de *Cryptococcus* durante a infecção e busca de novos alvos para diagnóstico e ação de antifúngicos.

Baseados na compreensão preliminar sobre o remodelamento celular de *Cryptococcus* spp. durante a infecção, publicamos um comentário sobre trabalho intitulado "*Cryptococcus gattii* evades CD11b-mediated fungal recognition by coating itself with capsular polysaccharides", apresentado no capítulo II desta tese. Nesse comentário, destacamos a importância de compreender o papel do polissacarídeo capsular (PC) de *C. gattii* no reconhecimento de *Cryptococcus* spp. por CD11b e como esse conhecimento pode influenciar nas estratégias para o desenvolvimento de novas vacinas contra a criptococose. Surpreendentemente, vimos que boa parte dos estudos com PC são realizados com *C. neoformans* e pouco

se sabe sobre o papel de PC em *C. gattii*. Essa lacuna reforça a necessidade de mais estudos direcionados a *C. gattii*, uma vez que, considerando a nossa experiência e as evidências da literatura, a patogênese da infecção por *C. gattii* é diferente de *C. neoformans*. Embora o conhecimento sobre a infecção causada por *C. gattii* seja mais recente do que *C. neoformans*, acreditamos que a pouca compreensão dessa espécie pode oferecer barreiras para os avanços no desenvolvimento de ferramentas de diagnóstico, novos tratamentos e vacinas no contexto da criptococose.

Posteriormente, nesse mesmo capítulo, apresentamos um cenário geral sobre a criptococose, abordando desde a compreensão da biologia fúngica e sua interação no ambiente até as limitações terapêuticas e vacinais atualmente existentes. Vimos que o tratamento da criptococose ainda permanece como um grande desafio no combate à doença. Infelizmente, isso ocorre não apenas pelo arsenal limitado de antifúngicos disponíveis, como também, por falhas na garantia de acesso aos tratamentos atualmente existentes e eficazes. Isso reforça a necessidade de ampliarmos a nossa visão para além do desenvolvimento e busca de novas terapias antifúngicas. Mais do que isso, é importante traçar estratégias para que os tratamentos atualmente eficazes estejam disponíveis para a população e que as drogas em desenvolvimento sejam mais acessíveis. Do contrário, todo o conhecimento produzido na busca de novos tratamentos para a criptococose se tornará obsoleto.

Na premissa de busca por novas estratégias terapêuticas, complementando uma problemática apresentada no capítulo anterior, trabalhamos com o reposicionamento de antimaláricos no contexto da criptococose, como apresentado no capítulo III. Demonstramos que a combinação entre antimaláricos e anfotericina B resultou em uma interação sinérgica e aumento da sobrevida em modelo murino. Considerando a elevada toxidade e custo da AMB, acreditamos que, futuramente, esses achados podem oferecer um avanço importante no tratamento da Criptococose.

Interessantemente, vimos que o estradiol e a testosterona, assim como os ATMs, também apresentam sinergismo com anfotericina B, sendo capazes de reduzir a concentração mínima necessária para a ação fungicida desse antifúngico, como apresentado no capitulo IV. Esses achados reforçam a possibilidade de otimizar os tratamentos atualmente existentes e tornar mais rápida a disponibilização de novas estratégias terapêuticas contra a criptococose.

7. CONCLUSÃO

O conjunto de dados apresentados nesta tese mostram a complexidade biológica de *Cryptococcus* spp. durante a interação com o hospedeiro e a perspectiva de novos tratamentos que poderão ser utilizados no cenário da criptococose.

A indução de células pequenas e a regulação ribossomal é um fator determinante para a adaptação de *Cryptococcus* spp. no início da infecção, invasão tecidual e escape dos pulmões para o sistema nervoso central. Alterações celulares subsequentes, como aumento da capsula polissacarídica, metabolismo de inositol e produção de energia foram determinantes para a virulência de *C. neoformans*. Para *C. gattii*, demonstramos que o aumento da cápsula durante a infecção não é suficiente para predizer a virulência.

Por fim, mas não menos importante, vimos que antimaláricos e hormônios sexuais interagem sinergicamente com a anfotericina B, sendo potenciais estratégias para o tratamento da Criptococose.

8. REFERÊNCIAS

(CLSI), C. A. L. S. I. **Method for Broth Dilution antifungal Susceptibility Testing of Yeasts; Approved Standard**. Third ed. Wayne, Pennsylvania, USA, 2012.

AKAIHE, C. L.; NWEZE, E. I. Epidemiology of Cryptococcus and cryptococcosis in Western Africa. **Mycoses**, 64, n. 1, p. 4-17, Jan 2021.

AKINS, R. A. An update on antifungal targets and mechanisms of resistance in Candida albicans. **Med Mycol**, 43, n. 4, p. 285-318, Jun 2005.

ARAUJO, G. E. S.; FONSECA, F. L.; PONTES, B.; TORRES, A. *et al.* Capsules from pathogenic and non-pathogenic Cryptococcus spp. manifest significant differences in structure and ability to protect against phagocytic cells. **PLoS One**, 7, n. 1, p. e29561, 2012.

ASHIRU, J. O.; AKANG, E. E. Cryptococcal meningitis with malaria. A case report. **Mycopathologia**, 127, n. 1, p. 15-17, Jul 1994.

BARCELLOS, V. A.; MARTINS, L. M. S.; FONTES, A. C. L.; REUWSAAT, J. C. V. *et al.* Genotypic and Phenotypic Diversity of. **Front Microbiol**, 9, p. 132, 2018.

BARNETT, J. A. A history of research on yeasts 14: medical yeasts part 2, Cryptococcus neoformans. **Yeast**, 27, n. 11, p. 875-904, Nov 2010.

BENNETT, J. E.; DISMUKES, W. E.; DUMA, R. J.; MEDOFF, G. *et al.* A comparison of amphotericin B alone and combined with flucytosine in the treatment of cryptoccal meningitis. **N Engl J Med**, 301, n. 3, p. 126-131, Jul 1979.

BOTTS, M. R.; GILES, S. S.; GATES, M. A.; KOZEL, T. R. *et al.* Isolation and characterization of Cryptococcus neoformans spores reveal a critical role for capsule biosynthesis genes in spore biogenesis. **Eukaryot Cell**, 8, n. 4, p. 595-605, Apr 2009.

BROWN, G. D.; DENNING, D. W.; GOW, N. A.; LEVITZ, S. M. *et al.* Hidden killers: human fungal infections. **Sci Transl Med**, 4, n. 165, p. 165rv113, Dec 2012.

BYRNES, E. J.; HEITMAN, J. Cryptococcus gattii outbreak expands into the Northwestern United States with fatal consequences. **F1000 Biol Rep**, 1, Aug 2009.

CANNON, R. D.; LAMPING, E.; HOLMES, A. R.; NIIMI, K. *et al.* Efflux-mediated antifungal drug resistance. **Clin Microbiol Rev**, 22, n. 2, p. 291-321, Table of Contents, Apr 2009.

CASADEVALL, A.; ROSAS, A. L.; NOSANCHUK, J. D. Melanin and virulence in Cryptococcus neoformans. **Curr Opin Microbiol**, 3, n. 4, p. 354-358, Aug 2000.

CASALINUOVO, I. A.; DI FRANCESCO, P.; GARACI, E. Fluconazole resistance in Candida albicans: a review of mechanisms. **Eur Rev Med Pharmacol Sci**, 8, n. 2, p. 69-77, 2004 Mar-Apr 2004.

CASSETTA, M. I.; MARZO, T.; FALLANI, S.; NOVELLI, A. *et al.* Drug repositioning: auranofin as a prospective antimicrobial agent for the treatment of severe staphylococcal infections. **Biometals**, 27, n. 4, p. 787-791, Aug 2014.

CHANG, Y. C.; STINS, M. F.; MCCAFFERY, M. J.; MILLER, G. F. *et al.* Cryptococcal yeast cells invade the central nervous system via transcellular penetration of the blood-brain barrier. **Infect Immun**, 72, n. 9, p. 4985-4995, Sep 2004.

CHARLIER, C.; NIELSEN, K.; DAOU, S.; BRIGITTE, M. *et al.* Evidence of a role for monocytes in dissemination and brain invasion by Cryptococcus neoformans. **Infect Immun**, 77, n. 1, p. 120-127, Jan 2009.

CHEN, S. C.; MEYER, W.; SORRELL, T. C. Cryptococcus gattii infections. **Clin Microbiol Rev**, 27, n. 4, p. 980-1024, Oct 2014.

CHRÉTIEN, F.; LORTHOLARY, O.; KANSAU, I.; NEUVILLE, S. *et al.* Pathogenesis of cerebral Cryptococcus neoformans infection after fungemia. **J Infect Dis**, 186, n. 4, p. 522-530, Aug 2002.

COELHO, C.; CASADEVALL, A. Cryptococcal therapies and drug targets: the old, the new and the promising. **Cell Microbiol**, 18, n. 6, p. 792-799, 06 2016.

COGLIATI, M. Global Molecular Epidemiology of Cryptococcus neoformans and Cryptococcus gattii: An Atlas of the Molecular Types. **Scientifica (Cairo)**, 2013, p. 675213, 2013.

Correction to 'SynergyFinder 2.0: visual analytics of multi-drug combination synergies'. **Nucleic Acids Res**, Jun 17 2022.

COSTA, M. C.; DE BARROS FERNANDES, H.; GONÇALVES, G. K. N.; SANTOS, A. P. N. *et al.* 17-β-Estradiol increases macrophage activity through activation of the G-protein-coupled estrogen receptor and improves the response of female mice to Cryptococcus gattii. **Cell Microbiol**, 22, n. 6, p. e13179, 06 2020.

CRUZ-TOPETE, D.; DOMINIC, P.; STOKES, K. Y. Uncovering sex-specific mechanisms of action of testosterone and redox balance. **Redox Biol**, 31, p. 101490, 04 2020.

DATTA, K.; BARTLETT, K. H.; MARR, K. A. Cryptococcus gattii: Emergence in Western North America: Exploitation of a Novel Ecological Niche. **Interdiscip Perspect Infect Dis**, 2009, p. 176532, 2009.

DE OLIVEIRA, H. C.; JOFFE, L. S.; SIMON, K. S.; CASTELLI, R. F. *et al.* Fenbendazole Controls. **Antimicrob Agents Chemother**, 64, n. 6, 05 21 2020.

DENHAM, S. T.; BRAMMER, B.; CHUNG, K. Y.; WAMBAUGH, M. A. *et al.* A dissemination-prone morphotype enhances extrapulmonary organ entry by Cryptococcus neoformans. **Cell Host Microbe**, Sep 02 2022.

DOLAN, K.; MONTGOMERY, S.; BUCHHEIT, B.; DIDONE, L. *et al.* Antifungal activity of tamoxifen:

in vitro and in vivo activities and mechanistic characterization. **Antimicrob Agents Chemother**, 53, n. 8, p. 3337-3346, Aug 2009.

DYLĄG, M.; COLON-REYES, R. J.; KOZUBOWSKI, L. Titan cell formation is unique to. **Virulence**, 11, n. 1, p. 719-729, 01 01 2020.

EFFERTH, T.; DUNSTAN, H.; SAUERBREY, A.; MIYACHI, H. *et al.* The anti-malarial artesunate is also active against cancer. **Int J Oncol**, 18, n. 4, p. 767-773, Apr 2001.

EFFERTH, T.; GIAISI, M.; MERLING, A.; KRAMMER, P. H. *et al.* Artesunate induces ROS-mediated apoptosis in doxorubicin-resistant T leukemia cells. **PLoS One**, 2, n. 8, p. e693, Aug 2007.

FELL, J. W.; BOEKHOUT, T.; FONSECA, A.; SCORZETTI, G. *et al.* Biodiversity and systematics of basidiomycetous yeasts as determined by large-subunit rDNA D1/D2 domain sequence analysis. **Int J Syst Evol Microbiol**, 50 Pt 3, p. 1351-1371, May 2000.

FERNANDES, K. E.; BROCKWAY, A.; HAVERKAMP, M.; CUOMO, C. A. *et al.* Phenotypic Variability Correlates with Clinical Outcome in. **mBio**, 9, n. 5, 10 2018.

FERNANDES, K. E.; DWYER, C.; CAMPBELL, L. T.; CARTER, D. A. Species in the Cryptococcus gattii Complex Differ in Capsule and Cell Size following Growth under Capsule-Inducing Conditions. **mSphere**, 1, n. 6, 2016 Nov-Dec 2016.

FERNANDES, K. E.; FRASER, J. A.; CARTER, D. A. Lineages Derived from Cryptococcus neoformans Type Strain H99 Support a Link between the Capacity to Be Pleomorphic and Virulence. **mBio**, 13, n. 2, p. e0028322, Apr 26 2022.

FERREIRA, G. F.; BALTAZAR, L. E. M.; SANTOS, J. R.; MONTEIRO, A. S. *et al.* The role of oxidative and nitrosative bursts caused by azoles and amphotericin B against the fungal pathogen Cryptococcus gattii. **J Antimicrob Chemother**, 68, n. 8, p. 1801-1811, Aug 2013.

FERREIRA, G. F.; SANTOS, D. A. Heteroresistance and fungi. **Mycoses**, 60, n. 9, p. 562-568, Sep 2017.

FERREIRA, G. F.; SANTOS, J. R.; COSTA, M. C.; HOLANDA, R. A. *et al.* Heteroresistance to Itraconazole Alters the Morphology and Increases the Virulence of Cryptococcus gattii. **Antimicrob Agents Chemother**, 59, n. 8, p. 4600-4609, Aug 2015.

FISHER, M. C.; ALASTRUEY-IZQUIERDO, A.; BERMAN, J.; BICANIC, T. *et al.* Tackling the emerging threat of antifungal resistance to human health. **Nat Rev Microbiol**, 20, n. 9, p. 557-571, 09 2022.

FYFE, M.; MACDOUGALL, L.; ROMNEY, M.; STARR, M. *et al.* Cryptococcus gattii infections on Vancouver Island, British Columbia, Canada: emergence of a tropical fungus in a temperate environment. **Can Commun Dis Rep**, 34, n. 6, p. 1-12, Jun 2008.

GARCÍA-RODAS, R.; CORDERO, R. J.; TREVIJANO-CONTADOR, N.; JANBON, G. *et al.* Capsule

growth in Cryptococcus neoformans is coordinated with cell cycle progression. **MBio**, 5, n. 3, p. e00945-00914, Jun 2014.

GARCÍA-RODAS, R.; TREVIJANO-CONTADOR, N.; ROMÁN, E.; JANBON, G. *et al.* Role of Cln1 during melanization of Cryptococcus neoformans. **Front Microbiol**, 6, p. 798, 2015.

GERSTEIN, A. C.; FU, M. S.; MUKAREMERA, L.; LI, Z. *et al.* Polyploid titan cells produce haploid and aneuploid progeny to promote stress adaptation. **mBio**, 6, n. 5, p. e01340-01315, Oct 13 2015.

GHANNOUM, M. A.; RICE, L. B. Antifungal agents: mode of action, mechanisms of resistance, and correlation of these mechanisms with bacterial resistance. **Clin Microbiol Rev**, 12, n. 4, p. 501-517, Oct 1999.

GIBSON, J. F.; JOHNSTON, S. A. Immunity to Cryptococcus neoformans and C. gattii during cryptococcosis. **Fungal Genet Biol**, 78, p. 76-86, May 2015.

GIEFING-KRÖLL, C.; BERGER, P.; LEPPERDINGER, G.; GRUBECK-LOEBENSTEIN, B. How sex and age affect immune responses, susceptibility to infections, and response to vaccination. **Aging Cell**, 14, n. 3, p. 309-321, Jun 2015.

GOPALAKRISHNAN, A. M.; KUMAR, N. Antimalarial action of artesunate involves DNA damage mediated by reactive oxygen species. **Antimicrob Agents Chemother**, 59, n. 1, p. 317-325, Jan 2015.

GOUVEIA-EUFRASIO, L.; RIBEIRO, N. Q.; SANTOS, J. R. A.; DA COSTA, M. C. *et al.* Randomized, phase 1/2, double-blind pioglitazone repositioning trial combined with antifungals for the treatment of cryptococcal meningitis - PIO study. **Contemp Clin Trials Commun**, 22, p. 100745, Jun 2021.

HAGEN, F.; KHAYHAN, K.; THEELEN, B.; KOLECKA, A. *et al.* Recognition of seven species in the Cryptococcus gattii/Cryptococcus neoformans species complex. **Fungal Genet Biol**, 78, p. 16-48, May 2015.

HOMMEL, B.; STURNY-LECLÈRE, A.; VOLANT, S.; VELUPPILLAI, N. *et al.* Cryptococcus neoformans resists to drastic conditions by switching to viable but non-culturable cell phenotype. **PLoS Pathog**, 15, n. 7, p. e1007945, 07 2019.

IYER, K. R.; REVIE, N. M.; FU, C.; ROBBINS, N. *et al.* Treatment strategies for cryptococcal infection: challenges, advances and future outlook. **Nat Rev Microbiol**, 19, n. 7, p. 454-466, 07 2021.

JARVIS, J. N.; LEEME, T. B.; MOLEFI, M.; CHOFLE, A. A. *et al.* Short-course High-dose Liposomal Amphotericin B for Human Immunodeficiency Virus-associated Cryptococcal Meningitis: A Phase 2 Randomized Controlled Trial. **Clin Infect Dis**, 68, n. 3, p. 393-401, 01 18 2019.

JUNG, H. Y.; KIM, B.; RYU, H. G.; JI, Y. *et al.* Amodiaquine improves insulin resistance and lipid

metabolism in diabetic model mice. **Diabetes Obes Metab**, 20, n. 7, p. 1688-1701, 07 2018.

JUNG, K. W.; YANG, D. H.; MAENG, S.; LEE, K. T. *et al.* Systematic functional profiling of transcription factor networks in Cryptococcus neoformans. **Nat Commun**, 6, p. 6757, Apr 2015.

KANDER, M. C.; CUI, Y.; LIU, Z. Gender difference in oxidative stress: a new look at the mechanisms for cardiovascular diseases. **J Cell Mol Med**, 21, n. 5, p. 1024-1032, 05 2017.

KAPTEIN, S. J.; EFFERTH, T.; LEIS, M.; RECHTER, S. *et al.* The anti-malaria drug artesunate inhibits replication of cytomegalovirus in vitro and in vivo. **Antiviral Res**, 69, n. 2, p. 60-69, Feb 2006.

KLEIN, B. S.; TEBBETS, B. Dimorphism and virulence in fungi. **Curr Opin Microbiol**, 10, n. 4, p. 314-319, Aug 2007.

KOVATS, S. Estrogen receptors regulate innate immune cells and signaling pathways. **Cell Immunol**, 294, n. 2, p. 63-69, Apr 2015.

KROCKENBERGER, M. B.; MALIK, R.; NGAMSKULRUNGROJ, P.; TRILLES, L. *et al.* Pathogenesis of pulmonary Cryptococcus gattii infection: a rat model. **Mycopathologia**, 170, n. 5, p. 315-330, Nov 2010.

KUMWENDA, P.; COTTIER, F.; HENDRY, A. C.; KNEAFSEY, D. *et al.* Estrogen promotes innate immune evasion of Candida albicans through inactivation of the alternative complement system. **Cell Rep**, 38, n. 1, p. 110183, 01 04 2022.

KWON-CHUNG, K. J. Morphogenesis of Filobasidiella neoformans, the sexual state of Cryptococcus neoformans. **Mycologia**, 68, n. 4, p. 821-833, 1976 Jul-Aug 1976.

KWON-CHUNG, K. J.; FRASER, J. A.; DOERING, T. L.; WANG, Z. *et al.* Cryptococcus neoformans and Cryptococcus gattii, the etiologic agents of cryptococcosis. **Cold Spring Harb Perspect Med**, 4, n. 7, p. a019760, Jul 2014.

LI, S. S.; MODY, C. H. Cryptococcus. **Proc Am Thorac Soc**, 7, n. 3, p. 186-196, May 2010.

LU, R.; HOLLINGSWORTH, C.; QIU, J.; WANG, A. *et al.* Efficacy of Oral Encochleated Amphotericin B in a Mouse Model of Cryptococcal Meningoencephalitis. **mBio**, 10, n. 3, 05 28 2019.

LUPETTI, A.; DANESI, R.; CAMPA, M.; DEL TACCA, M. *et al.* Molecular basis of resistance to azole antifungals. **Trends Mol Med**, 8, n. 2, p. 76-81, Feb 2002.

MANCINI, A.; LEONE, E.; FESTA, R.; GRANDE, G. *et al.* Effects of testosterone on antioxidant systems in male secondary hypogonadism. **J Androl**, 29, n. 6, p. 622-629, 2008 Nov-Dec 2008.

MARTINEZ, L. R.; NTIAMOAH, P.; GÁCSER, A.; CASADEVALL, A. *et al.* Voriconazole inhibits melanization in Cryptococcus neoformans. **Antimicrob Agents Chemother**, 51, n. 12, p. 4396-4400, Dec 2007.

MATSUDA, Y.; KAWATE, H.; OKISHIGE, Y.; ABE, I. *et al.* Successful management of cryptococcosis of the bilateral adrenal glands and liver by unilateral adrenalectomy with antifungal agents: a case report. **BMC Infect Dis**, 11, p. 340, Dec 2011.

MAY, R. C.; STONE, N. R.; WIESNER, D. L.; BICANIC, T. *et al.* Cryptococcus: from environmental saprophyte to global pathogen. **Nat Rev Microbiol**, 14, n. 2, p. 106-117, 02 2016.

MAYER, F. L.; SÁNCHEZ-LEÓN, E.; KRONSTAD, J. W. A chemical genetic screen reveals a role for proteostasis in capsule and biofilm formation by. **Microb Cell**, 5, n. 11, p. 495-510, Oct 31 2018.

MAZIARZ, E. K.; PERFECT, J. R. Cryptococcosis. **Infect Dis Clin North Am**, 30, n. 1, p. 179-206, Mar 2016.

MESA-ARANGO, A. C.; SCORZONI, L.; ZARAGOZA, O. It only takes one to do many jobs: Amphotericin B as antifungal and immunomodulatory drug. **Front Microbiol**, 3, p. 286, 2012.

MESHNICK, S. R. Artemisinin: mechanisms of action, resistance and toxicity. **Int J Parasitol**, 32, n. 13, p. 1655-1660, Dec 2002.

MONROE, A.; WILLIAMS, N. A.; OGOMA, S.; KAREMA, C. *et al.* Reflections on the 2021 World Malaria Report and the future of malaria control. **Malar J**, 21, n. 1, p. 154, May 27 2022.

MOODLEY, A.; RAE, W.; BHIGJEE, A.; CONNOLLY, C. *et al.* Early clinical and subclinical visual evoked potential and Humphrey's visual field defects in cryptococcal meningitis. **PLoS One**, 7, n. 12, p. e52895, 2012.

MOR, V.; RELLA, A.; FARNOUD, A. M.; SINGH, A. *et al.* Identification of a New Class of Antifungals Targeting the Synthesis of Fungal Sphingolipids. **MBio**, 6, n. 3, p. e00647, Jun 2015.

MORRIS, A. M. Review: voriconazole for prevention or treatment of invasive fungal infections in cancer with neutropenia. **Ann Intern Med**, 161, n. 2, p. JC8, Jul 2014.

MORTENSON, J. A.; BARTLETT, K. H.; WILSON, R. W.; LOCKHART, S. R. Detection of Cryptococcus gattii in selected urban parks of the Willamette Valley, Oregon. **Mycopathologia**, 175, n. 3-4, p. 351-355, Apr 2013.

NARA, S.; SANO, T.; OJIMA, H.; ONAYA, H. *et al.* Liver cryptococcosis manifesting as obstructive jaundice in a young immunocompetent man: report of a case. **Surg Today**, 38, n. 3, p. 271-274, 2008.

NETT, J. E.; ANDES, D. R. Antifungal Agents: Spectrum of Activity, Pharmacology, and Clinical Indications. **Infect Dis Clin North Am**, 30, n. 1, p. 51-83, Mar 2016.

NOONEY, L.; MATTHEWS, R. C.; BURNIE, J. P. Evaluation of Mycograb, amphotericin B, caspofungin, and fluconazole in combination against Cryptococcus neoformans by checkerboard and time-kill methodologies. **Diagn Microbiol Infect Dis**, 51, n. 1, p. 19-29, Jan 2005.

OKAGAKI, L. H.; STRAIN, A. K.; NIELSEN, J. N.; CHARLIER, C. *et al.* Cryptococcal cell morphology affects host cell interactions and pathogenicity. **PLoS Pathog**, 6, n. 6, p. e1000953, Jun 2010.

OLSZEWSKI, M. A.; ZHANG, Y.; HUFFNAGLE, G. B. Mechanisms of cryptococcal virulence and persistence. **Future Microbiol**, 5, n. 8, p. 1269-1288, Aug 2010.

PAPPAS, P. G. Cryptococcal infections in non-HIV-infected patients. **Trans Am Clin Climatol Assoc**, 124, p. 61-79, 2013.

PARK, B. J.; WANNEMUEHLER, K. A.; MARSTON, B. J.; GOVENDER, N. *et al.* Estimation of the current global burden of cryptococcal meningitis among persons living with HIV/AIDS. **AIDS**, 23, n. 4, p. 525-530, Feb 2009.

PERES-EMIDIO, E. C.; FREITAS, G. J. C.; COSTA, M. C.; GOUVEIA-EUFRASIO, L. *et al.* Infection Modulates the Immune Response and Increases Mice Resistance to. **Front Cell Infect Microbiol**, 12, p. 811474, 2022.

PERFECT, J. R. The antifungal pipeline: a reality check. **Nat Rev Drug Discov**, May 2017.

PERFECT, J. R.; BICANIC, T. Cryptococcosis diagnosis and treatment: What do we know now. **Fungal Genet Biol**, 78, p. 49-54, May 2015.

PERFECT, J. R.; DISMUKES, W. E.; DROMER, F.; GOLDMAN, D. L. *et al.* Clinical practice guidelines for the management of cryptococcal disease: 2010 update by the infectious diseases society of america. **Clin Infect Dis**, 50, n. 3, p. 291-322, Feb 2010.

QIAO, S.; TAO, S.; ROJO DE LA VEGA, M.; PARK, S. L. *et al.* The antimalarial amodiaquine causes autophagic-lysosomal and proliferative blockade sensitizing human melanoma cells to starvation- and chemotherapy-induced cell death. **Autophagy**, 9, n. 12, p. 2087-2102, Dec 2013.

RAJASINGHAM, R.; GOVENDER, N. P.; JORDAN, A.; LOYSE, A. *et al.* The global burden of HIV-associated cryptococcal infection in adults in 2020: a modelling analysis. **Lancet Infect Dis**, Aug 29 2022.

RAJASINGHAM, R.; SMITH, R. M.; PARK, B. J.; JARVIS, J. N. *et al.* Global burden of disease of HIV-associated cryptococcal meningitis: an updated analysis. **Lancet Infect Dis**, 17, n. 8, p. 873-881, 08 2017.

REAGAN-SHAW, S.; NIHAL, M.; AHMAD, N. Dose translation from animal to human studies revisited. **FASEB J**, 22, n. 3, p. 659-661, Mar 2008.

RIBEIRO, N. Q.; COSTA, M. C.; MAGALHÃES, T. F. F.; CARNEIRO, H. C. S. *et al.* Atorvastatin as a promising anticryptococcal agent. **Int J Antimicrob Agents**, 49, n. 6, p. 695-702, Jun 2017.

RIBEIRO, N. Q.; SANTOS, A. P. N.; EMÍDIO, E. C. P.; COSTA, M. C. *et al.* Pioglitazone as an adjuvant of amphotericin B for the treatment of cryptococcosis. **Int J Antimicrob Agents**, 54, n. 3, p. 301-308, Sep 2019.

RODRIGUES, M. L. Funding and Innovation in Diseases of Neglected Populations: The Paradox of Cryptococcal Meningitis. **PLoS Negl Trop Dis**, 10, n. 3, p. e0004429, Mar 2016.

ROSSI, S. A.; DE OLIVEIRA, H. C.; AGREDA-MELLON, D.; LUCIO, J. *et al.* Identification of Off-Patent Drugs That Show Synergism with Amphotericin B or That Present Antifungal Action against Cryptococcus neoformans and. **Antimicrob Agents Chemother**, 64, n. 4, 03 24 2020.

SANTOS, J. R.; GOUVEIA, L. F.; TAYLOR, E. L.; RESENDE-STOIANOFF, M. A. *et al.* Dynamic interaction between fluconazole and amphotericin B against Cryptococcus gattii. **Antimicrob Agents Chemother**, 56, n. 5, p. 2553-2558, May 2012.

SANTOS, J. R. A.; RIBEIRO, N. Q.; BASTOS, R. W.; HOLANDA, R. A. *et al.* High-dose fluconazole in combination with amphotericin B is more efficient than monotherapy in murine model of cryptococcosis. **Sci Rep**, 7, n. 1, p. 4661, Jul 2017.

SHANKAR, J.; RESTREPO, A.; CLEMONS, K. V.; STEVENS, D. A. Hormones and the resistance of women to paracoccidioidomycosis. **Clin Microbiol Rev**, 24, n. 2, p. 296-313, Apr 2011.

STEPHEN, C.; LESTER, S.; BLACK, W.; FYFE, M. *et al.* Multispecies outbreak of cryptococcosis on southern Vancouver Island, British Columbia. **Can Vet J**, 43, n. 10, p. 792-794, Oct 2002.

STONE, N. R.; RHODES, J.; FISHER, M. C.; MFINANGA, S. *et al.* Dynamic ploidy changes drive fluconazole resistance in human cryptococcal meningitis. **J Clin Invest**, 129, n. 3, p. 999-1014, 03 01 2019.

SUBRAMANIAN, S.; MATHAI, D. Clinical manifestations and management of cryptococcal infection. **J Postgrad Med**, 51 Suppl 1, p. S21-26, 2005.

SUN, S.; COELHO, M. A.; DAVID-PALMA, M.; PRIEST, S. J. *et al.* The Evolution of Sexual Reproduction and the Mating-Type Locus: Links to Pathogenesis of. **Annu Rev Genet**, 53, p. 417-444, 12 03 2019.

SYME, R. M.; SPURRELL, J. C.; AMANKWAH, E. K.; GREEN, F. H. *et al.* Primary dendritic cells phagocytose Cryptococcus neoformans via mannose receptors and Fcgamma receptor II for presentation to T lymphocytes. **Infect Immun**, 70, n. 11, p. 5972-5981, Nov 2002.

TREVIJANO-CONTADOR, N.; DE OLIVEIRA, H. C.; GARCÍA-RODAS, R.; ROSSI, S. A. *et al.* Cryptococcus neoformans can form titan-like cells in vitro in response to multiple signals. **PLoS Pathog**, 14, n. 5, p. e1007007, 05 2018.

TUITE, N. L.; LACEY, K. Overview of invasive fungal infections. **Methods Mol Biol**, 968, p. 1-23, 2013.

UPTON, A.; FRASER, J. A.; KIDD, S. E.; BRETZ, C. *et al.* First contemporary case of human infection with Cryptococcus gattii in Puget Sound: evidence for spread of the Vancouver Island outbreak. **J Clin Microbiol**, 45, n. 9, p. 3086-3088, Sep 2007.

URAI, M.; KANEKO, Y.; UENO, K.; OKUBO, Y. *et al.* Evasion of Innate Immune Responses by the Highly Virulent Cryptococcus gattii by Altering Capsule Glucuronoxylomannan Structure. **Front Cell Infect Microbiol**, 5, p. 101, 2015.

VELAGAPUDI, R.; HSUEH, Y. P.; GEUNES-BOYER, S.; WRIGHT, J. R. *et al.* Spores as infectious propagules of Cryptococcus neoformans. **Infect Immun**, 77, n. 10, p. 4345-4355, Oct 2009.

VOELZ, K.; MAY, R. C. Cryptococcal interactions with the host immune system. **Eukaryot Cell**, 9, n. 6, p. 835-846, Jun 2010.

VOM STEEG, L. G.; KLEIN, S. L. SeXX Matters in Infectious Disease Pathogenesis. **PLoS Pathog**, 12, n. 2, p. e1005374, Feb 2016.

VU, K.; THAM, R.; UHRIG, J. P.; THOMPSON, G. R. *et al.* Invasion of the central nervous system by Cryptococcus neoformans requires a secreted fungal metalloprotease. **MBio**, 5, n. 3, p. e01101-01114, Jun 2014.

WILLIAMSON, P. R.; JARVIS, J. N.; PANACKAL, A. A.; FISHER, M. C. *et al.* Cryptococcal meningitis: epidemiology, immunology, diagnosis and therapy. **Nat Rev Neurol**, 13, n. 1, p. 13-24, Jan 2017.

XU, X.; LIN, J.; ZHAO, Y.; KIRKMAN, E. *et al.* Glucosamine stimulates pheromone-independent dimorphic transition in Cryptococcus neoformans by promoting Crz1 nuclear translocation. **PLoS Genet**, 13, n. 9, p. e1006982, Sep 2017.

XUE, C. Cryptococcus and beyond--inositol utilization and its implications for the emergence of fungal virulence. **PLoS Pathog**, 8, n. 9, p. e1002869, Sep 2012.

XUE, C.; TADA, Y.; DONG, X.; HEITMAN, J. The human fungal pathogen Cryptococcus can complete its sexual cycle during a pathogenic association with plants. **Cell Host Microbe**, 1, n. 4, p. 263-273, Jun 14 2007.

YAUCH, L. E.; LAM, J. S.; LEVITZ, S. M. Direct inhibition of T-cell responses by the Cryptococcus capsular polysaccharide glucuronoxylomannan. **PLoS Pathog**, 2, n. 11, p. e120, Nov 2006.

ZARAGOZA, O. Multiple Disguises for the Same Party: The Concepts of Morphogenesis and Phenotypic Variations in Cryptococcus neoformans. **Front Microbiol**, 2, p. 181, 2011.

ZARAGOZA, O.; GARCÍA-RODAS, R.; NOSANCHUK, J. D.; CUENCA-ESTRELLA, M. *et al.* Fungal cell gigantism during mammalian infection. **PLoS Pathog**, 6, n. 6, p. e1000945, Jun 17 2010.

ZAVREL, M.; WHITE, T. C. Medically important fungi respond to azole drugs: an update. **Future Microbiol**, 10, n. 8, p. 1355-1373, 2015.

ZHAI, B.; WU, C.; WANG, L.; SACHS, M. S. *et al.* The antidepressant sertraline provides a promising therapeutic option for neurotropic cryptococcal infections. **Antimicrob Agents Chemother**, 56, n. 7, p. 3758-3766, Jul 2012.

9. ARTIGOS PUBLICADOS EM COLABORAÇÃO DURANTE O DOUTORADO

1. PERES-EMIDIO, ELUZIA C. ; **FREITAS, GUSTAVO J. C.** ; COSTA, MARLIETE C. ; GOUVEIA-EUFRASIO, LUDMILA ; SILVA, LÍVIA M. V. ; SANTOS, ANDERSON P. N. ; CARMO, PAULO H. F. ; BRITO, CAMILA B. ; ARIFA, RAQUEL D. N. ; BASTOS, RAFAEL W. ; RIBEIRO, NOELLY Q. ; OLIVEIRA, LORENA V. N. ; SILVA, MONIQUE F. ; PAIXÃO, TATIANE A. ; SALIBA, ALESSANDRA M. ; FAGUNDES, CAIO T. ; SOUZA, DANIELE G. ; SANTOS, DANIEL A. . Pseudomonas aeruginosa Infection Modulates the Immune Response and Increases Mice Resistance to *Cryptococcus* gattii. Frontiers in Cellular and Infection Microbiology, v. 12, p. 12-14, 2022.

2. DOS ANJOS CORDEIRO, JEANE MARTINHA ; SANTOS, LUCIANO CARDOSO ; DE OLIVEIRA, LUCIANA SANTOS ; SANTOS, BIANCA REIS ; SANTOS, EMILLY OLIVEIRA ; BARBOSA, ERIKLES MACÊDO ; DE MACÊDO, ISABELA OLIVEIRA ; **DE FREITAS, GUSTAVO JOSÉ COTA** ; SANTOS, DANIEL DE ASSIS ; DE LAVOR, MÁRIO SÉRGIO LIMA ; SILVA, JUNEO FREITAS . Maternal hypothyroidism causes oxidative stress and endoplasmic reticulum stress in the maternal-fetal interface of rats. FREE RADICAL BIOLOGY AND MEDICINE, v. 191, p. 24-39, 2022.

3. CARMO, PAULO H F ; **FREITAS, GUSTAVO J C** ; DORNELAS, JOÃO C M ; ALMEIDA, BRUNA C T ; BALTAZAR, LUDMILA M ; FERREIRA, GABRIELLA F ; PERES, NALU T A ; SANTOS, DANIEL A . Reactive oxygen and nitrogen species are crucial for the antifungal activity of amorolfine and ciclopirox olamine against the dermatophyte Trichophyton interdigitale. MEDICAL MYCOLOGY, v. 60, p. 12-16, 2022.

4. GOUVEIA-EUFRASIO, LUDMILA RIBEIRO, NOELLY QUEIROZ SANTOS, JULLIANA RIBEIRO ALVES DA COSTA, MARLIETE CARVALHO EMÍDIO, ELÚZIA CASTRO PERES; **DE FREITAS, GUSTAVO JOSÉ COTA;** DO CARMO, PAULO HENRIQUE FONSECA MIRANDA, BÁRBARA ALVES DE OLIVEIRA, JOÃO CARLOS MAIA DORNELAS DA SILVA, LÍVIA MARA VITORINO TEIXEIRA LEOCÁDIO, VICTOR AUGUSTO RANDI MAGALHÃES, VANESSA CAROLINE PENIDO, INDIARA PEREIRA, LEONARDO SOARES RABELO, LÍVIA FROTA DE ALMEIDA FARIA, FLÁVIO AUGUSTO TEIXEIRA DUTRA, MARIA RITA ASPAHAN, MAÍRA DE PAULA, LUDMILA DA SILVA, DIRCE INÊS TAVARES MELO, MÁRCIA GREGORY DE ANDRADE ZAMBELLI, VIRGINIA ANTUNES GOMES FARACO, ANDRÉ AUGUSTO DA COSTA CÉSAR, ISABELA ALVES, GLAUCIENE PRADO , et al. ; Randomized, phase 1/2, double-blind pioglitazone repositioning trial combined with antifungals for the treatment of cryptococcal meningitis - PIO study. Contemporary Clinical Trials Communications, v. 22, p. 100745, 2021.

5. BALTAZAR, LUDMILA MATOS; RIBEIRO, GABRIELA FIOR; **FREITAS, GUSTAVO J.** ; QUEIROZ-JUNIOR, CELSO MARTINS ; FAGUNDES, CAIO TAVARES; CHAVES-OLÓRTEGUI, CARLOS; TEIXEIRA, MAURO MARTINS; SOUZA, DANIELE G.. Protective Response in Experimental Paracoccidioidomycosis Elicited by Extracellular Vesicles Containing Antigens of Paracoccidioides brasiliensis. Cells, v. 10, p. 1813, 2021.

6. MAGALHÃES, THAIS FURTADO FERREIRA; COSTA, MARLIETE CARVALHO ; HOLANDA, RODRIGO ASSUNÇÃO; FERREIRA, GABRIELA FREITAS; CARVALHO, VANESSA SILVA DUTRA ; **FREITAS, GUSTAVO JOSE COTA** ; RIBEIRO, NOELLY QUEIROZ ; EMÍDIO, ELÚZIA CASTRO PERES ; CARMO, PAULO HENRIQUE FONSECA ; DE BRITO, CAMILA BERNARDO ; DE SOUZA, DANIELE GLÓRIA ; ROCHA, CLÁUDIA EMANUELA VIANA ; PAIXÃO, TATIANE ALVES ; DE RESENDE-STOIANOFF, MARIA APARECIDA ; SANTOS, DANIEL ASSIS . N-acetylcysteine reduces amphotericin B deoxycholate nephrotoxicity and improves the outcome of murine cryptococcosis. MEDICAL MYCOLOGY, v. 8, p. 9, 2020.

7. COSTA, MARLIETE C.; BARROS FERNANDES, HELIANA ; GONÇALVES, GLEISY K. N. ; SANTOS, ANDERSON P. N. ; FERREIRA, GABRIELLA F. ; **FREITAS, GUSTAVO J. C.** ; CARMO, PAULO H. F. ; HUBNER, JÔSY ; EMÍDIO, ELÚZIA C. P. ; SANTOS, JULLIANA R. A. ; SANTOS, JANE L. ; REIS, ADELINA

M. ; FAGUNDES, CAIO T. ; SILVA, ARISTÓBOLO M. ; SANTOS, DANIEL A. . 17-β-Estradiol increases macrophage activity through activation of the G-protein-coupled estrogen receptor and improves the response of female mice to *Cryptococcus* gattii. CELLULAR MICROBIOLOGY, v. 8, p. 9, 2020.

8. FOLLY, MARIANY L. C. ; FERREIRA, GABRIELLA F. ; SALVADOR, MAIARA R. ; SATHLER, ANA A. ; DA SILVA, GUILHERME F. ; SANTOS, JOICE CASTELO BRANCO ; SANTOS, JULLIANA R. A. DOS ; NUNES NETO, WALLACE RIBEIRO ; RODRIGUES, JOÃO FRANCISCO SILVA ; FERNANDES, ELIZABETH SOARES ; DA SILVA, LUÍS CLÁUDIO NASCIMENTO ; **DE FREITAS, GUSTAVO JOSÉ COTA** ; DENADAI, ÂNGELO M. ; RODRIGUES, IVANILDES V. ; MENDONÇA, LEONARDO M. ; MONTEIRO, ANDREA SOUZA ; SANTOS, DANIEL ASSIS ; CABRERA, GABRIELA M. ; SILESS, GASTÓN ; LANG, KAREN L. . Evaluation of in vitro Antifungal Activity of Xylosma prockia (Turcz.) Turcz. (Salicaceae) Leaves Against *Cryptococcus* spp.. Frontiers in Microbiology, v. 10, p. 7, 2020.

9. MACIEL, NATÁLIA OP; JOHANN, SUSANA ; BRANDÃO, LUCIANA R ; KUCHARÍKOVÁ, SONA ; MORAIS, CAMILA G ; OLIVEIRA, ALEXANDRE P ; **FREITAS, GUSTAVO JC** ; BORELLI, BEATRIZ M ; PELLIZZARI, FRANCIANE M ; SANTOS, DANIEL A ; DIJCK, PATRICK VAN ; ROSA, CARLOS A . Occurrence, antifungal susceptibility, and virulence factors of opportunistic yeasts isolated from Brazilian beaches. Memórias do Instituto Oswaldo Cruz, v. 114, p. 9, 2019.